

# DEEP LEARNING AND THE RATE OF APPROXIMATION BY FLOWS

JINGPU CHENG, QIANXIAO LI, TING LIN, AND ZUOWEI SHEN

ABSTRACT. We investigate the dependence of the approximation capacity of deep residual networks on its depth in a continuous dynamical systems setting. This can be formulated as the general problem of quantifying the minimal time-horizon required to approximate a diffeomorphism by flows driven by a given family  $\mathcal{F}$  of vector fields. We show that this minimal time can be identified as a geodesic distance on a sub-Finsler manifold of diffeomorphisms, where the local geometry is characterised by a variational principle involving  $\mathcal{F}$ . This connects the learning efficiency of target relationships to their compatibility with the learning architectural choice. Further, the results suggest that the key approximation mechanism in deep learning, namely the approximation of functions by composition or dynamics, differs in a fundamental way from linear approximation theory, where linear spaces and norm-based rate estimates are replaced by manifolds and geodesic distances.

## CONTENTS

1. Introduction	1
2. Problem formulation and main results	4
2.1. Notations	4
2.2. Formulation and main results	4
2.3. Implications for approximation theory and compositional models	7
3. The rate of approximation by flows: one dimensional ReLU networks	9
3.1. Proofs of the results for 1D ReLU control family	12
4. The rate of approximation by flows: the general case	22
4.1. Preliminaries on Banach sub-Finsler geometry	22
4.2. General characterization of approximation complexity via Finsler geometry	27
4.3. Interpolation distance, variational formula and asymptotic properties	32
5. Applications	36
5.1. 1D ReLU revisited	36
5.2. Other applications	39
Computations for the layer-normalization example	45
References	50

## 1. INTRODUCTION

Deep residual networks (ResNets) form the backbone of modern deep learning architectures, ranging from convolution networks for image processing [20] to transformers powering large language models [48]. At the same time, their success also pose interesting new mathematical questions. A deep residual network is built from repeated compositions of transformations

$$(1.1) \quad x(n+1) = x(n) + f_n(x(n)), \quad f_n \in \mathcal{F}, \quad n = 0, 1, 2, \dots, N-1,$$

where  $N$  is the depth of the network,  $x(n) \in \mathbb{R}^d$  is the hidden state of the network at layer  $n$  and  $f_n : \mathbb{R}^d \rightarrow \mathbb{R}^d$  is the trainable non-linear transformation applied at each layer, with  $\mathcal{F}$  being the

set of possible transformations that is determined by the architectural choice. For example, in fully connected ResNets,  $\mathcal{F}$  is the set of all functions that can be represented by a single-layer feedforward network [47, 46, 18], whereas for transformers,  $\mathcal{F}$  is the set of token-wise networks composed with self-attention maps [48, 13, 15].

With this compositional structure, one can build complex transformations  $x(0) \mapsto x(N)$  by increasing the number of layers  $N$ , and this is the main way of improving model learning capacity in modern artificial intelligence applications. These fall into the following two complementary formulations.

**(i) Approximation of functions in supervised learning.** In standard supervised learning tasks, we consider a set of inputs  $X \subset \mathbb{R}^d$  and a set of outputs  $Y \subset \mathbb{R}^m$ . The goal of learning is to approximate an unknown target function  $F : X \rightarrow Y$  that maps inputs to outputs. For example,  $X$  can be the set of natural images represented by pixel intensities, and  $Y$  is the corresponding classification of the image into types, such as cats, birds, cars, etc.  $F$  would then be the function that classify a given image into its type, realising an image recognition tool.

Residual networks tackles this approximation problem by considering the composition

$$(1.2) \quad \tilde{F} := \beta \circ \varphi_N \circ \alpha,$$

where  $x(0) \mapsto \varphi_N(x(0)) = x(N)$  is the map defined by the  $N$ -layer residual dynamics in (1.1), and  $\alpha : \mathbb{R}^d \rightarrow \mathbb{R}^d$  and  $\beta : \mathbb{R}^d \rightarrow Y$  are simple maps (e.g.,  $\beta$  can be affine functions for regression problems and indicator functions of a half-space for binary classification problems). The function  $\tilde{F}$  is then used to approximate the target  $F$ , with its approximation capacity imparted by the large number of building blocks in  $\varphi_N$ .

**(ii) Approximations of distributions in generative modelling.** Another highly relevant application relying on a similar dynamical approximation scheme is generative modelling [31, 21, 40], where the goal is to learn a model that can generate samples (e.g. images, text, crystal structure, etc.) from a target data distribution. In this case, a predominant approach is to model a transport map that pushes forward a simple reference distribution  $\mu_0$  (e.g., a Gaussian) to a complicated target data distribution  $\mu_1$ . More concretely, we aim to find a map  $\varphi$  such that

$$(1.3) \quad \varphi\#\mu_0 \approx \mu_1.$$

In practice, such transport maps are often modelled as the flow map of an ODE realized by the deep residual structure [21, 40, 42, 31] (serving as a discrete approximation) in (1.1).

In both scenarios discussed above, one requires the compositions of residual layers to approximate a complicated transformation on  $X$ . A primary mathematical question that arises is: how does such compositional structures build complexity, and how is it different from classical methods — such as finite elements, splines, and wavelets — which typically rely on linear combinations of simpler functions? A convenient way to study this is the *dynamical systems* approach, which idealises the compositions in (1.1) as a continuous dynamics

$$(1.4) \quad \dot{x}(t) = f_t(x(t)), \quad f_t \in \mathcal{F}, \quad t \in [0, T].$$

This connects the problem of expressivity of deep ResNets to the study of the approximation or controllability properties of flows of differential equations, and this approach has yielded a number of insights in deep learning [26, 45, 2, 33, 8]. Most notably, it was shown under fairly weak assumptions on  $\mathcal{F}$  that the family of flow maps of (1.4) is dense in appropriate spaces of maps from  $\mathbb{R}^d$  to itself [26, 8]. This implies in particular that as long as ResNets are sufficiently deep, they can be used to solve arbitrary tasks, such as image recognition, language modelling and reinforcement learning.

However, the follow-up (and perhaps the more important) question remains: what maps from  $\mathbb{R}^d$  to itself are more easily approximated by a relatively shallow network as opposed to a very deep one? This connects to the important practical problem of why and when one should use deep learning over other approximation schemes. A precise answer to this question is thus important in both theory and practice.

There are familiar analogues in classical approximation theory for which the corresponding issues are well-understood. For example, while Weierstrass [14] showed that polynomials are dense in the space of continuous functions on the unit interval, it does not tell us which continuous functions can be approximated well with a low polynomial order. The classical theorem due to Jackson [14] provides an answer to this question, where it is shown that

$$(1.5) \quad \inf_{p \in \mathcal{P}_n} \|F(x) - p(x)\|_{C([0,1])} \lesssim \|F^{(\alpha)}\|_{C([0,1])} n^{-\alpha}, \quad F \in C^\alpha([0, 1]),$$

where  $\mathcal{P}_n$  is the set of polynomials with degree up to and including  $n$ ,  $\alpha$  is a positive integer, and  $F^{(\alpha)}$  is the order  $\alpha$  derivative of  $F$ , which we assume to be  $\alpha$ -times continuously differentiable. Jackson's theorem identifies a proper subset of continuous functions ( $C^{(\alpha)}$ ) as target function spaces, on which we can establish a *rate of approximation*. In particular, we see that the smoother the target is, the faster the rate of approximation<sup>1</sup>. Under the same smoothness condition, a function with a smaller  $\|\cdot\|_{C([0,1])}$  admits a lower approximation error. This is a measure of the *complexity* of a target function under polynomial approximation. This result has immediate practical consequences: we now understand that it is precisely the continuously differentiable functions that admit effective approximations by polynomials, and the complexity is governed by the size of its derivatives – the smaller the better.

The purpose of this paper is to study the parallel problem for approximation by flows, as in eq. (1.4). In our setting, the cost is not the number of terms in a linear combination of monomials (polynomial degree) but the depth of the residual architecture, idealised as the time horizon  $T$  in eq. (1.4). We ask: for which target maps can the flow approximate arbitrarily well within a finite time  $T$ , and how does the minimal such  $T$  depend on the target and our choice of architecture  $\mathcal{F}$ ? We view this minimal time as a notion of complexity of the target. This differs subtly from the classical Jackson-style question, which fixes a budget (e.g., degree  $n$ ) and bounds the approximation error as a function of that budget. Here we invert the perspective: for a prescribed accuracy (arbitrarily small), we seek the minimal budget  $T$  that makes the approximation possible. A simple linear analogy illustrates this distinction. Consider a Hilbert space  $H$  with an orthonormal basis  $\{e_i\}_{i \geq 1}$ . If one fixes a linear budget  $S$  (say, an  $\ell^1$  or  $\ell^2$  constraint on coefficients), the set of functions that can be approximated arbitrarily well under that budget is just the corresponding ball in  $H$  – a trivial characterisation. By contrast, in the compositional/flow setting the hypothesis class is closed under composition, not addition, and the resulting minimal-budget characterisation is non-trivial. This is precisely the object we will study. The problem of minimal time of flows for approximation has been studied in specific settings in previous works. For instance, in [33], the authors studied the approximation using continuous-time ResNets with ReLU type activations. They provided an upper bound on the time to achieve a certain accuracy for general  $L^2$  functions. In [26], the authors provide a quantitative estimate on the minimal reachable time in 1D case for ReLU activations. In [17], the estimation of time for interpolating a set of measures using flow-based models with self-attention layers is studied. These works mainly focus on specific architectures and are based on constructive approaches. In contrast, our purpose is to develop a general framework for studying the minimal time problem for general flow-based models using a geometric viewpoint.

We now give a informal preview of the main results and insights. First, we show that the right space of maps on which we can quantify flow approximation should be a metric space respecting the compositional structure of the problem. That is, instead of discussing the complexity of approximating *one* map, we should instead study the complexity of connecting *two* maps by a flow. The approximation complexity will then be identified with the metric on this space. Next, this global picture is then supplemented by a local one, where we show that the metric is realised as the geodesic distance on this metric space viewed as a sub-Finsler manifold. Most importantly, the local lengths (Finsler norms) are characterised in a variational form involving the family of vector fields  $\mathcal{F}$ . Together, this gives a concrete picture of the quantitative aspects of flow (ResNet) approximation: the complexity of connecting two

<sup>1</sup>A converse due to Bernstein [14] shows that an approximation error decay rate of  $n^{\alpha+\delta}$  ( $\delta > 0$ ) implies  $F \in C^{(\alpha)}$ , meaning that only smooth functions can be efficiently approximated.

given maps by a continuous deep ResNet is a distance on a manifold of target maps, where the local geometry is generated by the expressiveness of each shallow layer architecture of the deep network. This framework addresses the basic question of quantitative measures of complexity for approximation via deep architectures, and holds for in general dimensions and architecture choices. In section 5 we give some examples of this approach for problems where the precise manifold can be identified and its associated geodesic distances can be computed or estimated.

## 2. PROBLEM FORMULATION AND MAIN RESULTS

In this section, we summarize our main results on the geometric framework for the complexity class of flow approximation. We begin by introducing the notations and the precise formulation of the problem, followed by the statement and explanation of the main results.

**2.1. Notations.** In the following, for a finite-dimensional manifold  $M$ , a vector field  $f \in \text{Vec}(M)$  and time  $t \geq 0$ , we denote its flow map  $\varphi_f^t$  as:

$$(2.1) \quad \varphi_f^t : x(0) \rightarrow x(t), \quad \dot{x}(t) = f(x(t)).$$

We adopt the following convention whenever possible:

- (1) We use  $f, g$  to denote the vector fields and  $\varphi_f^t$  as the flow map of  $f$  at time horizon  $t$ .
- (2) We use  $\psi, \xi$ , to denote the target mappings from a manifold  $M$  to itself.
- (3) We use  $u, v$  to denote tangent vectors.

Let  $X$  be a vector space. We write  $\overline{X}^{\|\cdot\|}$  as the closure of  $X$  under the norm  $\|\cdot\|$ . Moreover, if there is a natural linear inclusion  $\overline{X}^{\|\cdot\|} \hookrightarrow Y$  to some classical space  $Y$ , we will identify both  $X$  and  $\overline{X}^{\|\cdot\|}$  as their image in  $Y$  under this inclusion.

For  $u : M \rightarrow \mathbb{R}^k$ , we write  $u \in W^{1,\infty}(M)$  if  $u \in L^\infty(M)$  and its (weak) derivative satisfies  $\nabla u \in L^\infty(M)$ . We equip it with the norm

$$(2.2) \quad \|u\|_{W^{1,\infty}(M)} := \|u\|_{L^\infty(M)} + \|\nabla u\|_{L^\infty(M)}.$$

For a vector field  $f \in \text{Vec}(M)$ , we interpret  $f \in W^{1,\infty}(M)$  component-wise in local charts (equivalently, via any fixed smooth atlas on compact  $M$ ). We write  $\text{Diff}^{W^{1,\infty}}(M)$  for the group of homeomorphisms  $\psi : M \rightarrow M$  whose coordinate representations belong to  $W^{1,\infty}$ , i.e.

$$(2.3) \quad \psi, \psi^{-1} \in W^{1,\infty}(M).$$

**2.2. Formulation and main results.** Let  $M \subset \mathbb{R}^d$  be a smooth compact manifold (possibly with boundary). Consider the following control system:

$$(2.4) \quad \dot{x}(t) = f(x(t), \theta(t)), \quad x(0) = x_0 \in M, \quad \theta(t) \in \Theta, \quad t \in [0, T],$$

where for each parameter  $\theta \in \Theta$  the map  $x \mapsto f(x, \theta)$  is a vector field on  $M$ , i.e.,  $f(\cdot, \theta) \in \text{Vec}(M)$ . We refer to  $x(\cdot)$  as the state trajectory and to  $\theta(\cdot)$  as the control signal. The associated family of vector fields (hereafter called a *control family*) is

$$(2.5) \quad \mathcal{F} := \{x \mapsto f(x, \theta) \mid \theta \in \Theta\} \subset \text{Vec}(M),$$

which is the set of admissible control functions. We assume throughout that  $\mathcal{F}$  is symmetric, i.e.,  $f \in \mathcal{F}$  implies  $-f \in \mathcal{F}$ , and functions in  $\mathcal{F}$  are uniformly bounded and uniformly Lipschitz on  $M$ , i.e., there exists  $L > 0$  such that for all  $f \in \mathcal{F}$ ,

$$(2.6) \quad \|f\|_{L^\infty(M)} := \sup_{x \in M} \|f(x)\| \leq L, \quad \text{and} \quad \text{Lip}(f) := \sup_{x, y \in M, x \neq y} \frac{\|f(x) - f(y)\|}{\|x - y\|} \leq L.$$

For a given horizon  $T > 0$ , we denote by  $\mathcal{A}_{\mathcal{F}}(T)$  the class of all flow maps generated by time-splitting the dynamics in  $\mathcal{F}$  over a total duration  $T$ :

$$(2.7) \quad \mathcal{A}_{\mathcal{F}}(T) := \left\{ \varphi_{f_m}^{t_m} \circ \dots \circ \varphi_{f_1}^{t_1} \mid m \in \mathbb{N}, f_i \in \mathcal{F}, t_i > 0, \sum_{i=1}^m t_i = T \right\},$$

It is now known that under mild conditions on  $\mathcal{F}$ , the set

$$(2.8) \quad \mathcal{A}_{\mathcal{F}} := \bigcup_{T>0} \mathcal{A}_{\mathcal{F}}(T)$$

is dense in  $C(M, M)$  (the class of continuous maps  $M \rightarrow M$ ) with respect to natural topologies (e.g., uniform on compacta or  $L_{\text{loc}}^p$ ). For example, in [26, 45, 33, 2, 8] it is shown that when  $M = \mathbb{R}^d$  and  $\mathcal{F}$  is affine-invariant and contains a non-linear vector field, then  $\mathcal{A}_{\mathcal{F}}$  is dense in  $L_{\text{loc}}^p(\mathbb{R}^d, \mathbb{R}^d)$  for any  $p \in [1, \infty)$ . In [16], it is also shown that under similar condition,  $\mathcal{A}_{\mathcal{F}}$  is dense in  $C(M, M)$  topology in the set of orientation preserving diffeomorphisms over  $M$ . This means in particular that given sufficiently long time horizons, maps generated by flows of reasonable control families  $\mathcal{F}$  can learn arbitrary relationships to any desired accuracy.

The density results give basic guarantees on the viability of using deep learning for complex tasks. However, quantitative rate estimates for such approximation schemes is much less explored. Here, we focus on the minimal time needed to approximate a given target map. Specifically, for  $\psi \in \text{Diff}(M)$  we define

$$(2.9) \quad \mathbf{C}_{\mathcal{F}}(\psi) := \inf\{T > 0 \mid \psi \in \overline{\mathcal{A}_{\mathcal{F}}(T)}\}.$$

Here,  $\overline{\mathcal{A}_{\mathcal{F}}(T)}$  denotes the closure of  $\mathcal{A}_{\mathcal{F}}(T)$  in the  $C(M, M)$  topology. Thus,  $\mathbf{C}_{\mathcal{F}}(\psi)$  is the minimal time for which the flows-maps generated by (2.4) can approximate  $\psi$  arbitrarily well. In practice, this quantity corresponds to how deep a residual network with layer architecture  $\mathcal{F}$  needs to be to learn a relationship  $\psi$ . We take as our target space the class of diffeomorphisms that are reachable in finite time:

$$(2.10) \quad \mathcal{T} := \{\psi \in \text{Diff}(M) \mid \mathbf{C}_{\mathcal{F}}(\psi) < \infty\}.$$

Our goal is to characterize, or at least provide estimates for,  $\mathbf{C}_{\mathcal{F}}(\psi)$  for  $\psi \in \mathcal{T}$ .

The quantity  $\mathbf{C}_{\mathcal{F}}(\psi)$  serves as a notion of complexity for maps in  $\mathcal{T}$ . Approximation complexity in classical linear approximation theory is typically characterized by certain norms (e.g. Sobolev norms, Besov norms), where closure under linear combinations drives the analysis. In contrast, our hypothesis class  $\mathcal{A}_{\mathcal{F}}$  is generally not closed under linear combinations. Instead, it is closed under compositions. That is, given  $\psi, \xi$  in the class, we typically have  $\psi \circ \xi \in \mathcal{A}_{\mathcal{F}}$ , but not  $\alpha\psi + \beta\xi$  for all  $\alpha, \beta \in \mathbb{R}$ . This leads to fundamentally different approximation mechanisms. For example, the approximation of the identity function is trivial using the hypothesis space of flows/ResNets. However, the difference  $0 = \text{Id} - \text{Id}$  is not easy to uniformly approximate using flows/ResNets, at least in 1D [26]. In other words, the approximation error is not compatible with linear combinations of target functions.

A key observation is that approximation error/complexity should respect the algebraic structure of the hypothesis space. For a linear space  $\mathcal{H}$  closed under linear combinations, one has the triangle inequality

$$(2.11) \quad \inf_{h \in \mathcal{H}} \|h - (\psi + \xi)\| \leq \inf_{h \in \mathcal{H}} \|h - \psi\| + \inf_{h \in \mathcal{H}} \|h - \xi\|.$$

That is, the approximation error of  $\psi + \xi$  is controlled by the sum of the individual errors, compatible with linear structure. In our compositional setting, an analogous triangle inequality holds with respect to composition:

$$(2.12) \quad \mathbf{C}_{\mathcal{F}}(\psi \circ \xi) \leq \mathbf{C}_{\mathcal{F}}(\psi) + \mathbf{C}_{\mathcal{F}}(\xi).$$

In words, the minimal time to approximate  $\psi \circ \xi$  is at most the sum of the times for  $\psi$  and for  $\xi$ .

Here we arrive at an important observation:  $\mathbf{C}_{\mathcal{F}}(\psi)$  *cannot* be any kind of a norm of  $\psi$ , for otherwise the usual triangle inequality would imply the ease of approximation of  $\alpha\psi + \beta\xi$  provided the ease of approximation of  $\psi, \xi$ , which is false. This then hints at the next natural possibility: an appropriate metric satisfying the compositional triangle inequality should describe flow approximation complexity. This turns out to be the correct approach. Concretely, we extend  $\mathbf{C}_{\mathcal{F}}(\cdot)$  to a distance on  $\mathcal{T}$ . For  $\psi_1, \psi_2 \in \mathcal{T}$  define

$$(2.13) \quad d_{\mathcal{F}}(\psi_1, \psi_2) := \inf\{T > 0 \mid \psi_1 \in \overline{\mathcal{A}_{\mathcal{F}}(T) \circ \psi_2}\},$$

that is,  $d_{\mathcal{F}}(\psi_1, \psi_2)$  is the minimal time to connect  $\psi_2$  to  $\psi_1$  up to arbitrary accuracy. Recall that since  $\mathcal{F}$  is symmetric ( $f \in \mathcal{F}$  implies  $-f \in \mathcal{F}$ ),  $d_{\mathcal{F}}$  is a metric on  $\mathcal{T}$ . This metric can also be generalized to any pairs  $\psi_1, \psi_2 \in \text{Diff}(M)$ , by allowing  $d_{\mathcal{F}}(\psi_1, \psi_2)$  to take value  $+\infty$  when  $\psi_1$  is not reachable from  $\psi_2$ . With this metric, we have

$$\mathbf{C}_{\mathcal{F}}(\psi) = d_{\mathcal{F}}(\psi, \text{Id}), \quad \text{where Id is the identity map.}$$

The critical question is then: how does  $\mathcal{F}$  (the complexity of the control family, or in deep learning, the architectural choice of each layer) determine this metric? To answer this question, we develop a geometric viewpoint, where we consider  $\mathcal{T} \subseteq \mathcal{M} \subset \text{Diff}^0(M)$  as a subset of some  $\mathcal{M}$  with Banach manifold structure (e.g.,  $\text{Diff}^{W^{1,\infty}}(M)$  for suitable  $M$ ), and endow  $\mathcal{M}$  with a sub-Finsler structure – a generalisation of a sub-Riemannian structure [44, 1, 3] where a norm on each tangent space replaces the sub-Riemannian inner product. Crucially, as in sub-Riemannian manifolds one can still define a geodesic distance, which we show is exactly  $d_{\mathcal{F}}$ . This geodesic distance is called the Carnot-Carathéodory (CC) distance in the literature of sub-Riemannian geometry. For simplicity, we adopt the name “geodesic distance” in the rest of this paper, keeping in mind that in the most general case this should be understood as the CC distance. Remarkably, the local sub-Finsler norm admits a variational characterization tied to  $\mathcal{F}$ , yielding a new lens on approximation complexity for flow-based models. In the following, for  $s > 0$ , we define

$$(2.14) \quad \mathbf{CH}_s(\mathcal{F}) := \left\{ \sum_{i=1}^N a_i f_i : f_i \in \mathcal{F}, \sum_{i=1}^N |a_i| \leq s \right\}.$$

Then, the key intuition of the sub-Finsler structure is as follows. An infinitesimal change of a map  $\psi$  can be produced by composing it with a short-time flow: for a vector field  $v \in \text{Vec}(M)$  and small  $\varepsilon > 0$ ,

$$(\varphi_v^\varepsilon \circ \psi)(x) = \psi(x) + \varepsilon v(\psi(x)) + o(\varepsilon).$$

Thus the instantaneous velocity at  $\psi$  has the form  $u = v \circ \psi$ . If  $v$  belongs to the  $s$ -scaled convex hull  $\mathbf{CH}_s(\mathcal{F})$ , then (by time-rescaling) this short move can be realised using controls from  $\mathcal{F}$  with time proportional to  $s$ . This motivates measuring the “size” of an infinitesimal velocity  $u$  at  $\psi$  by the smallest such  $s$ :

$$(2.15) \quad \|u\|_\psi = \inf\{s > 0 \mid u \in \overline{\mathbf{CH}_s(\mathcal{F})}^{C^0} \circ \psi\},$$

with the convention  $\|u\|_\psi = +\infty$  when  $u$  is not of the form  $v \circ \psi$ . Here, the closure is taken in the  $C^0(M, \mathbb{R}^d)$  topology. Sections 4.1 and 4.2 provides the rigorous presentation of this notion, where this local quantity is defined intrinsically (as a sub-Finsler fiber norm on  $\mathcal{M}$ ) and proved to be well-posed.

Integrating this local norm along suitable paths in  $\mathcal{M}$  provides computable upper bounds on  $d_{\mathcal{F}}$ , and hence on  $\mathbf{C}_{\mathcal{F}}$ . This result is summarized in the following theorem, which is the main result of this paper. The geometric framework built in the main theorem is also illustrated in the diagram Figure 1.

**Theorem 2.1.** *Suppose  $(\mathcal{M}, \mathcal{F})$  is a compatible pair, as defined in Definition 4.8. Then, the flow-complexity metric  $d_{\mathcal{F}}$  coincides with the geodesic distance induced by the local norm (2.15). In particular, for all  $\psi_1, \psi_2 \in \mathcal{M}$ ,*

$$(2.16) \quad d_{\mathcal{F}}(\psi_1, \psi_2) = \inf \left\{ \int_0^1 \|\dot{\gamma}(t)\|_{\gamma(t)} dt \mid \gamma(0) = \psi_1, \gamma(1) = \psi_2 \right\}.$$

The proof is given in Section 4.2.

**Remark 2.1.** The norm in (2.15) is also called the atomic norm or Minkowski functional of the set  $\mathbf{CH}_s(\mathcal{F}) \circ \psi$ , and is a concept widely applied in convex analysis and inverse problems [7, 32].

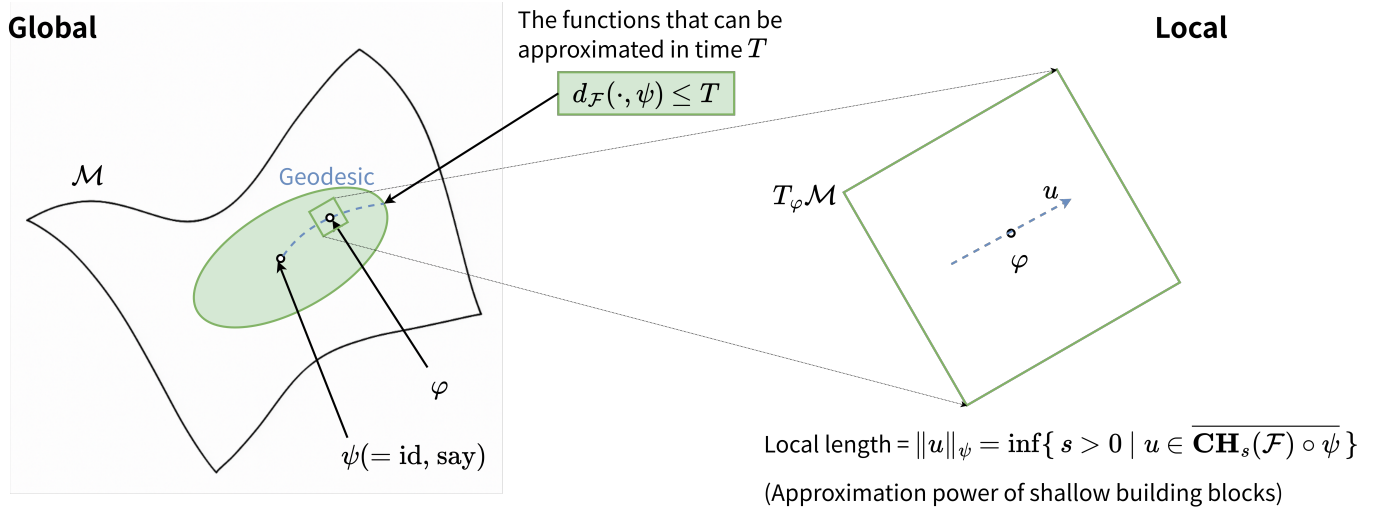


FIGURE 1. Diagram illustrating the connection built in the main result between the approximation complexity by flows and sub-Finsler geometry

The result above establishes a geometric framework for analyzing the complexity  $\mathbf{C}_{\mathcal{F}}(\psi)$  of approximating a target map  $\psi$  by flows of (2.4). Given  $\psi \in \mathcal{M}$ , one can estimate  $\mathbf{C}_{\mathcal{F}}(\psi)$  by constructing a path  $\gamma$  in  $\mathcal{M}$  connecting  $\text{Id}$  to  $\psi$ , and integrating the local norm  $\|\cdot\|_{\gamma(t)}$  along  $\gamma$ . The local norm itself is characterized by a variational principle involving the convex hull of the control family  $\mathcal{F}$ , which relates to the approximation results for shallow neural networks and is relatively well-studied [6, 29, 38, 39].

On the mathematical side, this result gives a quantitative characterization of the rate of approximation of diffeomorphisms by flows, where the vector field at each time is constrained to a family  $\mathcal{F}$ . On the application side, it also addresses, in an idealised setting, a key question of deep learning, namely which target relationships are best learned using deep as opposed to shallow networks. Notably, this has implications in the two approximation problems mentioned in the introduction.

**2.3. Implications for approximation theory and compositional models.** Approximation theory is fundamentally about metrics on functions. One needs a metric to quantify the approximation error (how close an approximant is to a target), and one also needs a notion of complexity of the target relative to a hypothesis class (how hard it is to approximate). A central feature that distinguishes deep neural networks from both shallow networks and classical linear approximation schemes is that complexity is built through function compositions, rather than linear combinations. From this viewpoint, a key question for an approximation theory of deep networks is: how does composition improve approximation, and how should we measure the corresponding complexity in a way that is compatible with composition? Without a good understanding of this question, it is difficult to understand the essential benefits of depth in deep learning.

Our first contribution to this question is the introduction of the distance  $d_{\mathcal{F}}(\cdot, \cdot)$  on the target space  $\mathcal{T}$  as a measure of compositional closeness. As shown in Equation (2.12), the complexity functional  $C_{\mathcal{F}}(\psi) = d_{\mathcal{F}}(\psi, \text{Id})$  satisfies a triangle inequality with respect to composition. This is precisely the compatibility one expects for a compositional hypothesis space: if  $\psi$  can be well-approximated by composing two intermediate maps, then the corresponding complexity should be bounded by the sum of the intermediate complexities.

Moreover, Theorem 2.1 provides a quantitative characterization of  $d_{\mathcal{F}}$  via a sub-Finsler geometry on  $\mathcal{T}$  induced by the layer class  $\mathcal{F}$ . In particular, the local norm at each point  $\psi$  is given by a variational principle involving the (scaled) convex hull of  $\mathcal{F}$ , which is closely related to approximation properties of shallow networks. This turns  $d_{\mathcal{F}}$  from an abstract definition into a quantity that is, at least in principle, computable or estimable: one may identify the target class  $\mathcal{T}$  and derive bounds on  $d_{\mathcal{F}}$  by analyzing the shallow approximation power of  $\mathcal{F}$ .

This framework has several implications for approximation using deep neural networks. Recall that a residual network with depth  $N$  builds an input–output map  $\mathbb{R}^d \rightarrow \mathbb{R}^d$ ,  $x_0 \mapsto x_N$ , via

$$(2.17) \quad x_{k+1} = x_k + \Delta t f_k(x_k), \quad f_k \in \mathcal{F}, \quad k = 0, \dots, N-1,$$

where  $\mathcal{F}$  is the class of transformations realizable by one layer. Letting  $N \rightarrow \infty$  while keeping the total horizon  $T = N\Delta t$  fixed yields the continuous-time idealization

$$(2.18) \quad \dot{x}(t) = f_t(x(t)), \quad f_t \in \mathcal{F}, \quad t \in [0, T],$$

whose flow map  $x(0) \mapsto x(T)$  represents the network input–output relation. In this setting, the horizon  $T$  plays the role of an idealized notion of depth.

The condition  $d_{\mathcal{F}}(\psi, \psi_0) < \infty$  has a direct approximation-theoretic meaning: it asserts that the target map  $\psi$  can be approximated arbitrarily well by composing  $\psi_0$  with a finite-time flow generated by controls in  $\mathcal{F}$ . More precisely,

$$(2.19) \quad d_{\mathcal{F}}(\psi, \psi_0) < \infty \iff \exists T < \infty \text{ such that } \forall \varepsilon > 0, \exists \phi_\varepsilon \in \mathcal{A}_{\mathcal{F}}(T) \text{ with } \|\phi_\varepsilon \circ \psi_0 - \psi\|_{C^0(M)} < \varepsilon.$$

Thus, within the continuous-time idealization, lying in the same  $d_{\mathcal{F}}$ -component is exactly the statement that one can reach (up to arbitrary accuracy) in finite depth by composing layers.

In supervised learning, one often models a target map  $F : K \subset \mathbb{R}^\ell \rightarrow \mathbb{R}^k$  as

$$(2.20) \quad F \approx \beta \circ \psi \circ \alpha,$$

where  $\psi \in \mathcal{A}_{\mathcal{F}}$  is a representation map generated by the deep dynamics, while  $\alpha$  and  $\beta$  belong to comparatively simple input/output classes (e.g. linear maps or shallow readouts). If a representation  $\psi$  that makes (2.20) feasible lies in  $\mathcal{T}$ , then (2.19) guarantees that  $\psi$  can be approximated within finite idealized depth. In particular, applying our framework for higher-dimensional flows, we show in Section 5.2.2 that for the introduced ReLU-based control family considered there, for any compact  $K$  and any sufficiently smooth target  $F$ , there exist linear maps  $\alpha, \beta$  and a horizon  $T > 0$  such that for every  $\varepsilon > 0$  one can find  $\phi_\varepsilon \in \mathcal{A}_{\mathcal{F}}(T)$  satisfying

$$(2.21) \quad \|\beta \circ \phi_\varepsilon \circ \alpha - F\|_{C^0(K)} < \varepsilon.$$

Importantly, the same *uniform* time horizon  $T$  works for arbitrarily small  $\varepsilon$ . This contrasts with approximation results in which the time needed to approximate a general target function may diverge as the required accuracy increases such as in [8, 26]. See Section 5.2.2 for further discussion.

In flow-based generative modelling, given a reference distribution  $\nu$  on  $M$  (a prior) and a target distribution  $\mu$ , one seeks a transport map  $\psi$  such that  $\psi_{\#}\nu = \mu$ . In general there may be infinitely many such maps, but their approximation complexity with respect to the model class  $\mathcal{A}_{\mathcal{F}}$  can be very different. Our framework provides a principled way to compare the complexity of different constructions: one may compare  $d_{\mathcal{F}}(\psi_1, \text{Id})$  and  $d_{\mathcal{F}}(\psi_2, \text{Id})$  for candidate transport maps  $\psi_1, \psi_2$  realizing the same pushforward. This is particularly relevant for flow matching [27], where multiple vector fields (and hence multiple flow maps) can be used to connect a given prior to the same target distribution. The metric  $d_{\mathcal{F}}$  offers a theoretical tool to quantify which constructions are more compatible with the chosen layer class, and therefore potentially easier to approximate in practice.

In the following sections, we demonstrate how to apply this framework to obtain estimates for  $d_{\mathcal{F}}$  through explicit examples. In the one-dimensional case  $M = [0, 1]$ , when  $\mathcal{F}$  is generated by neural

networks with activation  $\text{ReLU}(x) := \max\{0, x\}$ , we can compute  $d_{\mathcal{F}}$  in closed form for any pair of diffeomorphisms  $\psi_1, \psi_2 \in \mathcal{T}$  (see Proposition 3.1):

$$(2.22) \quad d_{\mathcal{F}}(\psi_1, \psi_2) = \|\ln \psi_1' - \ln \psi_2'\|_{\text{TV}([0,1])}.$$

Notice that the right-hand side is not a norm of  $\psi_1 - \psi_2$ , highlighting a fundamental difference from classical linear approximation theory. Furthermore, if we regard  $\psi_1, \psi_2$  as cumulative distribution functions, then the right-hand side coincides with the  $L^1$  distance between their score functions, a quantity frequently appearing in flow-based generative models. We give more details in Section 3 and Section 5.

We also provide a two-dimensional example in Section 5, where  $M = S^1 \subset \mathbb{R}^2$  is the unit circle and the control family is given by a two-dimensional ReLU control family equipped with a layer-normalization-type constraint. In this case, while an exact closed form for  $d_{\mathcal{F}}$  is difficult to obtain, we can still derive explicit estimates for pairs  $\psi_1, \psi_2$  with  $C^3$  regularity.

Moreover, viewing approximation complexity through  $d_{\mathcal{F}}$  suggests a practical guideline for model design. While deep models are often initialized at the identity map  $\text{Id}$ , the metric perspective indicates that the initialization need not be  $\text{Id}$ : the idealized depth required to reach a target  $\psi$  from an initial map  $\psi_0$  is  $d_{\mathcal{F}}(\psi, \psi_0)$ . If domain knowledge can be used to select an initialization  $\psi_0$  lying in the same component as  $\psi$  and closer in  $d_{\mathcal{F}}$ , then the compositional effort needed for approximation can be substantially reduced. This perspective, together with the connected-component obstruction, will be discussed further in Section 5.1.4.

Finally, although our framework is developed for the continuous-time idealization, the key insights also apply to the discrete-time setting. The dynamical formulation preserves the compositional structure of the hypothesis space, which is the key feature of deep neural networks. By applying suitable time-discretization schemes, one can translate estimates for  $d_{\mathcal{F}}$  into corresponding error and complexity bounds for the discrete-time approximation complexity  $\mathbf{C}_{\mathcal{F}}(\psi)$ , which is closer to practical implementations.

### 3. THE RATE OF APPROXIMATION BY FLOWS: ONE DIMENSIONAL RELU NETWORKS

We begin by illustrating the basic ideas and general philosophies of our approach using an example, where the control family is a set of one-dimensional neural network functions with the ReLU activation function. This is a simple case where many computations have closed form. At the same time, it extends the previous investigations of this example in [26]. Here we outline the main findings with the detailed proofs and computations deferred to section 3.1.

Let  $M := [0, 1]$  and consider the following control family in  $\text{Vec}(M)$ :

$$(3.1) \quad \mathcal{F} := \left\{ f(x) = \sum_{i=1}^2 w_i \text{ReLU}(a_i x + b_i) \mid f(0) = f(1) = 0, \sum_{i=1}^2 |w_i a_i| \leq 1 \right\} \subset \text{Vec}(M),$$

which is the set of shallow neural networks with bounded weights sum and fixed values at 0 and 1, with the activation function  $\text{ReLU}(x) := \max\{0, x\}$ . In the language of machine learning, each layer in this deep ResNet consists of a width-2 ReLU-activated fully connected neural network, operating in one hidden dimension. Observe that for  $f \in \mathcal{F}$ , its flow map  $\varphi_t^f$  has the following property:

$\varphi_t^f$  is an increasing function from  $[0, 1]$  to  $[0, 1]$  with  $\varphi_t^f(0) = 0$  and  $\varphi_t^f(1) = 1$ .

Now, we introduce our target function space as in (2.10), i.e. the set of all functions that can be uniformly approximated by the flow maps in  $\mathcal{A}_{\mathcal{F}}$  within finite time. In this example, we have a clearer description of the target function space: any function in  $\mathcal{M}$  is a non-decreasing function from  $[0, 1]$  to  $[0, 1]$  with fixed endpoints 0 and 1.

We are then interested in characterizing the complexity measure  $\mathbf{C}_{\mathcal{F}}(\psi)$  for  $\psi \in \mathcal{M}$ , as well as a closed-form characterization of  $\mathcal{M}$ . In [26], an estimation of  $\mathbf{C}_{\mathcal{F}}(\psi)$  is provided as following:

**Proposition 3.1** (Proposition 4.8 in [26]). *If  $\psi$  is a piece-wise smooth increasing function with  $\psi(0) = 0$ ,  $\psi(1) = 1$ , and  $\|\ln \psi'\|_{\text{TV}([0,1])} < \infty$ , then  $\psi \in \mathcal{M}$ . In particular,*

$$(3.2) \quad \mathbf{C}_{\mathcal{F}}(\psi) \leq \|\ln \psi'\|_{\text{TV}([0,1])} + |\ln \psi'(0)| + |\ln \psi'(1)|.$$

Here,  $\|\cdot\|_{\text{TV}([0,1])}$  denotes the total variation of a function on  $[0, 1]$ , defined as

$$(3.3) \quad \|g\|_{\text{TV}([0,1])} := \sup \left\{ \sum_{i=1}^{n-1} |g(x_{i+1}) - g(x_i)| \mid n \in \mathbb{N}, 0 \leq x_1 < x_2 < \dots < x_n \leq 1 \right\}.$$

Proposition 3.1 provides an upper bound of the complexity measure  $\mathbf{C}_{\mathcal{F}}(\psi)$  using a constructive approach [26], but it was not shown there whether this bound is tight, or if an exact formula for  $\mathbf{C}_{\mathcal{F}}(\psi)$  can be obtained.

A key observation is that  $\mathcal{M}$  is closed under function composition. That is, for any  $\psi_1, \psi_2 \in \mathcal{M}$ , we have  $\psi_1 \circ \psi_2 \in \mathcal{M}$ . This inherent algebraic structure parallels the linear structure in classical approximation theory, and thus motivates us to consider the compatibility of the complexity measure  $\mathbf{C}_{\mathcal{F}}(\psi)$  with respect to function composition. Specifically, for any  $\psi_1, \psi_2 \in \mathcal{M}$ , we expect the compositional triangle inequality in (2.12) to hold. From a dynamical system perspective, the complexity  $\mathbf{C}_{\mathcal{F}}(\psi)$  can be interpreted as the minimal time needed to steer the system from the identity map  $\text{Id}$  to the target function  $\psi$  using the ReLU control family (3.1). With this interpretation, the compositional triangle inequality in (2.12) can be understood as follows: to reach  $\psi_1 \circ \psi_2$  from  $\text{Id}$ , one can first reach  $\psi_2$  from  $\text{Id}$ , and then reach  $\psi_1 \circ \psi_2$  from  $\psi_2$ . The total time taken is the sum of the two individual times, which gives an upper bound for  $\mathbf{C}_{\mathcal{F}}(\psi_1 \circ \psi_2)$ .

This observation indicates that  $\mathbf{C}_{\mathcal{F}}(\psi)$  should be considered in a pairwise manner, rather than individually for each  $\psi$ . In other words, instead of focusing solely on the complexity of reaching a single target function from the identity, we should investigate the complexity of transitioning between any two target functions in  $\mathcal{M}$ , leading to the definition of a distance function on  $\mathcal{M}$ :

$$(3.4) \quad d_{\mathcal{F}}(\psi_1, \psi_2) := \inf \{ T > 0 \mid \psi_1 \in \overline{\mathcal{A}_{\mathcal{F}}(T) \circ \psi_2} \}.$$

Here

$$\overline{\mathcal{A}_{\mathcal{F}}(T) \circ \psi_2} := \{ \xi \in C([0, 1]) \mid \inf_{\phi \in \mathcal{A}_{\mathcal{F}}(T)} \|\xi - \phi \circ \psi_2\|_{C([0,1])} = 0 \}.$$

We can easily verify that  $d_{\mathcal{F}}(\cdot, \cdot)$  is indeed a metric on  $\mathcal{M}$ , i.e. it is positive definite, symmetric, and satisfies the triangle inequality. Furthermore, for any  $\psi_1, \psi_2 \in \mathcal{M}$ , it can be directly checked that:

$$(3.5) \quad \mathbf{C}_{\mathcal{F}}(f_2 \circ f_1) = d_{\mathcal{F}}(f_2 \circ f_1, \text{Id}) \leq d_{\mathcal{F}}(f_2 \circ f_1, f_1) + d_{\mathcal{F}}(f_1, \text{Id}) = \mathbf{C}_{\mathcal{F}}(f_2) + \mathbf{C}_{\mathcal{F}}(f_1),$$

which is the triangular inequality with respect to function compositions. With this additional structure identified,  $\mathcal{M}$  is not only a set of functions, but also a metric space equipped with the metric  $d_{\mathcal{F}}(\cdot, \cdot)$  that is compatible with function compositions, an inherent algebraic structure of  $\mathcal{M}$ .

The next question is then: how does this metric depend on the control family  $\mathcal{F}$ ? Unravelling this relation is crucial for understanding what maps on the unit interval are more amenable to approximation with a moderate time horizon.

We begin with a simple case by fixing a function  $\psi \in \mathcal{M}$  and considering another function  $\xi \in \mathcal{M}$  that is very close to  $\psi$  in the metric  $d_{\mathcal{F}}$ . How can we connect  $\psi$  and  $\xi$  with a flow? For a very small scale  $\tau > 0$  and  $\alpha_1, \dots, \alpha_n > 0$ , consider the flow map:

$$(3.6) \quad \varphi_{f_n}^{\alpha_n \tau} \circ \dots \circ \varphi_{f_1}^{\alpha_1 \tau} \in \mathcal{A}_{\mathcal{F}}, \text{ with } f_i \in \mathcal{F},$$

which admits the first-order approximation:

$$(3.7) \quad \varphi_{f_n}^{\alpha_n \tau} \circ \dots \circ \varphi_{f_1}^{\alpha_1 \tau}(x) = x + \tau \sum_{i=1}^n \alpha_i f_i(x) + o(\tau).$$

Therefore, the corresponding function in  $\mathcal{A}_{\mathcal{F}} \circ \psi$  is close to

$$(3.8) \quad \psi + \tau \sum_{i=1}^n \alpha_i f_i \circ \psi + o(\tau).$$

If  $u := \frac{\xi - \psi}{\tau}$  is close to  $\sum_{i=1}^n \alpha_i f_i \circ \psi$  for some  $f_i \in \mathcal{F}$  and  $\alpha_i > 0$ , then the map  $\xi = \psi + \tau u$  is approximately reachable from  $\psi$  within time  $\tau \sum_{i=1}^n \alpha_i$ . Therefore, given a perturbation function  $u$  and small  $t > 0$ , the distance  $d_{\mathcal{F}}(\psi, \psi + \tau u)$  is approximately given by the product of  $\tau$  and the minimal weight sum needed to approximate  $u$  using functions in  $\mathcal{F}$  composed with  $\xi$ . For  $s > 0$ , if we define

$$(3.9) \quad \mathbf{CH}_s(\mathcal{F}) := \left\{ \sum_{i=1}^n \alpha_i f_i \mid f_i \in \mathcal{F}, \alpha_i \geq 0, \sum_{i=1}^n \alpha_i \leq s \right\}$$

as the  $s$ -scaled convex hull of  $\mathcal{F}$  in  $\text{Vec}(M)$ . Then, the local norm

$$(3.10) \quad \|u\|_{\psi} := \inf \{ s > 0 \mid u \in \overline{\mathbf{CH}_s(\mathcal{F})}^{C^0} \circ \psi \},$$

represents the minimal weight sum needed to approximate  $u$  using functions in  $\mathcal{F}$  composed with  $\psi$ .

Then, based the above local analysis, for a perturbation function  $u$  and small  $\tau > 0$ , the function  $\psi + \tau u$  is approximately reachable from  $\psi$  within time  $\tau \|u\|_{\psi}$ .

In the one-dimensional ReLU example, we can explicitly compute  $\|\cdot\|_{\psi}$  by investigating the corresponding variational problem in (3.10), which is essentially a spline approximation problem. Here, we introduce the space  $\text{BV}^2([0, 1])$  defined as:

$$(3.11) \quad \text{BV}^2([0, 1]) := \{u \in C([0, 1]) \mid u' \text{ exists a.e., and } u' \in \text{BV}([0, 1])\}.$$

We consider the perturbation  $u$  to be in the space  $\text{BV}^2([0, 1])$  and with zero boundary conditions, defined as:

$$(3.12) \quad \text{BV}_0^2([0, 1]) := \{u \in \text{BV}^2([0, 1]) \mid u(0) = u(1) = 0\}.$$

**Proposition 3.2.** *For  $u \in \text{BV}_0^2([0, 1])$  and  $\psi \in \mathcal{M}$ , the following identity holds*

$$(3.13) \quad \|u\|_{\psi} = \inf \{ s > 0 \mid u \in \overline{\mathbf{CH}_s(\mathcal{F})}^{C^0} \circ \psi \} = \left\| \frac{u'}{\psi'} \right\|_{\text{TV}_{[0,1]}}.$$

With this local picture, we can imagine computing the global distance  $d_{\mathcal{F}}(\cdot, \cdot)$  by summing up the local costs along a path connecting two target functions. Specifically, consider  $\psi_1, \psi_2 \in \mathcal{M}$ , we can consider a sequence of intermediate functions  $\xi_0 = \psi_1, \xi_1, \dots, \xi_n = \psi_2$  in  $\mathcal{M}$ , such that each pair  $\xi_i, \xi_{i+1}$  are very close to each other, i.e.  $d_{\mathcal{F}}(\xi_i, \xi_{i+1})$  is very small. The distance  $d_{\mathcal{F}}(\psi_1, \psi_2)$  is then bounded by:

$$(3.14) \quad d_{\mathcal{F}}(\psi_1, \psi_2) \leq \sum_{i=0}^{n-1} d_{\mathcal{F}}(\xi_i, \xi_{i+1}) \approx \sum_{i=0}^{n-1} \|\xi_{i+1} - \xi_i\|_{\xi_i}.$$

Taking the limit as the partition gets finer, we arrive at the integral form:

$$(3.15) \quad d_{\mathcal{F}}(\psi_1, \psi_2) \leq \int_0^1 \left\| \frac{d}{dt} \gamma(t) \right\|_{\gamma(t)} dt$$

for any piece-wise smooth path  $\gamma : [0, 1] \rightarrow \mathcal{M}$  with  $\gamma(0) = \psi_1$  and  $\gamma(1) = \psi_2$ . By taking the infimum over all such paths, we obtain a characterization of  $d_{\mathcal{F}}(\cdot, \cdot)$  as the shortest length of the path connecting two points under the local norm  $\|\cdot\|_{\cdot}$ :

$$(3.16) \quad d_{\mathcal{F}}(\psi_1, \psi_2) = \inf \left\{ \int_0^1 \left\| \frac{d}{dt} \gamma(t) \right\|_{\gamma(t)} dt \mid \gamma : [0, 1] \rightarrow \mathcal{M} \text{ is piece-wise smooth, } \gamma(0) = \psi_1, \gamma(1) = \psi_2 \right\}.$$

The smoothness of the path  $\gamma$  depends on the manifold structure of  $\mathcal{M}$ , which will be rigorously introduced in the next section. With this characterization and the explicit form of the local norm  $\|\cdot\|_\psi$ , we can explicitly derive a path that minimizing the distance integral between any two functions  $\psi, \xi$  in  $\mathcal{M}$  (derived in (3.92)):

$$(3.17) \quad \tilde{\gamma}_t(x) = \frac{\int_0^x (\psi'_1(x))^{1-t} (\psi'_2(x))^t dx}{\int_0^1 (\psi'_1(x))^{1-t} (\psi'_2(x))^t dx}.$$

Finally, integrating the local norm along this path, we can derive a closed form expression of the distance  $d_{\mathcal{F}}(\cdot, \cdot)$ , and an explicit characterization of the manifold  $\mathcal{T}$ . Summarizing the results, we have:

**Theorem 3.1.**  $\mathcal{T}$  is characterized as:

$$(3.18) \quad \mathcal{T} = \{\psi \in \text{BV}^2([0, 1]) \mid \psi(0) = 0, \psi_1 = 1, \psi' \geq c > 0 \text{ a.e. for some } c\}.$$

For any  $\psi_1, \psi_2 \in \mathcal{T}$ , we have

$$(3.19) \quad d_{\mathcal{F}}(\psi_1, \psi_2) = \|\ln \psi'_1 - \ln \psi'_2\|_{\text{TV}([0,1])}$$

As a corollary, the complexity measure  $\mathbf{C}_{\mathcal{F}}(\psi)$  for any  $\psi \in \mathcal{T}$  is given by

$$(3.20) \quad \mathbf{C}_{\mathcal{F}}(\psi) = d_{\mathcal{F}}(\psi, \text{Id}) = \|\ln \psi'\|_{\text{TV}([0,1])}.$$

Compared with the estimation in Proposition 3.1 [26], Theorem 3.1 not only sharpens the upper bound, but also provides an exact characterization of the complexity measure  $\mathbf{C}_{\mathcal{F}}(\psi)$  for all  $\psi \in \mathcal{T}$ . Moreover, we also have a closed-form characterization of the target function space  $\mathcal{T}$ . These improvements are achieved by the extension of  $\mathbf{C}_{\mathcal{F}}(\cdot)$  to the distance function  $d_{\mathcal{F}}(\cdot, \cdot)$ , and the variational relationship between the local norm  $\|\cdot\|_\psi$  and the global distance  $d_{\mathcal{F}}(\cdot, \cdot)$  given in Equation (3.16). The local norm  $\|\cdot\|_\psi$  connects the distance  $d_{\mathcal{F}}(\cdot, \cdot)$  to the control family  $\mathcal{F}$  through the variational problem in Proposition 3.2, turning the difficult problem of computing the minimal time-horizon to an optimization problem over paths, which in this case is completely solvable. This analysis paves way for the general theory we will present in the next section.

**3.1. Proofs of the results for 1D ReLU control family.** We provide the proofs and computations behind the results stated in Section 3. The rigorous statement and proofs of the connections between the global distance  $d_{\mathcal{F}}(\cdot, \cdot)$ , the local norm  $\|\cdot\|_{\mathcal{F}}$ , together with the variational characterization ((3.2) and (3.19)) are deferred to Section 4.2, where the results are proved in a more general setting. Here, we only focus on the computations of the closed-form formulae relevant for the 1D ReLU control family.

**3.1.1. Proof of Proposition 3.2.** We first give the sketch of the proof of Proposition 3.2, and then provide the detailed computations. The proof is separated into the following steps:

- **Step 1:** We first consider the special case where  $\psi$  is the identity mapping on  $[0, 1]$ , and prove that

$$(3.21) \quad \|u'\|_{\text{TV}[0,1]} \geq \inf\{s > 0 \mid u \in \overline{\mathbf{CH}_s(\mathcal{F})}^{C^0} \circ \psi\}$$

for any  $u \in \text{BV}_0^2([0, 1])$ . This is done by first considering a discrete version with interpolation on equally distributed points. We study the weight  $\ell^1$  minimization problem defined by (3.24) and (3.25), and provide an exact formula for the minimum value of  $S_N(w, v)$  in Proposition 3.3. This provides a way of constructing the approximation  $\tilde{u}_N$  with controlled  $\ell^1$  norm. Then, we take the limit  $N \rightarrow \infty$  to obtain the desired inequality.

- **Step 2:** Next, we prove the reverse inequality

$$(3.22) \quad \|u'\|_{\text{TV}[0,1]} \leq \inf\{s > 0 \mid u \in \overline{\mathbf{CH}_s(\mathcal{F})}^{C^0} \circ \psi\}$$

in Proposition 3.5. This is proved by contradiction. Assume the opposite inequality holds, then one can construct an interpolation scheme with controlled  $\ell^1$  norm, which contradicts the exact formula in Proposition 3.3.

• **Step 3:** Finally, we extend the result to general  $\psi \in \mathcal{M}$  by a change of variable.

We now provide details for Step 1, assuming that  $\psi$  is the identity mapping  $[0, 1] \rightarrow [0, 1]$ . We consider a discrete version with interpolation on equally distributed points. Specifically, for a given positive integer  $N$ , we consider a shallow network with an additional constant bias term  $C_N$ :

$$(3.23) \quad \tilde{u}_N(x) := \sum_{i=0}^N \left( w_i \sigma\left(x - \frac{i}{N}\right) + v_i \sigma\left(\frac{i}{N} - x\right) \right) + C_N,$$

where  $\sigma(x) = \max\{0, x\}$  is the ReLU activation function,  $w_i, v_i$  and  $C_N$  are parameters to be determined later.

We study the following  $\ell^1$  minimization problem with interpolation constraints:

$$(3.24) \quad \min S_N(w, v) := \sum_{i=0}^N |w_i| + |v_i|,$$

$$(3.25) \quad \text{s.t. } \tilde{u}_N\left(\frac{i}{N}\right) = u\left(\frac{i}{N}\right), \quad i = 0, 1, \dots, N.$$

among all possible choices of  $\tilde{u}_N$ .

Let  $\text{dist}(x, A)$  be the distance between a point  $x$  and a set (interval)  $A$ . The following lemma is useful in the following argument.

**Lemma 3.1.** *The following results hold:*

$$(3.26) \quad |a - b| + |b| = |a| + 2 \text{dist}(b, [\min\{a, 0\}, \max\{a, 0\}]) \text{ for any } a, b \in \mathbb{R},$$

and

$$(3.27) \quad \text{dist}\left(\sum_{i=1}^n a_i, \sum_{i=1}^n A_i\right) \leq \sum_{i=1}^n \text{dist}(a_i, A_i) \text{ for any } a_i \in \mathbb{R}, \text{ and } A_i \subset \mathbb{R},$$

where the sum of the intervals is the Minkowski addition.

Moreover, if each  $A_i$  is a closed interval  $A_i = [\ell_i, r_i]$ , then equality holds in (3.27) whenever one of the following happens:

$$(i) \ a_i \in [\ell_i, r_i] \text{ for all } i, \quad (ii) \ a_i \leq \ell_i \text{ for all } i, \quad (iii) \ a_i \geq r_i \text{ for all } i.$$

*Proof.* We first prove (3.26). By symmetry it suffices to treat  $a \geq 0$ , so the interval is  $[0, a]$ .

• If  $b \in [0, a]$ , then

$$|a - b| + |b| = (a - b) + b = a = |a|, \quad \text{dist}(b, [0, a]) = 0.$$

• If  $b < 0$ , then

$$|a - b| + |b| = (a - b) + (-b) = a - 2b = a + 2(-b) = |a| + 2 \text{dist}(b, [0, a]).$$

• If  $b > a$ , then

$$|a - b| + |b| = (b - a) + b = 2b - a = a + 2(b - a) = |a| + 2 \text{dist}(b, [0, a]).$$

This proves (3.26).

Now we prove (3.27). Fix  $\varepsilon > 0$ . For each  $i$ , choose  $x_i \in A_i$  such that  $|a_i - x_i| \leq \text{dist}(a_i, A_i) + \varepsilon/n$ . Then  $x := \sum_{i=1}^n x_i \in \sum_{i=1}^n A_i$ , hence

$$(3.28) \quad \text{dist}\left(\sum_{i=1}^n a_i, \sum_{i=1}^n A_i\right) \leq \left| \sum_{i=1}^n a_i - x \right| = \left| \sum_{i=1}^n (a_i - x_i) \right| \leq \sum_{i=1}^n |a_i - x_i| \leq \sum_{i=1}^n \text{dist}(a_i, A_i) + \varepsilon.$$

Letting  $\varepsilon \rightarrow 0$  yields (3.27).

Finally, we prove the equality conditions. Assume  $A_i = [\ell_i, r_i]$ . Then  $\sum_i A_i = [\sum_i \ell_i, \sum_i r_i]$ . If (i) holds, then  $\sum_i a_i \in \sum_i A_i$ , so both sides are 0. If (ii) holds, then  $\text{dist}(a_i, A_i) = \ell_i - a_i$  and

$$(3.29) \quad \text{dist}\left(\sum_i a_i, \sum_i A_i\right) = \left(\sum_i \ell_i\right) - \left(\sum_i a_i\right) = \sum_i (\ell_i - a_i) = \sum_i \text{dist}(a_i, A_i).$$

Case (iii) is similar. □

The following proposition provides the exact solution of  $S_N(w, v)$  for the  $\ell_1$  minimization problem with interpolation constraints.

**Proposition 3.3.** *Let*

$$(3.30) \quad k_i = N\Delta^2 u\left(\frac{i}{N}\right) := N\left(u\left(\frac{i+1}{N}\right) - 2u\left(\frac{i}{N}\right) + u\left(\frac{i-1}{N}\right)\right), \quad i = 1, \dots, N-1,$$

and

$$(3.31) \quad K_+ = \sum_{i=1}^{N-1} \max\{k_i, 0\}, \quad K_- = \sum_{i=1}^{N-1} \min\{k_i, 0\}.$$

Then, we have

$$(3.32) \quad \min S_N(w, v) = \sum_{i=1}^{N-1} |k_i| + \text{dist}\left(-N\left(u\left(\frac{1}{N}\right) - u(0)\right), [K_-, K_+]\right).$$

*Proof.* First, notice that the terms  $w_N\sigma(x-1)$  and  $v_0\sigma(x)$  do not contribute to the interpolation, and thus  $w_N$  and  $v_0$  must be zero in an optimal  $\tilde{u}_N$ . Now, take  $x = 0, \frac{1}{N}, \dots, 1$ , by the interpolation condition (3.25), we have:

$$(3.33) \quad \frac{1}{N}\left(\sum_{i=j+1}^N iv_i + \sum_{i=0}^{j-1} (j-i)w_i\right) = u\left(\frac{j}{N}\right) - C_N, \quad j = 0, 1, \dots, N.$$

Here the summation is zero if the index is out of range. Now, we denote  $\tilde{k}_i = w_i + v_i$  for  $i = 0, \dots, N$ . By taking the second order difference, it follows that the conditions in (3.33) are equivalent to:

$$(3.34) \quad \tilde{k}_0 = N\left(u\left(\frac{1}{N}\right) - u(0)\right) + \sum_{i=1}^N v_i, \quad \tilde{k}_i = k_i, \quad i = 1, \dots, N-1,$$

and

$$(3.35) \quad \sum_{i=1}^N iv_i = u(0) - C_N.$$

Since  $C_N$  is a free variable, we can consider the problem without restriction (3.35). Therefore, we have:

$$(3.36) \quad \begin{aligned} S_N(w, v) &= \sum_{i=1}^{N-1} (|k_i - v_i| + |v_i|) + \left| N\left(u\left(\frac{1}{N}\right) - u(0)\right) + \sum_{i=1}^N v_i \right| + |v_N| \\ &\geq \sum_{i=1}^{N-1} (|k_i - v_i| + |v_i|) + \left| N\left(u\left(\frac{1}{N}\right) - u(0)\right) + \sum_{i=1}^{N-1} v_i \right|. \end{aligned}$$

Here, we use the inequality that  $|a + b| + |b| \geq |a|$  for any  $a, b \in \mathbb{R}$ . Continuing with (3.36), we have:

$$\begin{aligned}
(3.37) \quad S_N(w, v) &\geq \sum_{i=1}^{N-1} (|k_i - v_i| + |v_i|) + \left| N(u(\frac{1}{N}) - u(0)) + \sum_{i=1}^{N-1} v_i \right| \\
&= \sum_{i=1}^{N-1} |k_i| + 2 \sum_{i=1}^{N-1} \text{dist}(v_i, [\min\{k_i, 0\}, \max\{k_i, 0\}]) + \left| N(u(\frac{1}{N}) - u(0)) + \sum_{i=1}^{N-1} v_i \right| \\
&\geq \sum_{i=1}^{N-1} |k_i| + 2 \text{dist}\left(\sum_{i=1}^{N-1} v_i, \sum_{i=1}^{N-1} [\min\{k_i, 0\}, \max\{k_i, 0\}]\right) + \left| N(u(\frac{1}{N}) - u(0)) + \sum_{i=1}^{N-1} v_i \right| \\
&= \sum_{i=1}^{N-1} |k_i| + 2 \text{dist}\left(\sum_{i=1}^{N-1} v_i, [K_-, K_+]\right) + \left| N(u(\frac{1}{N}) - u(0)) + \sum_{i=1}^{N-1} v_i \right|,
\end{aligned}$$

where the second line uses (3.26), and the third line uses (3.27).

Let us denote  $V = \sum_{i=1}^{N-1} v_i$ . Then, it can be readily checked that the minimum of  $2 \text{dist}(V, [K_-, K_+]) + |N(u(\frac{1}{N}) - u(0)) + V|$  can be achieved at

$$(3.38) \quad V = \begin{cases} -N(u(\frac{1}{N}) - u(0)), & \text{if } -N(u(\frac{1}{N}) - u(0)) \in [K_-, K_+] \\ K_-, & \text{if } -N(u(\frac{1}{N}) - u(0)) < K_-, \\ K_+, & \text{if } -N(u(\frac{1}{N}) - u(0)) > K_+. \end{cases}$$

The minimum then can be calculated as  $\text{dist}(-N(u(\frac{1}{N}) - u(0)), [K_-, K_+])$ . Therefore, we have

$$(3.39) \quad S_N(w, v) \geq \sum_{i=1}^{N-1} |k_i| + \text{dist}(-N(u(\frac{1}{N}) - u(0)), [K_-, K_+]).$$

Moreover, this value can be achieved by taking  $v_N = 0$ , and for  $i < N$  we choose  $v_i$  in  $[\min\{k_i, 0\}, \max\{k_i, 0\}]$ , and  $\sum_{i=1}^{N-1} v_i = V$  to minimize the last equation in (3.37). The value of  $C_N$  is now given by:

$$(3.40) \quad C_N = u(0) - \frac{1}{N} \sum_{i=1}^N i v_i.$$

□

By taking a continuous limit on (3.32), we are ready to show the upper bound. The following lemma for the limit of second order difference of  $u \in \text{BV}^2([0, 1])$  is useful.

**Lemma 3.2.** *For any  $u \in \text{BV}^2([0, 1])$ , we have*

$$(3.41) \quad \lim_{N \rightarrow \infty} \sum_{i=1}^{N-1} |k_i| = \|u'\|_{\text{TV}[0,1]}.$$

*Proof.* Set

$$(3.42) \quad \delta_k := N(u(x_k) - u(x_{k-1})) = N \int_{x_{k-1}}^{x_k} g(x), dx, \quad k = 1, \dots, N.$$

Then

$$(3.43) \quad N(u(x_{k+1}) - 2u(x_k) + u(x_{k-1})) = \delta_{k+1} - \delta_k, \quad \text{so} \quad S_N = \sum_{k=1}^{N-1} |\delta_{k+1} - \delta_k|$$

Let  $\mathcal{A}_N$  be the set of continuous, piecewise linear  $\phi : [0, 1] \rightarrow \mathbb{R}$  with nodes  $\{x_k\}$ ,  $\phi(0) = \phi(1) = 0$ , and  $|\phi|_\infty \leq 1$ . On each  $[x_{k-1}, x_k]$  we have  $\phi'(x) = N(\phi(x_k) - \phi(x_{k-1})) =: N\Delta\phi_k$ , hence

$$(3.44) \quad \int_0^1 g\phi' = \sum_{k=1}^N N\Delta\phi_k \int_{x_{k-1}}^{x_k} g = \sum_{k=1}^N \delta_k \Delta\phi_k = - \sum_{k=1}^{N-1} (\delta_{k+1} - \delta_k)\phi(x_k).$$

Therefore,

$$(3.45) \quad \left| \int_0^1 g\phi' \right| \leq \sum_{k=1}^{N-1} |\delta_{k+1} - \delta_k| |\phi(x_k)| \leq S_N.$$

Choosing  $\phi \in \mathcal{A}_N$  with  $\phi(x_k) = \text{sgn}(\delta_{k+1} - \delta_k)$  (and linear interpolation with  $\phi(0) = \phi(1) = 0$ ) gives equality, hence

$$(3.46) \quad S_N = \sup_{\phi \in \mathcal{A}_N} \int_0^1 g\phi' dx$$

Using the dual representation of total variation,

$$(3.47) \quad \|g\|_{\text{TV}([0,1])} = \sup \left\{ \int_0^1 g\varphi' : \varphi \in C_0^1((0,1)), \|\varphi\|_\infty \leq 1 \right\},$$

and the inclusion  $\mathcal{A}_N \subset \{\varphi : \|\varphi\|_\infty \leq 1, \varphi(0) = \varphi(1) = 0, \varphi \text{ Lipschitz}\}$ , we have:

$$(3.48) \quad \limsup_{N \rightarrow \infty} S_N \leq \|g\|_{\text{TV}([0,1])}.$$

For any  $\psi \in C_0^1((0,1))$  with  $|\psi|_\infty \leq 1$ , let  $\phi_N \in \mathcal{A}_N$  be the piecewise linear interpolant of  $\psi$  on  $\{x_k\}$ . Then  $\phi_N \rightarrow \psi$  in  $W^{1,1}$ , hence

$$(3.49) \quad \int_0^1 g\phi_N' \rightarrow \int_0^1 g\psi'.$$

Therefore,  $S_N \geq \int_0^1 g\phi_N'$ . Taking  $\liminf$  and then the supremum over such  $\psi$  yields

$$(3.50) \quad \liminf_{N \rightarrow \infty} S_N \geq \|g\|_{\text{TV}([0,1])}.$$

Combining the two bounds gives  $S_N \rightarrow \|g\|_{\text{TV}([0,1])}$ .  $\square$

Combining Proposition 3.3 and Lemma 3.2, we can conclude Step 1 with the following upper bound.

**Proposition 3.4.** *For  $u \in \text{BV}_0^2([0,1])$ , the following identity holds*

$$(3.51) \quad \inf \{s \mid u \in \overline{\mathbf{CH}_s(\mathcal{F})}^{C^0}\} \leq \|u'\|_{\text{TV}[0,1]}$$

*Proof.* From (3.32), the assumption that  $u \in \text{BV}_0^2([0,1])$  and Lemma 3.2, we have

$$(3.52) \quad \lim_{N \rightarrow \infty} S_N(w, v) = \|u'\|_{\text{TV}[0,1]} + \text{dist} \left( -u'(0), \left[ \int_{[0,1]} \min\{u''(x), 0\} dx, \int_{[0,1]} \max\{u''(x), 0\} dx \right] \right).$$

Note that:

$$(3.53) \quad u'(0) - u'(1) = \int_{[0,1]} \min\{u''(x), 0\} dx + \int_{[0,1]} \max\{u''(x), 0\} dx,$$

the right hand side of equation (3.52) can be rewritten in a symmetric form:

$$(3.54) \quad \|u'\|_{\text{TV}[0,1]} + \frac{1}{2} \max\{|u'(0) + u'(1)| - \|u'\|_{\text{TV}[0,1]}, 0\}.$$

According to the following lemma, we have that

$$(3.55) \quad \lim_{N \rightarrow \infty} S_N(w, v) = \|u'\|_{\text{TV}[0,1]}.$$

**Lemma 3.3.** For  $u \in \text{BV}_0^2([0, 1])$ , we have  $|u'(0) + u'(1)| \leq \|u'\|_{\text{TV}[0,1]}$ .

*Proof of the lemma.* Since  $u \in \text{BV}_0^2([0, 1])$ , we have  $u' \in \text{BV}([0, 1]) \subset L^1(0, 1)$  and  $u$  is absolutely continuous with

$$(3.56) \quad u(1) - u(0) = \int_0^1 u'(s) ds = 0.$$

If  $u'(1) = 0$ , then

$$(3.57) \quad |u'(0) + u'(1)| = |u'(0) - u'(1)| \leq \|u'\|_{\text{TV}[0,1]}.$$

Assume now  $u'(1) > 0$  (the case  $u'(1) < 0$  is analogous). From  $\int_0^1 u' = 0$  it follows that  $u'$  cannot be nonnegative a.e. unless  $u' = 0$  a.e.; hence there exists  $t \in (0, 1)$  such that  $u'(t)$  exists and  $u'(t) \leq 0$ . Then  $u'(t)u'(1) \leq 0$ , so

$$(3.58) \quad |u'(t) + u'(1)| = ||u'(1)| - |u'(t)|| \leq |u'(1)| + |u'(t)| = |u'(1) - u'(t)|.$$

Therefore,

$$(3.59) \quad \begin{aligned} |u'(0) + u'(1)| &\leq |u'(0) - u'(t)| + |u'(t) + u'(1)| \\ &\leq |u'(0) - u'(t)| + |u'(1) - u'(t)| \\ &\leq \|u'\|_{\text{TV}[0,1]}, \end{aligned}$$

where the last inequality follows from the definition of total variation by taking the partition  $\{0, t, 1\}$ :  $\|u'\|_{\text{TV}[0,1]} \geq |u'(t) - u'(0)| + |u'(1) - u'(t)|$ .  $\square$

Here,  $u'(0)$  and  $u'(1)$  are the one-sided limits of  $u'$  at the endpoints, which is well-defined since  $u \in \text{BV}_0^2([0, 1])$ .

For each fixed finite  $N$ , we define a function:

$$(3.60) \quad \bar{u}_N := \tilde{u}_N - C_N + \frac{1}{N}\sigma(x + NC_N).$$

where  $C_N$  is the value of the constant term in the previous proof. It is then clear that  $\bar{u}_N$  is in  $\text{Span } \mathcal{F}$ . It follows that

$$(3.61) \quad |\bar{u}_N - \tilde{u}_N|_{C([0,1])} \leq \frac{1}{N}.$$

Also, we have that the sum of weights in  $\bar{u}_N$  is no more than  $\min S_N(w, v) + \frac{1}{N}$ . Notice that  $\tilde{u}_N$  is a piecewise linear interpolant of  $u$ . Since  $u \in \text{BV}_0^2([0, 1])$ , when  $N \rightarrow \infty$  we obtain  $\bar{u}_N \rightarrow u$ . This implies

$$(3.62) \quad \begin{aligned} \inf\{s \mid u \in \overline{\text{CH}_s(\mathcal{F})}^{C^0}\} &\leq \lim_{N \rightarrow \infty} \left( \min S_N(w, v) + \frac{1}{N} \right) \\ &= \|u'\|_{\text{TV}[0,1]} + \frac{1}{2} \max\{|u'(0) + u'(1)| - \|u'\|_{\text{TV}[0,1]}, 0\} \\ &= \|u'\|_{\text{TV}[0,1]}. \end{aligned}$$

The last equality uses the following fact: that  $\square$

Now, we provide the details for Step 2, i.e., we show the cost function (defined as the right-hand side of (3.62)) is also the lower bound.

**Proposition 3.5.** For  $u \in \text{BV}_0^2([0, 1])$ , the following identity holds

$$(3.63) \quad \inf\{s \mid u \in \overline{\text{CH}_s(\mathcal{F})}^{C^0}\} \geq \|u'\|_{\text{TV}[0,1]}$$

*Proof.* Suppose the opposite holds, then there exists a sequence

$$(3.64) \quad g_k(x) = \sum_{i=1}^{N_k} \alpha_i \sigma(x - b_i) + \sum_{j=1}^{M_k} \beta_j \sigma(x - c_j), k = 1, 2, \dots,$$

such that

$$(3.65) \quad \lim_{k \rightarrow \infty} g_k = u, \text{ and } \lim_{k \rightarrow \infty} \left( \sum_{i=1}^{N_k} |\alpha_i| + \sum_{j=1}^{M_k} |\beta_j| \right) = \|u'\|_{\text{TV}[0,1]} - \varepsilon,$$

for some  $\varepsilon > 0$ . We can assume that for each  $k$ ,  $\|g_k - u\|_{C([0,1])} \leq \frac{1}{k}$  by choosing a proper subsequence, and  $\left( \sum_{i=1}^{N_k} |\alpha_i| + \sum_{j=1}^{M_k} |\beta_j| \right) < \|u'\|_{\text{TV}[0,1]}$ .

The key is to adjust the node points  $b_i, c_i$  to some equidistributed points. To see this, we introduce the following modifications: For each  $b_i \in [0, 1]$ , let  $\tilde{b}_i$  be one of  $\{0, \frac{1}{k}, \dots, \frac{k-1}{k}, 1\}$  that is closest to  $b_i$ , for  $i = 1, 2, \dots, N_k$ . Similarly, we define  $\tilde{c}_i$ . For all  $b_i < 0$  and  $c_j > 1$ , we rewrite  $\alpha_i \sigma(x - b_i) = \alpha_i \sigma(x) - \alpha_i b_i$  and  $\beta_j \sigma(c_j - x) = \beta_j \sigma(1 - x) - \beta_j (c_j - 1)$  for  $x \in [0, 1]$ . Subsequently, we define

$$(3.66) \quad \begin{aligned} \tilde{g}_k(x) &:= \sum_{i: b_i \in [0,1]} \alpha_i \sigma(x - \tilde{b}_i) + \sum_{j: c_j \in [0,1]} \beta_j \sigma(x - \tilde{c}_j) \\ &+ \sum_{i: b_i < 0} (\alpha_i \sigma(x) - \alpha_i b_i) + \sum_{j: c_j > 1} (\beta_j \sigma(1 - x) - \beta_j (c_j - 1)) \\ &= \sum_{i=0}^k \left( w_i \sigma(x - \frac{i}{k}) + v_i \sigma(\frac{i}{k} - x) \right) + C_k, \end{aligned}$$

where  $w_i$  and  $v_i$  are the weights after merging, and  $C_k$  is the constant term after merging. It then holds that

$$(3.67) \quad \sum_{i=1}^k (|w_i| + |v_i|) \leq \sum_{i=1}^{N_k} |\alpha_i| + \sum_{j=1}^{M_k} |\beta_j| \leq \|u'\|_{\text{TV}[0,1]} - \varepsilon.$$

Also, for sufficiently large  $k$  we have:

$$(3.68) \quad \|\tilde{g}_k - g_k\|_{C([0,1])} \leq \frac{\|u'\|_{\text{TV}[0,1]}}{2} \cdot \frac{1}{k},$$

thus

$$(3.69) \quad \|\tilde{g}_k - u\|_{C([0,1])} \leq \frac{1}{k} (\|u'\|_{\text{TV}[0,1]} + 1).$$

Now we fix  $k$ , and specify the error as  $\varepsilon_i = \tilde{g}_k(\frac{i}{k}) - u(\frac{i}{k})$ , for  $i = 0, 1, \dots, k$ , with  $|\varepsilon_j| \leq \|\tilde{g}_k - u\|_{C(K)}$ . Now we pivot at  $\tilde{g}_k$ , and the coefficients solve the following linear system:

$$(3.70) \quad \frac{1}{N} \left( \sum_{i=j+1}^N i v_i + \sum_{i=0}^{j-1} (j-i) w_i \right) = u\left(\frac{j}{N}\right) - C_k + \varepsilon_j, \quad j = 0, 1, \dots, N.$$

In the following, we denote  $u_i = u(\frac{i}{k})$  for simplicity, and define:

$$(3.71) \quad \begin{aligned} \Delta^2 u_i &:= u_{i+1} - 2u_i + u_{i-1}, \quad i = 1, \dots, k-1, & \Delta^2 u_0 &:= u_1 - u_0, & \Delta^2 u_k &:= u_k - u_{k-1}. \\ \Delta^2 \varepsilon_i &:= \varepsilon_{i+1} - 2\varepsilon_i + \varepsilon_{i-1}, \quad i = 1, \dots, k-1, & \Delta^2 \varepsilon_0 &:= \varepsilon_1 - \varepsilon_0, & \Delta^2 \varepsilon_k &:= \varepsilon_k - \varepsilon_{k-1}. \end{aligned}$$

Thanks to (3.70) and Proposition 3.3, we have:

$$(3.72) \quad \sum_{i=0}^k |w_i| + |v_i| \geq k \sum_{i=1}^{k-1} |\Delta^2 u_i + \Delta^2 \varepsilon_i| + \text{dist} \left( -k(\Delta^2 u_0 + \Delta^2 \varepsilon_0), [\tilde{K}_-, \tilde{K}_+] \right)$$

where

$$(3.73) \quad \tilde{K}_+ = k \sum_{i=1}^{k-1} \max\{\Delta^2 u_i + \Delta^2 \varepsilon_i, 0\}, \quad \tilde{K}_- = k \sum_{i=1}^{k-1} \min\{\Delta^2 u_i + \Delta^2 \varepsilon_i, 0\}.$$

The term  $u_k$  and  $\varepsilon_k$  do not appear explicitly in the terms of (3.72). Nevertheless, we can perform a symmetrization for this discrete counterpart. It follows from  $k(\Delta^2 u_0 + \Delta^2 \varepsilon_0) + \tilde{K}_- + \tilde{K}_+ = k(\Delta^2 u_k + \Delta^2 \varepsilon_k)$  that:

$$(3.74) \quad \begin{aligned} & \text{dist} \left( -k(\Delta^2 u_0 + \Delta^2 \varepsilon_0), [\tilde{K}_-, \tilde{K}_+] \right) \\ &= \text{dist} \left( -k(\Delta^2 u_0 + \Delta^2 \varepsilon_0) - \frac{\tilde{K}_- + \tilde{K}_+}{2}, \left[ \frac{\tilde{K}_- - \tilde{K}_+}{2}, \frac{\tilde{K}_+ - \tilde{K}_-}{2} \right] \right) \\ &= \text{dist} \left( -k \frac{\Delta^2 u_0 + \Delta^2 \varepsilon_0 + \Delta^2 u_k + \Delta^2 \varepsilon_k}{2}, \left[ \frac{\tilde{K}_- - \tilde{K}_+}{2}, \frac{\tilde{K}_+ - \tilde{K}_-}{2} \right] \right) \\ &= \frac{k}{2} \max \left\{ |\Delta^2 u_0 + \Delta^2 \varepsilon_0 + \Delta^2 u_k + \Delta^2 \varepsilon_k| - \sum_{i=1}^{k-1} |\Delta^2 u_i + \Delta^2 \varepsilon_i|, 0 \right\} \end{aligned}$$

Therefore, (3.72) can be rewritten in a symmetric form:

$$(3.75) \quad \sum_{i=0}^k (|w_i| + |v_i|) \geq \sum_{i=1}^{k-1} k |\Delta^2 u_i + \Delta^2 \varepsilon_i| + \frac{k}{2} \max \left\{ |\Delta^2 u_0 + \Delta^2 \varepsilon_0 + \Delta^2 u_k + \Delta^2 \varepsilon_k| - \sum_{i=1}^{k-1} |\Delta^2 u_i + \Delta^2 \varepsilon_i|, 0 \right\},$$

The rest of the proof is aimed at reducing the error term  $\varepsilon_i$  in the right-hand side. In particular, we prove that for any  $\delta > 0$  and sufficiently large  $k$  we have

$$(3.76) \quad \sum_{i=0}^k (|w_i| + |v_i|) \geq k \sum_{i=1}^{k-1} |\Delta^2 u_i| + \frac{1}{2} k \max \left\{ \left( |\Delta^2 u_0 + \Delta^2 u_k| - \sum_{i=1}^{k-1} |\Delta^2 u_i| \right), 0 \right\} - \delta.$$

Now we start from (3.75). The first step is to relax  $|x|$  and  $\max\{x, 0\}$ , namely,

$$(3.77) \quad |x| = \max_{\phi \in [-1, 1]} \phi x, \quad \max\{x, 0\} = \max_{\theta \in [0, 1]} \theta x.$$

We then have the following estimation:

$$(3.78) \quad \begin{aligned} \text{RHS of (3.75)} &\geq k \sum_{i=1}^{k-1} |\Delta^2 u_i + \Delta^2 \varepsilon_i| + \frac{\theta}{2} k \left( |\Delta^2 u_0 + \Delta^2 \varepsilon_0 + \Delta^2 u_k + \Delta^2 \varepsilon_k| - \sum_{i=1}^{k-1} |\Delta^2 u_i + \Delta^2 \varepsilon_i| \right) \\ &= k \sum_{i=1}^{k-1} \left( 1 - \frac{\theta}{2} \right) |\Delta^2 u_i + \Delta^2 \varepsilon_i| + \frac{\theta}{2} k |\Delta^2 u_0 + \Delta^2 \varepsilon_0 + \Delta^2 u_k + \Delta^2 \varepsilon_k| \\ &\geq k \left( 1 - \frac{\theta}{2} \right) \sum_{i=1}^{k-1} \phi_i (\Delta^2 u_i + \Delta^2 \varepsilon_i) + \frac{\theta}{2} k |\Delta^2 u_0 + \Delta^2 \varepsilon_0 + \Delta^2 u_k + \Delta^2 \varepsilon_k|, \end{aligned}$$

for all  $\theta \in [0, 1]$  and  $\phi_i \in [-1, 1]$  for  $i = 1, \dots, k-1$ . For arbitrarily defined  $\phi_0$  and  $\phi_k$ , the following discrete integration by parts hold:

$$(3.79) \quad \sum_{i=1}^{k-1} \phi_i \Delta^2 \varepsilon_i = \sum_{i=1}^{k-1} \varepsilon_i \Delta^2 \phi_i + \phi_{k-1} \varepsilon_k + \phi_1 \varepsilon_0 - \varepsilon_{k-1} \phi_k - \varepsilon_1 \phi_0,$$

where  $\Delta^2\phi_i = \phi_{i+1} - 2\phi_i + \phi_{i-1}$  is the discrete central difference. We then have the estimation:

$$(3.80) \quad \begin{aligned} \sum_{i=1}^{k-1} \phi_i(\Delta^2 u_i + \Delta^2 \varepsilon_i) &= \sum_{i=1}^{k-1} \phi_i \Delta^2 u_i + \sum_{i=1}^{k-1} \varepsilon_i \Delta^2 \phi_i + \phi_{k-1} \varepsilon_k + \phi_1 \varepsilon_0 - \varepsilon_{k-1} \phi_k - \varepsilon_1 \phi_0 \\ &\geq \underbrace{\sum_{i=1}^{k-1} \phi_i \Delta^2 u_i - \frac{C}{k} \sum_{i=1}^{k-1} |\Delta^2 \phi_i|}_{A} + \phi_{k-1} \varepsilon_k + \phi_1 \varepsilon_0 - \varepsilon_{k-1} \phi_k - \varepsilon_1 \phi_0. \end{aligned}$$

Here,  $C := \|u'\|_{\text{TV}[0,1]} + 1$  is independent with  $k$ . Therefore, it follows that the right-hand side of (3.75) is not less than

$$(3.81) \quad k(1 - \frac{\theta}{2})A + \underbrace{k(1 - \frac{\theta}{2})(\phi_{k-1} \varepsilon_k + \phi_1 \varepsilon_0 - \varepsilon_{k-1} \phi_k - \varepsilon_1 \phi_0) + \frac{\theta}{2}k|\Delta^2 u_0 + \Delta^2 \varepsilon_0 + \Delta^2 u_k + \Delta^2 \varepsilon_k|}_{B}.$$

For a fixed  $\delta > 0$ , and  $a = \text{sign}(\Delta^2 \varepsilon_0 + \Delta^2 \varepsilon_1)$ , there exists a function  $\phi \in C^2([0, 1])$ , such that

- (a)  $|\phi|_{C([0,1])} \leq 1$ ;
- (b)  $\phi(0) = \phi(1) = a$ ;
- (c)  $\int_{[0,1]} \phi(x)u''(x)dx := \int_{[0,1]} \phi d(Du') > \|u'\|_{\text{TV}([0,1])} - \delta$ .

Fix  $\delta$  and  $a$ , for each  $k$ , we choose  $\phi_i = \phi(\frac{i}{k})$  for  $i = 0, 1, \dots, k$ . For the term  $A$ , we have

$$(3.82) \quad \begin{aligned} &\liminf_{k \rightarrow \infty} k \sum_{i=1}^{k-1} \phi_i \Delta^2 u_i - C \sum_{i=1}^{k-1} |\Delta^2 \phi_i| \\ &= \liminf_{k \rightarrow \infty} \int_{[0,1]} \phi(x)u''(x)dx - \frac{C}{k} \int_{[0,1]} |\phi''(x)|dx \\ &\geq \|u'\|_{\text{TV}([0,1])} - \delta. \end{aligned}$$

For the term  $B$ , we have

$$(3.83) \quad \begin{aligned} &k(1 - \frac{\theta}{2})(\phi_{k-1} \varepsilon_k + \phi_1 \varepsilon_0 - \varepsilon_{k-1} \phi_k - \varepsilon_1 \phi_0) + k\frac{\theta}{2}(|\Delta^2 u_0 + \Delta^2 \varepsilon_0 + \Delta^2 u_k + \Delta^2 \varepsilon_k|) \\ &= k(1 - \frac{\theta}{2})(|\Delta^2 \varepsilon_0 + \Delta^2 \varepsilon_k| + (a - \phi_{k-1})\varepsilon_k + (\phi_1 - a)\varepsilon_0) + k\frac{\theta}{2}(|\Delta^2 u_0 + \Delta^2 \varepsilon_0 + \Delta^2 u_k + \Delta^2 \varepsilon_k|) \\ &\geq k(1 - \frac{\theta}{2})|\Delta^2 \varepsilon_0 + \Delta^2 \varepsilon_k| + k\frac{\theta}{2}(|\Delta^2 u_0 + \Delta^2 u_k + \Delta^2 \varepsilon_0 + \Delta^2 \varepsilon_k|) - C(|\phi_{k-1} - a| + |\phi_1 - a|) \\ &\geq k\frac{\theta}{2}(|\Delta^2 \varepsilon_0 + \Delta^2 \varepsilon_k| + |\Delta^2 u_0 + \Delta^2 u_k + \Delta^2 \varepsilon_0 + \Delta^2 \varepsilon_k|) - C(|\phi_{k-1} - a| + |\phi_1 - a|) \\ &\geq k\frac{\theta}{2}|\Delta^2 u_0 + \Delta^2 u_k| - C(|\phi_{k-1} - a| + |\phi_1 - a|). \end{aligned}$$

As  $k \rightarrow \infty$ ,  $\phi_{k-1} \rightarrow a$  and  $\phi_1 \rightarrow a$ . Therefore, for sufficiently large  $k$ , we have that:

$$(3.84) \quad B \geq k\frac{\theta}{2}|\Delta^2 u_0 + \Delta^2 u_k| - \delta.$$

Combining all results above, we have shown that for sufficiently large  $k$ ,

$$(3.85) \quad \sum_{i=0}^k (|w_i| + |v_i|) \geq k \sum_{i=1}^{k-1} |\Delta^2 u_i| + \frac{\theta}{2}k \left( |\Delta^2 u_0 + \Delta^2 u_k| - \sum_{i=1}^{k-1} |\Delta^2 u_i| \right) - \delta$$

for all  $\theta \in [0, 1]$ . Recall the dual form of  $\max\{x, 0\}$  in (3.77), we have shown that:

$$(3.86) \quad \sum_{i=0}^k (|w_i| + |v_i|) \geq \|u'\|_{\text{TV}[0,1]} - 3\delta.$$

Since  $\delta$  can be arbitrarily small, we then have a contradiction to (3.67).  $\square$

Therefore, we show

$$(3.87) \quad \inf\{s \mid u \in \overline{\mathbf{CH}_s(\mathcal{F})}^{C^0}\} = \|u'\|_{\text{TV}[0,1]}$$

for all  $u \in \text{BV}_0^2([0, 1])$ .

3.1.2. *Proof of Theorem 3.1.* Now, we can provide the proof of Theorem 3.1. In the proof, we will use some of the geometric concepts that will be introduced later in Section 4.2.

*Proof of Theorem 3.1.* We first show that

$$(3.88) \quad \mathcal{M} \subseteq \{\psi \in \text{BV}^2([0, 1]) \mid \psi(0) = 0, \psi(1) = 1, \psi' \geq c > 0 \text{ a.e. for some } c\}.$$

Notice that all the functions in  $\mathcal{F}$  are uniformly Lipschitz and uniformly bounded in the  $\text{BV}^2$  norm. By a Grownwall's inequality estimate, flows in  $\mathcal{A}_{\mathcal{F}}$  are also uniformly bounded in the  $\text{BV}^2$  norm. Therefore, for any  $\psi \in \mathcal{M}$  that is the limit of flows in  $\mathcal{A}_{\mathcal{F}}(T)$  for some  $T < \infty$ , we have deduced that  $\psi \in \text{BV}^2([0, 1])$  by the Helly selection principle. Therefore, we have shown that  $\mathcal{M}$  is a subset of  $\text{BV}^2([0, 1])$ .

We then consider a map:

$$(3.89) \quad \alpha : \mathcal{M} \rightarrow \text{BV}([0, 1]) : \psi \mapsto \log \psi'.$$

The local norm on  $\mathcal{M}$  then induces a local norm, i.e. the pushforward, on  $\text{Im}(\alpha) \subset \text{BV}([0, 1])$ . For given  $\xi = \alpha(\psi) \in \text{Im}(\alpha)$  and  $h \in \text{BV}([0, 1])$ , this norm is given by:

$$(3.90) \quad \|h\|_{\xi}^{\text{Im}(\alpha)} = \|(d\alpha^{-1}(\xi))h\|_{\psi} = \left\| \int_0^x e^{g(t)} h(t) dt \right\|_{\psi} = \left\| \int_0^x f'(t) h(t) dt \right\|_{\psi} = \|h\|_{\text{TV}[0,1]}$$

With this induced metric,  $\alpha$  gives an isometric embedding from  $\mathcal{M}$  onto  $\text{Im}(\alpha) \subset \text{BV}([0, 1])$ . Notice that under this embedding, the metric is independent of  $\xi \in \mathcal{N}$ , which means the metric is "flat" in  $\mathcal{N}$ .

Then, it is easy to check that the modified straight line:

$$(3.91) \quad \gamma_t(x) = (1-t)\xi_1(x) + t\xi_2(x) - \log \int_0^1 e^{(1-t)\xi_1(x) + t\xi_2(x)} dx,$$

is a path with minimal length connecting  $\xi_1 = \alpha(\psi_1)$  and  $\xi_2 = \alpha(\psi_2)$  in  $\mathcal{N}$ .

In the original space  $\mathcal{M}$ , this path is given by:

$$(3.92) \quad \tilde{\gamma}_t(x) = \frac{\int_0^x (\psi_1'(x))^{1-t} (\psi_2'(x))^t dx}{\int_0^1 (\psi_1'(x))^{1-t} (\psi_2'(x))^t dx}.$$

Integrating the local norm along  $\gamma_t$ , we achieve the distance:

$$(3.93) \quad \begin{aligned} d_{\mathcal{N}}(\xi_1, \xi_2) &= \int_0^1 \|\xi_2' - \xi_1'\|_{\gamma_t} dt = \int_0^1 \|\xi_2' - \xi_1'\|_{\text{TV}[0,1]} dt \\ &= \|\xi_2 - \xi_1\|_{\text{TV}[0,1]}. \end{aligned}$$

Going back to  $\mathcal{M}$ , we have

$$(3.94) \quad d_{\mathcal{M}}(\psi_1, \psi_2) = \|\log \psi_2' - \log \psi_1'\|_{\text{TV}[0,1]}.$$

As a corollary, this result shows that for any  $\psi_1, \psi_2 \in \{\psi \in \text{BV}^2([0, 1]) \mid \psi(0) = 0, \psi(1) = 1, \psi' \geq c > 0 \text{ a.e. for some } c\}$ ,  $d_{\mathcal{F}}(\psi_1, \psi_2) < \infty$ . Therefore, we have shown that

$$(3.95) \quad \mathcal{M} = \{\psi \in \text{BV}^2([0, 1]) \mid \psi(0) = 0, \psi(1) = 1, \psi' \geq c > 0 \text{ a.e. for some } c\}.$$

This completes the proof.  $\square$

## 4. THE RATE OF APPROXIMATION BY FLOWS: THE GENERAL CASE

We now generalize the approach motivated in the ReLU example to analyze the rate of approximation by flows driven by general control families  $\mathcal{F}$  in  $d$  dimensions. Before we introduce the formulation of the general concepts, let us first summarize the approach in the previous section. We considered the class  $\mathcal{M}$  of maps that can be approximated, starting from the identity, by flows generated by  $\mathcal{F}$  in finite time. This class has a compositional structure rather than a linear one. We quantified the approximation complexity by the minimal reachable time  $\mathbf{C}_{\mathcal{F}}(\psi)$  by extending it to a distance  $d_{\mathcal{F}}$  on  $\mathcal{M}$ , the minimal time to transport one map to another via flows induced by  $\mathcal{F}$ . To connect this global quantity to  $\mathcal{F}$ , we examined the infinitesimal behavior of  $d_{\mathcal{F}}$  and obtained a local norm  $\|\cdot\|$ , which characterizes the complexity of transporting a function to its nearby functions. This norm captures the “shallow” approximation capability of  $\mathcal{F}$ , while the global transport cost emerges by integrating this norm along a curve.

As what we will develop in the following, the correspondence between global distance and local infinitesimal cost is naturally expressed in a sub-Finsler framework on  $\text{Diff}(M)$ , the group of diffeomorphisms on  $M$ :  $\mathcal{F}$  induces a horizontal distribution (the admissible directions) and a fiberwise norm on it; curves that follow the distribution are horizontal, and their lengths are the time-integrals of this norm. The resulting geodesic distance (the length of shortest horizontal paths) turns out to coincide with the minimal reachable time  $d_{\mathcal{F}}$ . Intuitively, directions outside the distribution have infinite local norm, so only horizontal motion is allowed.

In what follows, we formalize this viewpoint in a Banach sub-Finsler setting on  $\text{Diff}(M)$ . Section 4.1 introduces the basic objects (horizontal distribution, local norm, horizontal curves and length), Section 4.2 defines the associated geodesic distance and relates it to flow approximation, and Section 4.2 proves the main theorem that identifies  $d_{\mathcal{F}}$  with this sub-Finsler geodesic distance and gives the variational characterization of the local norm. This yields a practical recipe for estimating the complexity of approximating maps by flows: estimate the local norm (linked to shallow approximations by  $\mathcal{F}$ ), design horizontal paths, and integrate the norm to bound  $d_{\mathcal{F}}$  and  $\mathbf{C}_{\mathcal{F}}$ . In some cases, one can also design optimal horizontal paths that completely characterizes  $d_{\mathcal{F}}$ , and hence  $\mathbf{C}_{\mathcal{F}}$ .

**4.1. Preliminaries on Banach sub-Finsler geometry.** Since there are sometimes differing conventions for infinite-dimensional manifolds and Finsler geometry, we concretely describe our adopted settings.

Banach manifold generalizes the notion of manifold to infinite dimensions. Locally, an  $n$ -dimensional manifold looks like an open set in  $\mathbb{R}^n$ , while a Banach manifold looks like an open set in a Banach space  $(X, \|\cdot\|)$ . We adopt the definition of Banach manifolds as follows [12]:

**Definition 4.1** (Banach Manifold). *Let  $\mathcal{M}$  be a topological space. We call  $\mathcal{M}$  a  $C^r$  Banach (where  $r$  is a positive integer or  $\infty$ ) manifold modeled on a Banach space  $(X, \|\cdot\|)$  with codimension  $0 \leq k < \infty$ , if there exists a collection of charts  $(U_i, \beta_i)$ ,  $i \in I$ , such that:*

- (1)  $U_i \subset \mathcal{M}$  is open and  $\mathcal{M} = \bigcup_{i \in I} U_i$ ;
- (2) Each  $\beta_i$  is a homeomorphism from  $U_i$  onto a subspace  $X_i \subset X$  with codimension  $k$ ;
- (3) The crossover map

$$(4.1) \quad \beta_j \circ \beta_i^{-1} : \beta_i(U_i \cap U_j) \subset X_i \rightarrow \beta_j(U_i \cap U_j) \subset X_j$$

*is a  $C^r$  function for every  $i, j \in I$ , in the sense of Fréchet derivatives.*

*The collection of charts  $(U_i, \beta_i)$  is called an atlas of  $\mathcal{M}$ .*

**Example 4.1.** *The simplest example of a Banach manifold is an open subset  $\Omega$  of  $X$ . In this case, it is an  $X$ -manifold with codimension 0, where the atlas contains only one chart  $(\Omega, \text{Id})$ .*

**Example 4.2.** *Another important example is the space of diffeomorphisms on a compact manifold  $M$ . Let  $M \subset \mathbb{R}^d$  be a compact  $C^\infty$  manifold, and fix a  $C^\infty$  Riemannian metric on  $M$  with exponential map*

$\exp_x : T_x M \rightarrow M$ . Define

$$(4.2) \quad \text{Diff}^1(M) := \{\psi : M \rightarrow M : \psi \text{ is } C^1 \text{ and bijective, and } \psi^{-1} \in C^1(M, M)\}.$$

We now describe a canonical family of local charts on  $\text{Diff}^1(M)$  using short geodesics.

Fix  $\psi \in \text{Diff}^1(M)$ . Consider the Banach space

$$(4.3) \quad \text{Vec}^1(M) := \{u \in C^1(M, \mathbb{R}^d) \mid u(x) \in T_x M, \text{ for all } x \in M\}$$

to be the set of  $C^1$  vector fields on  $M$  equipped with the norm in  $C^1(M, \mathbb{R}^d)$ . For  $\varepsilon > 0$  small enough, define

$$(4.4) \quad \beta_\psi : B_{\text{Vec}^1(M)}(0, \varepsilon) \longrightarrow C^1(M, M), \quad \beta_\psi(u)(x) := \exp_{\psi(x)}(u(\psi(x))).$$

For  $\varepsilon$  sufficiently small,  $\beta_\psi(u)$  is a  $C^1$  diffeomorphism, and its image  $U_\psi := \beta_\psi(B_{\text{Vec}^1(M)}(0, \varepsilon))$  is an open neighborhood of  $\psi$  in  $\text{Diff}^1(M)$  ([50]). Moreover, for  $\phi \in U_\psi$  the inverse chart is given pointwise by  $w(x) := \exp_{\psi(x)}^{-1}(\phi(x))$ , and the corresponding vector field is  $v := w \circ \psi^{-1}$ . In words, for each  $x \in M$ , we start at the point  $\psi(x)$  and move along the unique geodesic with initial velocity  $u(x)$  (which is small), and declare the endpoint to be  $\beta_\psi(u)(x)$ .

The collection of charts  $\{(U_\psi, \beta_\psi^{-1})\}_{\psi \in \text{Diff}^1(M)}$  forms an atlas, thereby endowing  $\text{Diff}^1(M)$  with the structure of a Banach manifold modeled on  $C^1$  maps (codimension 0). Transition maps  $\beta_{\psi_2}^{-1} \circ \beta_{\psi_1}$  are  $C^1$  in the Fréchet sense (actually  $C^\infty$  according to [50]), since they are obtained by composing the smooth finite-dimensional maps  $(p, v) \mapsto \exp_p(v)$  and  $(p, q) \mapsto \exp_p^{-1}(q)$  pointwise.

Similar to finite-dimensional manifolds, we can now define the tangent space at a point  $x \in \mathcal{M}$ .

**Definition 4.2** (Tangent Spaces of Banach Manifolds). Let  $\mathcal{M}$  be a  $C^1$  Banach manifold modeled on  $X$  and  $x_0 \in \mathcal{M}$ . Define

$$(4.5) \quad W_{x_0} := \{\gamma \in C^1(E, \mathcal{M}) \mid E \text{ is an open interval containing } 0, \gamma(0) = x_0\}$$

be the set of all  $C^1$  curves passing through  $x_0$ . Let

$$(4.6) \quad K_{x_0} := \{\phi \in C^1(N(x_0), \mathbb{R}) \mid N(x_0) \subset \mathcal{M} \text{ is a neighborhood of } x_0, \phi(x_0) = 0\}$$

be the set of all smooth functions vanishing at  $x_0$ . Define an equivalent relation on  $W_{x_0}$  by  $\gamma_1 \sim \gamma_2$  iff  $(\phi\gamma_1)'(0) = (\phi\gamma_2)'(0)$  for all  $\phi \in K_{x_0}$ . An equivalence class  $[\gamma]$  of this relationship is called a tangent vector at  $x_0$ . The set of such tangent vectors

$$(4.7) \quad T_{x_0}\mathcal{M} := \{[\gamma] \mid \gamma \in W_{x_0}\}$$

forms a linear space, which is called the tangent space at  $x_0$ .

Note that for finite-dimensional manifold  $\mathcal{M}$  with dimension  $n$ , the tangent space is isomorphic to  $\mathbb{R}^n$ . A corresponding result holds for Banach manifolds.

**Proposition 4.1.** Let  $\mathcal{M}$  be an  $X$ -Banach manifold with co-dimension  $k$ . For any  $x_0 \in \mathcal{M}$ , the tangent space  $T_{x_0}\mathcal{M}$  is isomorphic as a linear space to a subspace  $Y \subset X$  with  $\text{codim } Y = k$ . Specifically, the map

$$(4.8) \quad \Phi_{x_0} : T_{x_0}\mathcal{M} \rightarrow Y \subset X, \quad [\gamma] \mapsto (\beta \circ \gamma)'(0),$$

is a linear bijection, where  $(U, \beta)$  is a chart such that  $x_0 \in U$ , and  $Y$  is the subspace corresponding to  $\beta$  with codimension  $k$ .

*Proof.* It is straightforward to see  $\Phi_{x_0}$  is well-defined and linear by the definition of tangent space. We then directly check the following:

- $\text{Ker } \Phi_{x_0} = \{0\}$ : If

$$(4.9) \quad \Phi_{x_0}([\gamma]) = (\beta \circ \gamma)'(0) = 0,$$

then for any  $\phi \in K_{x_0}$ , we have:

$$(4.10) \quad (\phi \circ \gamma)'(0) = [(\phi \circ \beta^{-1}) \circ (\beta \circ \gamma)]'(0) = (\phi \circ \beta^{-1})'(\beta \circ \gamma(0)) \cdot (\beta \circ \gamma)'(0) = 0.$$

By the definition of tangent vectors, we have  $[\gamma] = 0$ .

- $\text{Im } \Phi_{x_0} = Y$ : For any  $x \in X$ , consider the path  $\gamma(t) := \beta^{-1}(\beta(x_0) + tx)$ , which is a smooth curve passing through  $x_0$  with  $\gamma'(0) = x$ . It then follows that

$$(4.11) \quad \Phi_{x_0}([\gamma]) = (\beta \circ \gamma)'(0) = (\beta \circ \beta^{-1}(\beta(x_0) + tx))'(0) = x.$$

□

Our goal is to model the diffeomorphisms over  $M \subset \mathbb{R}^d$  as a Banach manifold, and study the “travelling” on this manifold via flows generated by a control family  $\mathcal{F}$ . Starting from the identity map, as we increase the time-horizon, we will be able to reach an increasingly complex set of diffeomorphisms. The allowed directions of this travel are of course determined by  $\mathcal{F}$ . In particular, we motivated earlier that only the directions  $u$  for which the local norm (3.10) is finite are allowed. In the most general case, the allowed directions at each point does not fill the whole tangent space. Rather, it is a suitably defined subspace which we call a *distribution*, following the language in sub-Riemannian geometry. We now formally introduce this and associated notions. Here, as in the finite-dimensional case, the union of all tangent spaces

$$(4.12) \quad T\mathcal{M} := \bigcup_{x \in \mathcal{M}} T_x \mathcal{M}$$

is called the tangent bundle of  $\mathcal{M}$ .

**Definition 4.3** ( $C^r$  submersion between Banach manifolds). *Let  $\mathcal{N}, \mathcal{M}$  be  $C^r$  Banach manifolds. A  $C^r$  map  $F : \mathcal{N} \rightarrow \mathcal{M}$  is a  $C^r$  submersion at  $p \in \mathcal{N}$  if the differential*

$$(4.13) \quad dF_p : T_p \mathcal{N} \rightarrow T_{F(p)} \mathcal{M}$$

*is a split surjection, i.e. surjective and admits a bounded right inverse (equivalently,  $\ker dF_p$  is a complemented closed subspace of  $T_p \mathcal{N}$ ). If this holds for all  $p \in \mathcal{N}$ , we call  $F$  a  $C^r$  submersion.*

The definition of vector bundles and distributions can be generalized to Banach manifolds as follows. Here, we follow the definitions in [3].

**Definition 4.4** (Banach vector bundle). *A  $C^r$  Banach vector bundle over  $\mathcal{M}$  is a triple  $(\mathcal{E}, \pi, F)$  where:*

- $\mathcal{E}$  and  $\mathcal{M}$  are  $C^r$  Banach manifolds, and  $\pi : \mathcal{E} \rightarrow \mathcal{M}$  is a  $C^r$  surjective submersion in the sense of Definition 4.3;
- Each fiber  $\mathcal{E}_x := \pi^{-1}(x)$  is a Banach space linearly isomorphic to a fixed model Banach space  $F$ ;
- There exists an open cover  $\{U_i\}_{i \in \alpha}$  of  $\mathcal{M}$  and  $C^r$  bundle charts (local trivializations)

$$(4.14) \quad \tau_i : \pi^{-1}(U_i) \xrightarrow{\cong} U_i \times F$$

*that are fiberwise linear and such that the transition maps*

$$(4.15) \quad g_{ij} : U_i \cap U_j \rightarrow \text{GL}(F), \quad \tau_i \circ \tau_j^{-1}(x, v) = (x, g_{ij}(x)v),$$

*are  $C^r$  (for the operator-norm topology) and satisfy the cocycle relations  $g_{ii} = \text{Id}_F$ ,  $g_{ij} = g_{ji}^{-1}$ ,  $g_{ik} = g_{ij}g_{jk}$  on triple overlaps.*

*In any trivialization,  $\pi$  has the local form  $(x, v) \mapsto x$ , and  $d\pi_{(x,v)}(\xi, \eta) = \xi$ .*

Classically, a distribution is specified by a subbundle  $\mathcal{D} \subset T\mathcal{M}$  via the inclusion map. In Banach manifold setting, this concept can also be generalized. Here, we follow the notion of *relative tangent space* or *anchored bundle* [3], which covers the subbundle case in a more general way.

**Definition 4.5** (Relative tangent space / Anchored bundle). *Let  $\mathcal{M}$  be a smooth Banach manifold. A relative tangent space on  $\mathcal{M}$  is a triple  $(\mathcal{E}, \pi, \rho)$  where*

- $\pi : \mathcal{E} \rightarrow \mathcal{M}$  is a smooth Banach vector bundle morphism with typical fiber a Banach space (denoted again by  $F$ );
- $\rho : \mathcal{E} \rightarrow T\mathcal{M}$  is a smooth vector-bundle morphism (the anchor).

The associated horizontal distribution is  $\mathcal{D} := \rho(\mathcal{E}) \subset T\mathcal{M}$ .

Intuitively, an anchored bundle  $(\mathcal{E}, \pi, \rho)$  over  $\mathcal{M}$  assigns to each point  $x \in \mathcal{M}$  a subspace of the tangent space  $T_x\mathcal{M}$  through the anchor map  $\rho$ , which varies smoothly with  $x$ . In the context of our minimal reachable time problem, the distribution  $\mathcal{D}$  is determined by the control family  $\mathcal{F}$ : it represents the set of all locally admissible velocities that can be generated by  $\mathcal{F}$  at each point.

We equip each fiber  $\mathcal{E}_x$  with a norm that depends continuously on  $x$  induces a fiberwise norm on the image  $\mathcal{D} := \rho(\mathcal{E}) \subset T\mathcal{M}$ . This generalizes the Riemannian/sub-Riemannian case (inner products) to a sub-Finsler setting (arbitrary norms). If  $\rho_x$  is injective, we simply transport the norm to  $\mathcal{D}_x$ ; otherwise we take the minimal-norm preimage.

**Definition 4.6** (sub-Finsler structure). *Let  $(\mathcal{E}, \pi, \rho)$  be an anchored  $C^r$  Banach vector bundle over  $\mathcal{M}$ . Assume  $\mathcal{E}$  is endowed with a fiberwise norm field, i.e. for each  $x \in \mathcal{M}$  a Banach norm  $\|\cdot\|_x$  on the fiber  $\mathcal{E}_x$ , depending continuously on  $x$  (equivalently, the map  $(x, v) \mapsto \|v\|_x$  is continuous on  $\mathcal{E}$ ). The induced sub-Finsler structure on the anchored distribution  $\mathcal{D} := \rho(\mathcal{E}) \subset T\mathcal{M}$  is the family of fiberwise norms:*

$$(4.16) \quad \|\xi\|_{\mathcal{D},x} := \inf \{ \|v\|_x : v \in \mathcal{E}_x, \rho_x v = \xi \}, \quad \xi \in T_x\mathcal{M},$$

with the convention  $\|\xi\|_{\mathcal{D},x} = +\infty$  if  $\xi \notin \mathcal{D}_x$ . If each  $\rho_x$  is injective, then  $\|\xi\|_{\mathcal{D},x} = \|\rho_x^{-1}\xi\|_x$  for  $\xi \in \mathcal{D}_x$ .

With an anchored normed bundle in place, a curve is horizontal if its velocity lies in  $\mathcal{D}$  almost everywhere, and its length is the time integral of the local norm. Minimizing length over horizontal curves yields the geodesic distance, exactly as in finite-dimensional sub-Riemannian geometry, now in the Banach setting.

**Definition 4.7** (Horizontal curves, length and distance.). *A curve  $\gamma : [0, T] \rightarrow \mathcal{M}$  is absolutely continuous if it is absolutely continuous in local charts; then  $\dot{\gamma}(t)$  exists for a.e.  $t$  and lies in  $T_{\gamma(t)}\mathcal{M}$ . We call  $\gamma$  horizontal if*

$$(4.17) \quad \dot{\gamma}(t) \in \mathcal{D}_{\gamma(t)} \quad \text{for a.e. } t \in [0, T],$$

equivalently, there exists a measurable control  $v(t) \in E_{\gamma(t)}$  with

$$(4.18) \quad \dot{\gamma}(t) = \rho_{\gamma(t)} v(t) \quad \text{a.e.}$$

The length of a horizontal curve is

$$(4.19) \quad L(\gamma) := \int_0^T \|\dot{\gamma}(t)\|_{\mathcal{D},\gamma(t)} dt$$

and  $L(\gamma) := +\infty$  if  $\gamma$  is not horizontal. Length is invariant under absolutely continuous reparametrizations.

The associated geodesic distance (Carnot–Carathéodory distance) on  $\mathcal{M}$  is

$$(4.20) \quad d(x_0, x_1) := \inf \{ L(\gamma) : \gamma \text{ horizontal, } \gamma(0) = x_0, \gamma(T) = x_1 \} \in [0, +\infty].$$

This is an extended metric on  $\mathcal{M}$ ; when any two points can be joined by a horizontal curve of finite length, it is a genuine metric.

The geodesic distance  $d$  encodes precisely the same infinitesimal cost prescribed by the sub-Finsler structure: along admissible (horizontal) directions, the metric has a first-order expansion whose slope equals the local fiber norm; along non-admissible directions, the local cost is infinite. Formally, the metric derivative of  $t \mapsto d(x, \gamma(t))$  at  $t = 0$  recovers the sub-Finsler norm at  $x$ . This ensures the consistency between the global path-length distance and the local norm structure.

**Proposition 4.2** (Recovering the local sub-Finsler norm from the geodesic distance). *Let  $(\mathcal{E}, \pi, \rho)$  be an anchored Banach vector bundle over a  $C^1$  Banach manifold  $\mathcal{M}$ , endowed with a continuous fiberwise norm  $\|\cdot\|_x$ , and let  $(\mathcal{D}, \|\cdot\|_{\mathcal{D}})$  and  $d$  be the induced sub-Finsler structure and geodesic distance. Fix  $x \in \mathcal{M}$  and  $v \in T_x\mathcal{M}$ .*

(1) *If  $v \in \mathcal{D}_x$ , then for any  $C^1$  horizontal curve  $\gamma$  with  $\gamma(0) = x$  and  $\gamma'(0) = v$ ,*

$$(4.21) \quad \|v\|_{\mathcal{D},x} = \lim_{t \rightarrow 0} \frac{d(x, \gamma(t))}{t}.$$

*In particular, the limit exists and is independent of the chosen horizontal  $\gamma$  with  $\gamma'(0) = v$ .*

(2) *If  $v \notin \mathcal{D}_x$ , then for any  $C^1$  curve  $\gamma$  with  $\gamma(0) = x$  and  $\gamma'(0) = v$ ,*

$$(4.22) \quad \lim_{t \rightarrow 0^+} \frac{d(x, \gamma(t))}{t} = +\infty.$$

*Proof.* We work in a local  $C^1$  chart around  $x$  so that  $\mathcal{M}$  is identified with an open set of a Banach space  $X$  and the anchored bundle  $(\mathcal{E}, \pi, \rho)$  becomes trivial with a continuous field of norms  $\|\cdot\|_y$  on the fiber  $F$ . In these coordinates the sub-Finsler speed is  $\|\dot{\gamma}(t)\|_{\mathcal{D},\gamma(t)} = \inf\{\|u(t)\|_{\gamma(t)} : \rho_{\gamma(t)}u(t) = \dot{\gamma}(t)\}$ . Local triviality and continuity imply uniform equivalence of the involved norms on a neighborhood of  $x$ .

**(i) Horizontal  $v \in \mathcal{D}_x$ .**

*Upper bound.* Let  $\gamma$  be horizontal,  $C^1$ , with  $\gamma(0) = x$  and  $\gamma'(0) = v$ . By definition of length and continuity of the fiber norms,

$$(4.23) \quad d(x, \gamma(t)) \leq L(\gamma|_{[0,t]}) = \int_0^t \|\dot{\gamma}(s)\|_{\mathcal{D},\gamma(s)} ds = t \|v\|_{\mathcal{D},x} + o(t),$$

$$\text{hence } \limsup_{t \rightarrow 0^+} \frac{d(x, \gamma(t))}{t} \leq \|v\|_{\mathcal{D},x}.$$

*Lower bound.* Fix a sequence  $\{t_k\}_{k=1}^{\infty} \rightarrow 0^+$ . For each  $k$ , let  $\sigma_k$  be a horizontal curve joining  $x$  to  $\gamma(t_k)$  with  $L(\sigma_k) \leq d(x, \gamma(t_k)) + \frac{1}{k}$ . Reparameterize each  $\sigma_k$  on  $[0, t_k]$  so that  $\dot{\sigma}_k = \rho_{\sigma_k}u_k$  with  $u_k \in L^1([0, t_k]; F)$  and  $\int_0^{t_k} \|u_k(s)\|_{\sigma_k(s)} ds = L(\sigma_k)$ . Set the averaged controls

$$(4.24) \quad \bar{u}_k := \frac{1}{t_k} \int_0^{t_k} u_k(s) ds \in F.$$

By continuity of  $\rho$  and the  $C^1$  expansion of  $\gamma$ ,

$$(4.25) \quad \frac{\gamma(t_k) - x}{t_k} = \frac{1}{t_k} \int_0^{t_k} \dot{\sigma}_k(s) ds = \frac{1}{t_k} \int_0^{t_k} \rho_{\sigma_k(s)}u_k(s) ds = \rho_x \bar{u}_k + o(1) \quad (k \rightarrow \infty).$$

Hence  $\rho_x \bar{u}_k \rightarrow v$ . By lower semicontinuity and the convexity of the fiber norm,

$$(4.26) \quad \liminf_{k \rightarrow \infty} \frac{d(x, \gamma(t_k))}{t_k} \geq \liminf_{k \rightarrow \infty} \frac{1}{t_k} \int_0^{t_k} \|u_k(s)\|_{\sigma_k(s)} ds \geq \liminf_{k \rightarrow \infty} \|\bar{u}_k\|_x \geq \inf_{\rho_x u = v} \|u\|_x = \|v\|_{\mathcal{D},x}.$$

Combining with the upper bound gives the limit and its value, independent of the chosen horizontal  $\gamma$ .

*(ii) Non-horizontal  $v \notin \mathcal{D}_x$ .* Suppose by contradiction that  $\liminf_{t \rightarrow 0^+} d(x, \gamma(t))/t < +\infty$  for some  $C^1$  curve  $\gamma$  with  $\gamma(0) = x$ ,  $\gamma'(0) = v$ . Then there exist  $t_k \rightarrow 0^+$  and horizontal  $\sigma_k$  from  $x$  to  $\gamma(t_k)$  with  $L(\sigma_k) \leq C t_k$ . Repeat the averaging argument above:  $\rho_x \bar{u}_k \rightarrow v$  and  $\|\bar{u}_k\|_x \leq C$  along a subsequence. Passing to the limit yields  $v \in \rho_x(F) = \mathcal{D}_x$ , a contradiction. Hence  $\lim_{t \rightarrow 0^+} d(x, \gamma(t))/t = +\infty$ .

This proves both statements.  $\square$

We have now introduced the Banach sub-Finsler toolkit needed to study approximation complexity: Banach manifolds and charts, tangent bundles, anchored bundles (distributions), fiber-wise norms (sub-Finsler structures), horizontal curves, and the associated geodesic distance. This framework gives

a geometric interpretation of the distance  $d_{\mathcal{F}}(\cdot, \cdot)$ : it coincides with the geodesic distance induced by a right-invariant sub-Finsler structure on the Banach manifold of  $W^{1,\infty}$ -diffeomorphisms.

In the next subsection we make this relation precise by identifying the relevant Banach manifold, the anchored bundle and its fiber-wise norm, and by stating and proving the main theorem that characterizes  $d_{\mathcal{F}}$  in terms of the sub-Finsler geometry developed above.

**4.2. General characterization of approximation complexity via Finsler geometry.** We now adopt the Banach Finsler geometry framework to study the approximation complexity for a general control family  $\mathcal{F}$ . Specifically, let  $M \subset \mathbb{R}^d$  be a compact smooth manifold with or without boundary, and  $\mathcal{F} \subset \text{Vec}(M)$  be a control family.

We assume that  $\mathcal{F}$  is uniformly bounded in the  $W^{1,\infty}$  norm, i.e.

$$(4.27) \quad \sup_{f \in \mathcal{F}} \|f\|_{W^{1,\infty}(M, \mathbb{R}^d)} < \infty.$$

Define the  $s$ -scaled convex hull of  $\mathcal{F}$  as

$$(4.28) \quad \mathbf{CH}_s(\mathcal{F}) := \left\{ \sum_{i=1}^N a_i f_i : f_i \in \mathcal{F}, \sum_{i=1}^N |a_i| \leq s \right\}.$$

Then, we consider the extended norm on  $\text{Vec}(M)$  defined as:

$$(4.29) \quad \|v\|_{\mathcal{F}} := \inf \{s \geq 0 : v \in \overline{\mathbf{CH}_s(\mathcal{F})}^{C^0}\},$$

with the convention  $\|v\|_{\mathcal{F}} = +\infty$  if  $v \notin \overline{\text{span } \mathcal{F}}^{C^0}$ . The norm  $\|\cdot\|_{\mathcal{F}}$  is naturally finite on  $\text{span } \mathcal{F}$ . Here, the closure is taken in the  $C^0(M, \mathbb{R}^d)$  topology. We denote by  $X_{\mathcal{F}}$  the closure of  $\text{span } \mathcal{F}$  under the  $\|\cdot\|_{\mathcal{F}}$  norm. Since  $\mathcal{F}$  is uniformly bounded in  $W^{1,\infty}$ ,  $\mathbf{CH}_s(\mathcal{F})$  is also uniformly bounded in  $W^{1,\infty}$  for each  $s$ . Since the  $C^0$  closure of a uniformly  $W^{1,\infty}$ -bounded set is still uniformly  $W^{1,\infty}$ -bounded, we have  $X_{\mathcal{F}} \subset W^{1,\infty}(M, \mathbb{R}^d)$ .

We make the following definition on the regularity of  $\mathcal{F}$  and the choice of the base Banach manifold  $\mathcal{M}$  on which we place the sub-Finsler structure.

**Definition 4.8** (Compatible pair). *Let  $\mathcal{M} \subset \text{Diff}(M)$  and  $\mathcal{F} \subset \text{Vec}(M)$ . We say that  $(\mathcal{M}, \mathcal{F})$  is a compatible pair if the following hold:*

- (1) ( $C^1$  Banach manifold structure via exponential charts)  $\mathcal{M}$  carries a  $C^1$  Banach manifold structure modeled on a subspace  $X \subset \text{Vec}(M)$  whose local charts are given by Riemannian exponential maps (as in Example 4.2).
- (2) (right translation is  $C^1$ ) For each  $\psi \in \mathcal{M}$ , the right-translation map  $R_{\psi} : \mathcal{M} \rightarrow \mathcal{M}$ ,  $R_{\psi}(\eta) = \eta \circ \psi$ , is of class  $C^1$ .
- (3) (admissible velocities) For every  $\psi \in \mathcal{M}$  and  $f \in X_{\mathcal{F}}$ ,  $f \circ \psi \in T_{\psi} \mathcal{M}$ .
- (4) (Invariance of  $\mathcal{M}$  under Carathéodory controls) For any measurable  $u(\cdot) : [0, T] \rightarrow X_{\mathcal{F}}$ , the ODE

$$(4.30) \quad \dot{\gamma}(t) = u(t) \circ \gamma(t), \quad \gamma(0) = \text{Id},$$

admits a unique absolutely continuous solution on  $[0, T]$ , and  $\gamma(t) \in \mathcal{M}$  for all  $t \in [0, T]$ .

The conditions in the above definition are quite natural and are satisfied in many settings of interest, including the one considered in section 3. In particular, the following example illustrates a typical and general class of compatible pairs.

**Example 4.3.** *A typical type of compatible pairs is the following.*

*Suppose  $M \subset \mathbb{R}^d$  is the closure of a bounded open set,  $\mathcal{M} = \text{Diff}^{W^{1,\infty}}(M)$  consists of  $W^{1,\infty}$  diffeomorphisms fixing the boundary, and  $\mathcal{F} \subset W^{1,\infty}(M, \mathbb{R}^d)$  such that  $f$  vanishes on the boundary for all  $f \in \mathcal{F}$ . Then  $(\mathcal{M}, \mathcal{F})$  is a compatible pair.*

*Indeed, (1) holds with model space*

$$(4.31) \quad X := \{u \in W^{1,\infty}(M, \mathbb{R}^d) : u|_{\partial M} = 0\},$$

and the local charts around  $\psi \in \mathcal{M}$  can be chosen as the affine maps

$$(4.32) \quad \beta_\psi : B_X(0, \varepsilon) \rightarrow \mathcal{M}, \quad \beta_\psi(u) := (\text{Id} + u) \circ \psi,$$

for  $\varepsilon > 0$  sufficiently small. Since  $u|_{\partial M} = 0$  and  $\psi$  fixes  $\partial M$ , we have  $\beta_\psi(u)$  also fixes  $\partial M$ ; moreover for  $\varepsilon$  small,  $\text{Id} + u$  is bi-Lipschitz on  $M$ , hence  $\beta_\psi(u) \in \text{Diff}^{W^{1,\infty}}(M)$ . In these charts, all transition maps are smooth (in fact affine), so  $\mathcal{M}$  is a  $C^1$  Banach manifold.

(2) is immediate: right translation is composition on the right,  $R_\varphi(\eta) = \eta \circ \varphi$ , and in the above charts it corresponds to the affine map  $u \mapsto u \circ \varphi$ , which is  $C^1$  as a map  $X \rightarrow X$  (composition by a fixed  $W^{1,\infty}$  diffeomorphism is bounded on  $W^{1,\infty}$ ).

(3) holds because  $f|_{\partial M} = 0$  for all  $f \in \mathcal{F}$  implies  $X_{\mathcal{F}} \subset X$ , and hence for any  $\psi \in \mathcal{M}$  we have  $X_{\mathcal{F}} \circ \psi \subset X \circ \psi = T_\psi \mathcal{M}$  under the above charts.

Finally, (4) follows from standard well-posedness and stability results for Carathéodory ODEs with Lipschitz vector fields. Indeed, for a measurable  $u(\cdot) : [0, T] \rightarrow X_{\mathcal{F}}$  we have  $\|Du(t)\|_{L^\infty} \lesssim \|u(t)\|_{\mathcal{F}}$ , hence  $t \mapsto \|Du(t)\|_{L^\infty}$  is integrable on  $[0, T]$ . Existence and uniqueness of an absolutely continuous solution to  $\dot{\gamma}(t) = u(t) \circ \gamma(t)$  then follow from the Carathéodory theory. Moreover, Grönwall's inequality gives a uniform bi-Lipschitz bound on  $\gamma(t)$  (and on its inverse by time-reversal), and the condition  $u(t)|_{\partial M} = 0$  implies that boundary points are stationary trajectories. Therefore  $\gamma(t)$  fixes  $\partial M$  and belongs to  $\text{Diff}^{W^{1,\infty}}(M) = \mathcal{M}$  for all  $t \in [0, T]$ .

In fact, the 1D example considered in section 3 is a special case of this setting, where  $M = [0, 1]$  and  $\mathcal{F}$  consists of ReLU-type controls vanishing at the boundary.

We now consider a target space  $\mathcal{T}$  consisting of maps that can be approximated by the flows driven with  $\mathcal{F}$  within a finite time:

$$(4.33) \quad \mathcal{T} := \{\psi \in \mathcal{M} \mid \mathbf{C}_{\mathcal{F}}(\psi) < \infty\}.$$

The complexity measure  $\mathbf{C}_{\mathcal{F}}$  (defined in (2.9)) can be extended to a distance function  $d_{\mathcal{F}}$  on  $\mathcal{T}$ :

$$(4.34) \quad d_{\mathcal{F}}(\psi_1, \psi_2) := \inf\{T > 0 \mid \psi_1 \in \overline{\mathcal{A}_{\mathcal{F}}(T) \circ \psi_2}^{C^0}\},$$

In fact, this distance can be generalized to an extended metric on  $\mathcal{M}$ , by defining  $d_{\mathcal{F}}(\psi_1, \psi_2) := +\infty$  if  $\psi_1 \notin \overline{\mathcal{A}_{\mathcal{F}}(T) \circ \psi_2}^{C^0}$  for all  $T > 0$ . With this extended distance,  $\mathcal{T}$  can be viewed as the connected component of the identity in the extended metric space  $(\mathcal{M}, d_{\mathcal{F}})$ . We then show that  $\mathcal{M}$  can be endowed with a sub-Finsler structure such that the associated geodesic distance coincides with  $d_{\mathcal{F}}$ .

Consider the anchored Banach bundle  $(\mathcal{E}, \pi, \rho)$  over  $\mathcal{M}$  defined as:

$$(4.35) \quad \mathcal{E} := \mathcal{M} \times X_{\mathcal{F}}, \quad \pi(\psi, v) := \psi, \quad \rho(\psi, v) := v \circ \psi, \text{ for all } (\psi, v) \in \mathcal{E}.$$

Its image defines the horizontal distribution

$$(4.36) \quad \mathcal{D}_\psi := \rho_\psi(X_{\mathcal{F}}) = X_{\mathcal{F}} \circ \psi \subset T_\psi \mathcal{M},$$

endowed with the fiberwise norm

$$(4.37) \quad \|u\|_\psi := \|u \circ \psi^{-1}\|_{\mathcal{F}}, \quad u \in \mathcal{D}_\psi, \quad \|u\|_\psi = +\infty \text{ if } u \notin \mathcal{D}_\psi.$$

This gives a sub-Finsler structure  $(\mathcal{D}, \|\cdot\|_{\mathcal{D}})$  on  $\mathcal{M}$ .

With these preparations, we can give detailed explanations of the main theorem stated in Theorem 2.1. If we assume  $(\mathcal{M}, \mathcal{F})$  is a compatible pair of a control family  $\mathcal{F}$  and a base manifold  $\mathcal{M}$  as defined in Definition 4.8. Then, the following statements hold:

- (1) The maps  $\|\cdot\|_\psi : T_\psi \mathcal{M} \rightarrow [0, \infty]$  defined in (4.37) gives a sub-Finsler structure on the distribution  $\mathcal{D}$  over  $\text{Diff}^1(M)$ .
- (2) For any  $\psi_1, \psi_2 \in \mathcal{M}$ ,

$$(4.38) \quad d_{\mathcal{F}}(\psi_1, \psi_2) = \inf \left\{ \int_0^1 \|\dot{\gamma}(t)\|_{\gamma(t)} dt : \gamma \text{ horizontal, } \gamma(0) = \psi_1, \gamma(1) = \psi_2 \right\}.$$

That is, the geodesic distance associated with the sub-Finsler structure  $(\mathcal{D}, \|\cdot\|_{\mathcal{D}})$  coincides with  $d_{\mathcal{F}}$  on  $\mathcal{M}$ .

**Remark 4.1.** *This distance defined by the right hand side in (4.38) is typically called the Carnot-Carathéodory in the literature of sub-Riemannian geometry. We adopt the name "geodesic distance" for simplicity here.*

*Moreover, when  $\mathcal{D}_{\psi} = T_{\psi}\mathcal{M}$  for all  $\psi \in \mathcal{M}$ , i.e.  $\mathcal{F}$  spans the whole tangent space, the map  $\|\cdot\|_{\psi}$  gives a Finsler structure on  $\mathcal{M}$ . In this case,  $\mathcal{M}$  becomes a Finsler manifold, and  $d_{\mathcal{F}}$  becomes an actual geodesic distance.*

This theorem offers a general geometric perspective to understand the approximation complexity of diffeomorphisms induced by a given control family  $\mathcal{F}$ . In particular, the local norm  $\|\cdot\|_{\psi}$  characterizes the local complexity of transporting a function to its nearby functions, while the global distance  $d_{\mathcal{F}}(\cdot, \cdot)$  quantifies the overall complexity of transporting one function to another via the shortest path integral of the local norm along curves connecting the two functions.

In general, a closed-form characterization of the distance  $d_{\mathcal{F}}(\cdot, \cdot)$  on  $\mathcal{M}$  may not be available. However, this theorem still provides a feasible approach to estimate it. Specifically, we can follow the steps below:

- First, we estimate the local norm  $\|\cdot\|_{\psi}$  at different  $\psi$  in  $\mathcal{M}$ . This relates to the approximation complexity of each shallow layer of neural networks, which has been widely studied in the literature [29, 38, 39].
- Next, we construct proper horizontal paths connecting the two target functions in  $\mathcal{M}$ . This step may require insights into the structure of  $\mathcal{M}$  and the dynamics induced by  $\mathcal{F}$ .
- Finally, we compute or estimate the path integral of the local norm along these paths to obtain upper bounds on  $d_{\mathcal{F}}(\cdot, \cdot)$ .

From the deep learning perspective, the distance  $d_{\mathcal{F}}$  measures the idealized depth of network to approximate a target function with layer-wise architecture induced by  $\mathcal{F}$ . Therefore, this theorem provides a general framework to identify what kind of target functions are more efficiently approximated by deep networks compared to shallow ones, and how this efficiency depends on the choice of the control family  $\mathcal{F}$ . Roughly speaking, if the target function can be connected to the identity map via a path passing through functions with small local norms, then it can be efficiently approximated by deep networks. For some control families, as we discuss later in Section 5, explicit characterisations or estimates can be obtained.

Let us now place this geometric framework in the broader context of approximation theory for neural networks. Classical results for shallow networks focus on universal approximation and Jackson-type estimates for one-hidden-layer architectures, where approximation complexity is typically quantified in terms of Sobolev, Besov, or Barron-type norms of the target function [11, 22, 6, 29, 39, 38]. In contrast, the theory of deep networks must account for the compositional structure. One line of work studies discrete-depth architectures directly, deriving explicit approximation bounds for specific architectures via constructive methods [28, 35, 37, 36, 53, 54]. A second line of work, closer to our approach, idealizes residual networks [20] as continuous-time systems and analyses the associated flow maps, viewing depth as a time horizon for an ODE or control system [49, 34, 25]. Within this flow-based perspective, the universal approximation results for a very broad class of architectures have been established [2, 26, 8, 33, 45, 9]. Approximation complexity estimates have also been studied for specific architectures [17, 33, 26], often by explicit constructions. Although the passage from discrete layers to flows is an idealization, it preserves the key distinguishing feature of deep models, where complexity generated by function composition, while making available tools from dynamical systems and control theory. Our work contributes to this flow-based perspective by identifying a geometric structure on the complexity class defined by the flow approximation problem, and showing that concrete estimates can be derived within this structure. This geometry is intrinsically non-linear and differs from the linear space setting of classical approximation theory, and we believe it provides a reasonable way to understand the complexity induced by function compositions.

In the rest of this part, we present the proof of Theorem 2.1.

We first show that the fiberwise norm in (4.37) defines a sub-Finsler structure on the right-invariant distribution induced by  $X_{\mathcal{F}}$ . Recall the anchored bundle

$$(4.39) \quad \mathcal{E} := \mathcal{M} \times X_{\mathcal{F}} \xrightarrow{\pi} \mathcal{M}, \quad \pi(\psi, v) = \psi, \quad \rho(\psi, v) = \iota(v) \circ \psi.$$

By compatibility condition (3) in Definition 4.8, the image of  $\rho$  defines a distribution

$$(4.40) \quad \mathcal{D}_{\psi} := \rho_{\psi}(X_{\mathcal{F}}) = X_{\mathcal{F}} \circ \psi \subset T_{\psi}\mathcal{M}, \quad \psi \in \mathcal{M}.$$

We endow  $\mathcal{D}$  with the fiberwise (extended) norm

$$(4.41) \quad \|\xi\|_{\psi} := \begin{cases} \|\xi \circ \psi^{-1}\|_{\mathcal{F}}, & \xi \in \mathcal{D}_{\psi}, \\ +\infty, & \xi \notin \mathcal{D}_{\psi}. \end{cases}$$

Equivalently, if  $\xi = v \circ \psi$  for some  $v \in X_{\mathcal{F}}$ , then  $\|\xi\|_{\psi} := \|v\|_{\mathcal{F}}$ . This is well-defined because right composition by  $\psi$  is a bijection on its image. For each fixed  $\psi$ ,  $\xi \mapsto \|\xi\|_{\psi}$  is a norm on  $\mathcal{D}_{\psi}$ , since  $v \mapsto v \circ \psi$  is a linear isomorphism  $X_{\mathcal{F}} \rightarrow \mathcal{D}_{\psi}$ .

It remains to check the local regularity required of a sub-Finsler structure in charts. Let  $(U_{\psi}, \beta_{\psi})$  be a  $C^1$  exponential chart of  $\mathcal{M}$  around  $\psi$ , modeled on a Banach space  $X$ . Since  $(\mathcal{M}, \mathcal{F})$  is a compatible pair, right translation  $R_{\varphi} : \eta \mapsto \eta \circ \varphi^{-1}$  is  $C^1$  on  $\mathcal{M}$  for  $\varphi$  in a neighborhood of  $\psi$ . In particular, in the chart  $(U_{\psi}, \beta_{\psi})$  the map

$$(4.42) \quad (\varphi, \xi) \longmapsto (dR_{\varphi})_{\varphi}[\xi]$$

is continuous, and (by construction of the right-invariant distribution) this continuity is exactly what is needed to ensure that  $\|\cdot\|_{\varphi}$  varies continuously with  $\varphi$  on the distribution  $\mathcal{D}_{\varphi}$ . More concretely, for  $\xi \in \mathcal{D}_{\varphi}$  we can write  $\xi = v \circ \varphi$  with  $v \in X_{\mathcal{F}}$ , and then

$$(4.43) \quad \|\xi\|_{\varphi} = \|v\|_{\mathcal{F}},$$

so the only dependence on  $\varphi$  is through the identification of  $\mathcal{D}_{\varphi}$  with  $X_{\mathcal{F}}$  via right translation, which is  $C^1$  by condition (2). This establishes that  $\{\|\cdot\|_{\psi}\}_{\psi \in \mathcal{M}}$  defines a sub-Finsler structure on  $\mathcal{D}$ .

We then show the equality of  $d_{\mathcal{F}}$  and the geodesic distance. Let  $d(\cdot, \cdot)$  denote the geodesic distance induced by the sub-Finsler norm, i.e.

$$(4.44) \quad d(\psi_1, \psi_2) := \inf \left\{ \int_0^1 \|\dot{\gamma}(t)\|_{\gamma(t)} dt : \gamma \text{ horizontal}, \gamma(0) = \psi_2, \gamma(1) = \psi_1 \right\}.$$

We first show that  $d \leq d_{\mathcal{F}}$ . We will use the following lemma, which is a Young measure-type compactness result [5] for measurable functions taking values in a compact set of vector fields.

**Lemma 4.1.** *Let  $K$  be a compact metric space and let  $u_n : [0, T] \rightarrow K$  be a sequence of measurable maps. Then there exist a subsequence  $u_{n_k}$  and a measurable family  $\nu_t \in \mathcal{P}(K)$  such that for every  $\Phi \in C(K, \mathbb{R})$  and every  $\varphi \in L^{\infty}([0, T], \mathbb{R})$ ,*

$$(4.45) \quad \int_0^T \varphi(t) \Phi(u_{n_k}(t)) dt \longrightarrow \int_0^T \varphi(t) \left( \int_K \Phi(v) d\nu_t(v) \right) dt.$$

Moreover, if  $K$  is convex and closed in a locally convex vector space (in particular in  $C^0(M)$ ), then the barycenter

$$(4.46) \quad u(t) := \int_K v d\nu_t(v)$$

belongs to  $K$  for a.e.  $t$ .

*Proof.* Define probability measures  $\mu_n \in \mathcal{P}([0, T] \times K)$  by

$$\int \zeta(t, v) d\mu_n(t, v) := \frac{1}{T} \int_0^T \zeta(t, u_n(t)) dt, \quad \forall \zeta \in C([0, T] \times K).$$

Since  $[0, T] \times K$  is compact,  $\{\mu_n\}$  is tight and hence relatively compact in the weak topology; extract  $\mu_n \rightharpoonup \mu$ . The time-marginal of each  $\mu_n$  is  $dt/T$ , hence the same holds for  $\mu$ . By disintegration there exists a measurable family  $\nu_t \in \mathcal{P}(K)$  such that  $d\mu(t, v) = \frac{1}{T} dt d\nu_t(v)$ , which yields (4.45). If  $K$  is convex and closed in a locally convex space, then (4.46) lies in  $K$  by Jensen/barycenter properties of convex closed sets.  $\square$

Fix  $\psi_1, \psi_2 \in \mathcal{M}$ . By applying a right translation, it suffices to prove the claim for  $(\psi_1 \circ \psi_2^{-1}, \text{Id})$ . Thus, we assume  $\psi_2 = \text{Id}$  below.

Let  $T > d_{\mathcal{F}}(\psi_1, \text{Id})$ . By definition of  $d_{\mathcal{F}}$ , there exists a sequence  $\xi_n \in \mathcal{A}_{\mathcal{F}}(T) \circ \text{Id}$  with

$$(4.47) \quad \xi_n \rightarrow \psi_1 \quad \text{in } C^0(M).$$

For each  $n$ , choose a piecewise-constant control  $u_n : [0, T] \rightarrow \mathbf{CH}_1(\mathcal{F})$  driving a curve  $\gamma_n : [0, T] \times \mathcal{M} \rightarrow \mathcal{M}$  such that

$$(4.48) \quad \gamma_n(t, x) = x + \int_0^t u_n(s, \gamma_n(s, x)) ds, \quad \gamma_n(0, \cdot) = \text{Id}, \quad \gamma_n(T, \cdot) = \xi_n.$$

Reparametrize if necessary so that

$$(4.49) \quad \|u_n(t)\|_{\mathcal{F}} \leq 1 \quad \text{for a.e. } t \in [0, T].$$

Set  $K := \overline{\mathbf{CH}_1(\mathcal{F})}^{C^0}$ . Since  $\mathcal{F}$  is uniformly bounded in  $W^{1, \infty}$ ,  $K$  is compact in  $C^0(M)$  according to the Arzelà–Ascoli theorem. By the Grönwall inequality, each  $\gamma_n(t, \cdot)$  is uniformly Lipschitz in  $x$ , and the family  $\{\gamma_n\}$  is equicontinuous in  $t$  with respect to the  $C^0$ -metric. By Arzelà–Ascoli, after extracting a subsequence,

$$(4.50) \quad \gamma_n \rightarrow \gamma \quad \text{in } C^0([0, T] \times M),$$

for some continuous  $\gamma$  with  $\gamma(0, \cdot) = \text{Id}$  and  $\gamma(T, \cdot) = \psi_1$ .

By the compactness of  $K$ , we can apply Lemma 4.1 to the measurable maps  $u_n : [0, T] \rightarrow K$  to obtain a measurable map  $t \rightarrow \nu_t \in \mathcal{P}(K)$  and define the barycenter

$$(4.51) \quad u(t) := \int_K v d\nu_t(v) \in K, \quad \|u(t)\|_{\mathcal{F}} \leq 1 \quad \text{for a.e. } t.$$

The inclusion in  $K$  uses that  $K$  is convex.

Fix  $x \in M$  and  $t \in [0, T]$ . From (4.48) we write

$$\gamma_n(t, x) - x = \int_0^t u_n(s, \gamma_n(s, x)) ds.$$

We claim that

$$(4.52) \quad \int_0^t u_n(s, \gamma_n(s, x)) ds \longrightarrow \int_0^t u(s, \gamma(s, x)) ds.$$

Indeed, decompose

$$\int_0^t [u_n(s, \gamma_n(s, x)) - u_n(s, \gamma(s, x))] ds + \int_0^t [u_n(s, \gamma(s, x)) - u(s, \gamma(s, x))] ds =: (I)_n + (II)_n.$$

For  $(I)_n$ , use the uniform Lipschitz bound on  $u_n(s, \cdot)$  and (4.50):

$$|(I)_n| \leq \int_0^t L \|\gamma_n(s, \cdot) - \gamma(s, \cdot)\|_{C^0} ds \longrightarrow 0.$$

For  $(II)_n$ , by uniform continuity of  $s \mapsto \gamma(s, x)$ , choose a partition  $0 = t_0 < \dots < t_m = t$  such that

$$(4.53) \quad \sup_{s \in [t_{j-1}, t_j]} \|\gamma(s, x) - \gamma(t_{j-1}, x)\| \leq \delta, \quad j = 1, \dots, m,$$

with  $\delta > 0$  to be chosen momentarily. Set  $y_j := \gamma(t_{j-1}, x)$ . Then, by the Lipschitz bound,

$$(4.54) \quad \left| \int_{t_{j-1}}^{t_j} u_n(s, \gamma(s, x)) ds - \int_{t_{j-1}}^{t_j} u_n(s, y_j) ds \right| \leq L \delta (t_j - t_{j-1}),$$

where  $L$  is a uniform Lipschitz constant for  $u_n(s, \cdot)$ , and similarly with  $u$  in place of  $u_n$ . Summing over  $j$  gives

$$(4.55) \quad |(II)_n| \leq \sum_{j=1}^m \left| \int_{t_{j-1}}^{t_j} [u_n(s, y_j) - u(s, y_j)] ds \right| + 2L\delta t.$$

Now, for each fixed  $y \in M$ , the map  $\Phi_y : K \rightarrow \mathbb{R}^d$ ,  $\Phi_y(v) := v(y)$  is continuous. Applying Lemma 4.1 with  $\Phi = \Phi_{y_j}$  and  $\varphi = \mathbf{1}_{[t_{j-1}, t_j]}$  yields

$$(4.56) \quad \int_{t_{j-1}}^{t_j} u_n(s, y_j) ds \rightarrow \int_{t_{j-1}}^{t_j} u(s, y_j) ds \quad \text{for each } j.$$

Hence  $\limsup_{n \rightarrow \infty} |(II)_n| \leq 2L\delta t$ . Since  $\delta$  can be made arbitrarily small, we get  $(II)_n \rightarrow 0$ , proving (4.52). Passing to the limit in (4.48) using (4.50) gives, for all  $x$  and  $t$ ,

$$(4.57) \quad \gamma(t, x) = x + \int_0^t u(s, \gamma(s, x)) ds.$$

Thus  $\gamma$  is a Carathéodory solution driven by the control  $u(\cdot)$ . According to the condition (4) in Definition 4.8,  $\gamma(t, \cdot) \in \mathcal{M}$  for all  $t$ . Moreover, we have  $\|u(t)\|_{\mathcal{F}} \leq 1$  for a.e.  $t$ , so  $\gamma$  is an admissible (horizontal) curve from  $\text{Id}$  to  $\psi_1$  and

$$(4.58) \quad L(\gamma) = \int_0^T \|u(t)\|_{\mathcal{F}} dt \leq T.$$

Therefore  $d(\psi_1, \text{Id}) \leq T$ . Since  $T > d_{\mathcal{F}}(\psi_1, \text{Id})$  was arbitrary, we conclude  $d(\psi_1, \text{Id}) \leq d_{\mathcal{F}}(\psi_1, \text{Id})$ , and by right-invariance the same holds for general  $(\psi_1, \psi_2)$ :

$$(4.59) \quad d(\psi_1, \psi_2) \leq d_{\mathcal{F}}(\psi_1, \psi_2).$$

Finally, let us show that  $d_{\mathcal{F}} \leq d$ . Let  $\gamma : [0, 1] \rightarrow \mathcal{M}$  be horizontal with  $\dot{\gamma}(t) = v(t) \circ \gamma(t)$  and  $v(\cdot)$  measurable with  $\int_0^1 \|v(t)\|_{\mathcal{F}} dt < \infty$ . We approximate  $t \mapsto v(t)$  in  $L^1$  by simple functions taking values in  $\mathbf{CH}_1(\mathcal{F})$ . On each subinterval where the control function  $f = \sum_{i=1}^N a_i f_i$  is the convex combination of finitely many vector fields  $f_i \in \mathcal{F}$ , we apply the corresponding piecewise-constant controls with total time equal to the sum of the coefficients  $\sum_{i=1}^N |a_i|$ , so that the endpoint converges to  $\gamma(1)$  while the total time converges to  $\int_0^1 \|v(t)\|_{\mathcal{F}} dt$ . Taking infima over all horizontal  $\gamma$  gives  $d_{\mathcal{F}}(\psi_1, \psi_2) \leq d(\psi_1, \psi_2)$ .

Combining the two inequalities we obtain  $d = d_{\mathcal{F}}$  on  $\text{Diff}^1(M)$ . This completes the proof.

**4.3. Interpolation distance, variational formula and asymptotic properties.** Our geometric framework is closely related to the analysis of reachability and minimal-time problems in classical control theory, related to finite-dimensional sub-Riemannian geometry [30, 1]. The key difference is that the manifold  $\mathcal{M}$  we study is generally infinite-dimensional, and the local metric may not be induced from an inner product. Another related concept is the universal interpolation problem of flows studied in [8, 10]. In [8], it is shown that for a control family  $\mathcal{F}$  and a target function  $\psi$ , if any set of finite samples  $\{(x_i, \psi(x_i))\}_{i=1}^m$  can be interpolated by some flow in  $\mathcal{A}_{\mathcal{F}}(T)$  within a uniform time  $T$  independent of  $m$  and the samples, then the control family  $\mathcal{F}$  can also approximate  $\psi$  uniformly within a finite time.

Given these connections, it is thus natural to consider what the finite-dimensional geometry induced by the corresponding finite-point interpolation problem is, and how it relates to the infinite dimensional geometry we studied before.

In the following, we will use  $x, y, z$  to denote points in  $M$  or  $T_x M$ , and use  $\mathbf{x}, \mathbf{y}, \mathbf{z}$  to denote points in  $M^m$  or  $T_{\mathbf{x}} M^m$  (the  $m$ -fold product). We still use  $\varphi, \psi$  to denote flows in  $\mathcal{A}_{\mathcal{F}}$ .

We first show how the control function induces a metric in  $M^m$ . We begin with the case when  $m = 1$ . In this case, we recover the classical metric induced by the minimal time control [44]. That is, for  $x, y \in M$ , we define

$$(4.60) \quad d_{\mathcal{F}}^{[1]}(x, y) = \inf\{T > 0 \mid \exists \varphi \in \overline{\mathcal{A}_{\mathcal{F}}(T)}, \varphi(x) = y\}.$$

For the general case, consider  $\mathbf{x} = (x_1, x_2, \dots, x_m) \in M^m$  and  $\mathbf{y} = (y_1, y_2, \dots, y_m) \in M^m$ . Then we can define similarly

$$(4.61) \quad d_{\mathcal{F}}^{[m]}(\mathbf{x}, \mathbf{y}) = \inf\{T > 0 \mid \exists \varphi \in \overline{\mathcal{A}_{\mathcal{F}}(T)}, \varphi(x_i) = y_i, i = 1, \dots, m\}.$$

In fact, the minimum can be achieved as shown in the following.

**Proposition 4.3.** *There exists  $\varphi \in \overline{\mathcal{A}_{\mathcal{F}}(d_{\mathcal{F}}^{[m]}(\mathbf{x}, \mathbf{y}))}$ , such that  $\varphi(x_i) = y_i$  for  $i = 1, \dots, m$ .*

*Proof.* First, we notice that for any  $\varphi_1 \in \mathcal{A}_{\mathcal{F}}(t_1 + t_2)$ , there exists  $\varphi_2 \in \mathcal{A}_{\mathcal{F}}(t_1)$  such that

$$(4.62) \quad \|\varphi_2 - \varphi_1\|_{C(M)} \leq (e^{t_2} - 1)\|\varphi_1\|_{C(M)}.$$

This follows by truncating the dynamics of  $\varphi_1$ .

For any positive integer  $N > 0$ , there exists  $\varphi_N \in \mathcal{A}_{\mathcal{F}}(d_{\mathcal{F}}^{[m]}(\mathbf{x}, \mathbf{y}) + \frac{1}{N})$  such that

$$(4.63) \quad |\varphi_N(x_i) - y_i| < \frac{1}{N}.$$

According to the above fact, there exists  $\tilde{\varphi}_N \in \mathcal{A}_{\mathcal{F}}(d_{\mathcal{F}}^{[m]}(\mathbf{x}, \mathbf{y}))$  such that

$$(4.64) \quad \|\tilde{\varphi}_N(x_i) - y_i\| \leq \frac{e^{\frac{1}{N}}}{N}.$$

Since  $\mathcal{F}$  is uniformly bounded and uniformly Lipschitz, the sequence  $\{\tilde{\varphi}_N\}_{N=1}^{\infty}$  is uniformly bounded and uniformly equicontinuous. By the Arzela-Ascoli theorem, the sequence  $\{\tilde{\varphi}_N\}_{i=1}^{\infty}$  has a convergece subsequence. Denote this limit as  $\tilde{\varphi} \in \overline{\mathcal{A}_{\mathcal{F}}(d_{\mathcal{F}}^{[m]}(\mathbf{x}, \mathbf{y}))}$ , then we have  $\tilde{\varphi}(x_i) = y_i$ .  $\square$

Our goal is now to connect this minimal-time distance to  $d_{\mathcal{F}}$ . We fix a sequence of sampling sets  $Z^{[m]} = \{z_i^{[m]}\}_{i=1}^m \subset M$  that asymptotically covers  $M$ , that is,

$$(4.65) \quad \lim_{n \rightarrow \infty} \min_{i \in [n]} |y - z_i| = 0, \text{ for all } y \in M.$$

We next define the sampling map

$$(4.66) \quad I^{[m]} : \text{Diff}(M) \rightarrow M^m, \quad I^{[m]}(\psi) := (\psi(z_1^{[m]}), \dots, \psi(z_m^{[m]})).$$

For  $\psi_1, \psi_2 \in \text{Diff}(M)$  write  $\mathbf{x} = I^{[m]}(\psi_1)$ ,  $\mathbf{y} = I^{[m]}(\psi_2) \in M^m$ . Now, we can show that for each  $m$ , the minimal-time distance  $d_{\mathcal{F}}^{[m]}$  admits a variational characterization in terms of the geodesic distance  $d_{\mathcal{F}}$ , linking finite-dimensional control theory to our formulation.

**Proposition 4.4.** *We have*

$$d_{\mathcal{F}}^{[m]}(\mathbf{x}, \mathbf{y}) = \min_{I^{[m]}\psi_1 = \mathbf{x}, I^{[m]}\psi_2 = \mathbf{y}} d_{\mathcal{F}}(\psi_1, \psi_2).$$

*Proof.* We first fix  $\psi_1$  and  $\psi_2$ , since  $d_{\mathcal{F}}^{[m]}(I^{[m]}\psi_1, I^{[m]}\psi_2) \leq d_{\mathcal{F}}(\psi_1, \psi_2)$ . We then have  $d_{\mathcal{F}}^{[m]}(\mathbf{x}, \mathbf{y}) \leq d_{\mathcal{F}}(\psi_1, \psi_2)$  whenever  $I^{[m]}\psi_1 = \mathbf{x}$  and  $I^{[m]}\psi_2 = \mathbf{y}$ .

Conversely, let  $\delta > 0$ , for  $\mathbf{x}, \mathbf{y} \in M^m$ , we take  $T = d_{\mathcal{F}}^{[m]}(\mathbf{x}, \mathbf{y})$  and consider flow maps in  $\mathcal{A}_{\mathcal{F}}(T)$ . For any  $\varepsilon > 0$ , there exists  $\varphi \in \overline{\mathcal{A}_{\mathcal{F}}(T)}$  such that  $\varphi(x_i) = y_i$  by Proposition 4.3. For any  $\psi_1$  such that  $I^{[m]}\psi_1 = \mathbf{x}$ , we take  $\psi_2 = \varphi \circ \psi_1 \in \overline{\mathcal{A}_{\mathcal{F}}(T) \circ \psi_1}$ . Therefore,  $d_{\mathcal{F}}(\psi_1, \psi_2) \leq T \leq d_{\mathcal{F}}(\psi_1, \psi_2) + \delta$ . Take  $\delta$  to be arbitrarily small, we conclude the result.  $\square$

Conversely, we can show that the infinite-dimensional distance  $d_{\mathcal{F}}$  is actually the limit of the finite-dimensional Carnot-Carathéodory distance  $d_{\mathcal{F}}^{[m]}$  as  $m \rightarrow \infty$ .

**Proposition 4.5.** *Fix  $\psi_1, \psi_2 \in \mathcal{M}$ , then*

$$(4.67) \quad \lim_{m \rightarrow \infty} d_{\mathcal{F}}^{[m]}(I^{[m]}(\psi_1), I^{[m]}(\psi_2)) = d_{\mathcal{F}}(\psi_1, \psi_2).$$

*Proof.* The upper bound  $d_{\mathcal{F}}^{[m]} \leq d_{\mathcal{F}}$  follows from Proposition 4.4. For lower bound, if for some  $\eta > 0$ , infinitely many  $m$  satisfy  $d_{\mathcal{F}}^{[m]} \leq d_{\mathcal{F}} - \eta$ , then by Proposition 4.3 we obtain  $\varphi_m \in \mathcal{A}_{\mathcal{F}}(T)$  with  $T \leq d_{\mathcal{F}} - \eta/2$  matching the samples. Equicontinuity of functions in  $\mathcal{A}_{\mathcal{F}}(T)$  and density of  $Z^{[m]}$  give a subsequence  $\varphi_m \rightarrow \varphi$  uniformly with  $\varphi \circ \psi_2 = \psi_1$ , contradicting the minimality of  $d_{\mathcal{F}}$ .  $\square$

Recall the relation between local sub-Finsler norms and the global metric  $d_{\mathcal{F}}$  established in Theorem 2.1 for the infinite-dimensional case. We now establish the analogous relations for the finite-dimensional manifold  $M^m$  equipped with the distance  $d_{\mathcal{F}}^{[m]}$ .

Write  $\psi^{[m]} := I^{[m]}(\psi) \in M^m$ . For  $\mathbf{u} \in T_{\psi^{[m]}}M^m \simeq (\mathbb{R}^d)^m$ , define the corresponding local norm by

$$(4.68) \quad \|\mathbf{u}\|_{\psi^{[m]}} := \inf \left\{ s > 0 \mid \exists g \in \overline{\mathbf{CH}_s(\mathcal{F})} \text{ s.t. } g \circ \psi(z_i^{[m]}) = u_i, i = 1, \dots, m \right\},$$

with the convention that the infimum over an empty set equals infinity. We then have the following analogue of (2.15) in finite interpolation problems.

**Proposition 4.6.** *Let  $\psi \in \mathcal{M}$  and  $\mathbf{u} \in T_{\psi^{[m]}}M^m$ . For any  $C^1$  curve  $\gamma : [0, \varepsilon] \rightarrow M^m$  with  $\gamma(0) = \psi^{[m]}$  and  $\gamma'(0) = \mathbf{u}$ ,*

$$(4.69) \quad \|\mathbf{u}\|_{\psi^{[m]}} = \lim_{t \rightarrow 0} \frac{d_{\mathcal{F}}^{[m]}(\psi^{[m]}, \gamma(t))}{t}.$$

*Proof.* The argument is similar to the proof (2.15) in Theorem 2.1.

*Upper bound:* If for some  $s > 0$ ,  $\mathbf{u}$  is realized at the samples by some  $g \in \overline{\mathbf{CH}_s(\mathcal{F})}$  (i.e.  $g \circ \psi(z_i^{[m]}) = u_i$ ), concatenate short flows of generators with total time  $st + o(t)$  to produce a horizontal curve in  $M^m$  starting at  $\psi^{[m]}$  whose endpoint at time  $t$  matches  $\gamma(t)$  to first order. Therefore,  $d_{\mathcal{F}}^{[m]}(\psi^{[m]}, \gamma(t)) \leq st + o(t)$ . Taking the limit  $t \rightarrow 0^+$  and then the infimum over  $s$  gives the upper bound. **Lower bound:** the uniformly Lipschitz property of admissible flows and sub-additivity of  $d_{\mathcal{F}}^{[m]}$  imply that any admissible flow of time  $o(t)$  realizing  $\gamma(t)$  forces  $\mathbf{u}$  to be attained by some  $g \in \overline{\mathbf{CH}_s(\mathcal{F})}$  with  $s$  arbitrarily close to the metric slope  $\liminf_{t \rightarrow 0^+} \frac{d_{\mathcal{F}}^{[m]}(\psi^{[m]}, \gamma(t))}{t}$ .  $\square$

Similar to the infinite-dimensional case, we can also characterize the distance  $d_{\mathcal{F}}^{[m]}$  in terms of lengths of curves in  $M^m$  induced by the local norms. Specifically, let  $\gamma : [0, 1] \rightarrow M^m$  be an absolutely continuous curve, and define its discrete length by

$$(4.70) \quad L^{[m]}(\gamma) := \int_0^1 \|\dot{\gamma}(t)\|_{\gamma(t)} dt.$$

We then have the following, whose proof is similar to that of (2.16) in Theorem 2.1.

**Proposition 4.7.** For all  $\mathbf{x}, \mathbf{y} \in M^m$ ,

$$(4.71) \quad d_{\mathcal{F}}^{[m]}(\mathbf{x}, \mathbf{y}) = \inf \left\{ L^{[m]}(\gamma) \mid \gamma : [0, 1] \rightarrow M^m \text{ absolutely continuous, } \gamma(0) = \mathbf{x}, \gamma(1) = \mathbf{y} \right\}.$$

Finally, recall the variational characterization of the local norm in (2.15) for the infinite-dimensional manifold  $\mathcal{M}$ :

$$(4.72) \quad \|u\|_{\psi} = \inf \left\{ s > 0 \mid u \in \overline{\mathbf{CH}_s(\mathcal{F}) \circ \psi} \right\}.$$

Write  $\mathbf{u}^{[m]} := I^{[m]}(u) \in T_{\psi^{[m]}}M^m$ .

The following proposition shows that the discrete local norms converge to the continuous local norm as the number of samples increases.

**Proposition 4.8.** Let  $\psi \in \mathcal{M}$  and  $u \in T_{\psi}\mathcal{M}$ . We then have:

$$(4.73) \quad \lim_{m \rightarrow \infty} \|\mathbf{u}^{[m]}\|_{\psi^{[m]}} = \|u\|_{\psi}.$$

*Proof. Upper bound for left-hand side:* Fix  $\varepsilon > 0$ . By definition of  $\|u\|_{\psi}$ , choose  $g_{\varepsilon} \in \overline{\mathbf{CH}_{\|u\|_{\psi} + \varepsilon}(\mathcal{F})}$  such that  $u = g_{\varepsilon} \circ \psi$  on  $M$ . Evaluating at the samples gives, for every  $m$  and  $i = 1, \dots, m$ ,

$$(4.74) \quad g_{\varepsilon}(\psi(z_i^{[m]})) = u(z_i^{[m]}).$$

Hence, by the definition of the finite-sample local norm,

$$(4.75) \quad \|u^{[m]}\|_{\psi^{[m]}} \leq \|u\|_{\psi} + \varepsilon \quad \text{for all } m.$$

Taking  $\limsup_{m \rightarrow \infty}$  and then  $\varepsilon \rightarrow 0^+$  yields

$$(4.76) \quad \limsup_{m \rightarrow \infty} \|\mathbf{u}^{[m]}\|_{\psi^{[m]}} \leq \|u\|_{\psi}.$$

*Lower bound for left-hand side:* Assume, by contradiction, that there exists  $\eta > 0$  and an infinite subsequence  $(m_k)$  such that

$$(4.77) \quad \|\mathbf{u}^{[m_k]}\|_{\psi^{[m_k]}} \leq \|u\|_{\psi} - \eta \quad \text{for all } k.$$

By the discrete variational definition, for each  $k$  there exists  $g_k \in \overline{\mathbf{CH}_{\|u\|_{\psi} - \eta}(\mathcal{F})}$  such that

$$(4.78) \quad g_k(\psi(z_i^{[m_k]})) = u(z_i^{[m_k]}), \quad i = 1, \dots, m_k.$$

The family  $\{g_k\}$  is uniformly bounded and uniformly equicontinuous on  $M$ ; by the Arzelà-Ascoli theorem, passing to a further subsequence (not relabeled) we may assume

$$(4.79) \quad g_k \rightarrow g \quad \text{uniformly on } M,$$

for some  $g \in \overline{\mathbf{CH}_{\|u\|_{\psi} - \eta}(\mathcal{F})}$  (closedness of the hull).

We claim that  $g \circ \psi = u$  on  $M$ , which contradicts the definition of  $\|u\|_{\psi}$ . Fix any  $y \in M$ . Since  $Z^{[m]}$  asymptotically covers  $M$  (defined in (4.65)), there exists a choice of indices  $i(k) \in \{1, \dots, m_k\}$  such that

$$(4.80) \quad z_{i(k)}^{[m_k]} \rightarrow y \quad (k \rightarrow \infty).$$

By continuity of  $\psi$  and  $u$  and uniform convergence  $g_k \rightarrow g$ ,

$$(4.81) \quad u(z_{i(k)}^{[m_k]}) \rightarrow u(y), \quad g_k(\psi(z_{i(k)}^{[m_k]})) \rightarrow g(\psi(y)).$$

Using the matching property (4.78) at the indices  $i(k)$ , we conclude

$$(4.82) \quad g(\psi(y)) = u(y).$$

Since  $y \in M$  was arbitrary,  $g \circ \psi = u$  on all of  $M$ . But  $g \in \overline{\mathbf{CH}_{\|u\|_{\psi} - \eta}(\mathcal{F})}$ , hence the definition of  $\|u\|_{\psi}$  would force  $\|u\|_{\psi} \leq \|u\|_{\psi} - \eta$ , a contradiction.

Therefore no such subsequence can exist, and we must have

$$(4.83) \quad \liminf_{m \rightarrow \infty} \|\mathbf{u}^{[m]}\|_{\psi^{[m]}} \geq \|u\|_{\psi}.$$

Combining the two steps gives  $\lim_{m \rightarrow \infty} \|\mathbf{u}^{[m]}\|_{\psi^{[m]}} = \|u\|_{\psi}$ .  $\square$

We have shown that the infinite-dimensional sub-Finsler geometry on  $\text{Diff}(M)$  (both its *local* norm and its *global* minimal-time distance  $d_{\mathcal{F}}$ ) arises as the limit of the corresponding finite-sample interpolation geometry as the sampling sets densify. Specifically, as  $Z^{[m]}$  becomes dense we have the convergence of distances

$$(4.84) \quad \lim_{m \rightarrow \infty} d_{\mathcal{F}}^{[m]}(I^{[m]}(\psi_1), I^{[m]}(\psi_2)) = d_{\mathcal{F}}(\psi_1, \psi_2),$$

and the convergence of local norms

$$(4.85) \quad \lim_{m \rightarrow \infty} \|I^{[m]}(u)\|_{I^{[m]}(\psi)} = \|u\|_{\psi},$$

Thus the finite-sample sub-Finsler structure is a consistent discretization of the infinite dimensional one. The relations established in this subsection can be summarized in the following commutative diagram.

$$(4.86) \quad \begin{array}{ccc} d_{\mathcal{F}}(\cdot, \cdot) & \begin{array}{c} \xleftarrow{\text{derivative}} \\ \xrightarrow{\text{integral}} \end{array} & \|\cdot\|_{\psi} \\ \uparrow \downarrow \text{sampling} & & \uparrow \downarrow \text{sampling} \\ d_{\mathcal{F}}^{[m]}(\cdot, \cdot) & \begin{array}{c} \xleftarrow{\text{integral}} \\ \xrightarrow{\text{integration}} \end{array} & \|\cdot\|_{\psi^{[m]}} \end{array}$$

This is fully consistent with the relation between universal interpolation and approximation studied in [8]: there, the existence of a *uniform* time  $T$  that interpolates any finite sample of a target  $\psi$  is shown to be equivalent to  $C^0$  approximation of  $\psi$  in finite time. The results here provide a geometric refinement of that equivalence: uniform control of the discrete distances  $d_{\mathcal{F}}^{[m]}$  over dense samples is equivalent to control of the global distance  $d_{\mathcal{F}}$ , and the discrete local norms converge to the continuous sub-Finsler norm that determines  $d_{\mathcal{F}}$  via the geodesic (path-length) formula. Practically, this links finite-sample interpolation complexity to the intrinsic (sub-Finsler) complexity of flow approximation.

## 5. APPLICATIONS

The geometric picture we presented holds generally for any control family  $\mathcal{F}$  over a smooth compact manifold  $M \subset \mathbb{R}^d$  satisfying our assumptions. For a given control family  $\mathcal{F}$ , our framework provides a way to characterize or estimate the approximation complexity  $C_{\mathcal{F}}(\psi)$  for given target function  $\psi \in \mathcal{M}$ , by studying the induced sub-Finsler norm and geodesics. Moreover, our framework also generalizes the approximation complexity  $C_{\mathcal{F}}$  to a distance  $d_{\mathcal{F}}(\psi_1, \psi_2)$  between any two diffeomorphisms  $\psi_1, \psi_2 \in \mathcal{M}$ , which may provide new insights to function/distribution approximation and model building. In the following, we will demonstrate the applicability and discuss the insights of our framework using specific examples.

**5.1. 1D ReLU revisited.** Let us revisit the results for 1D ReLU control family studied in Section 3 following the geometric framework established in the previous section. In particular, we will identify all the spaces involved precisely, and show how the manifold viewpoint reveal new insights to ReLU flow approximation.

5.1.1. *A complete summary for the ReLU case.* We start from the target function space  $\mathcal{T}$  associated with the 1D ReLU control family  $\mathcal{F}$  defined in (3.1). In our geometric viewpoint,  $\mathcal{T}$  is the connected component of the identity in  $\mathcal{M} = \text{Diff}^{W^{1,\infty}}([0, 1])$  under the topology induced by the geodesic distance induced by the sub-Finsler norm defined by the control family  $\mathcal{F}$ . According to the general results, the horizontal (tangent) space at each  $\psi \in \mathcal{M}$  can be identified as:

$$(5.1) \quad X_{\mathcal{F}} \circ \psi := \{ f \circ \psi \mid f \in X_{\mathcal{F}} \}.$$

With the local sub-Finsler norm given by

$$(5.2) \quad \|u\|_{\psi} = \inf \{ s > 0 \mid u \in \overline{\mathbf{CH}_s(\mathcal{F})}^{C^0} \circ \psi \},$$

Moreover,  $d_{\mathcal{F}}$  can be identified as the geodesic distance given by:

$$(5.3) \quad d_{\mathcal{F}}(\psi_1, \psi_2) = \inf \left\{ \int_0^1 \|\dot{\gamma}(t)\|_{\gamma(t)} dt : \gamma \text{ horizontal, } \gamma(0) = \psi_1, \gamma(1) = \psi_2 \right\}.$$

In the 1D ReLU case, fortunately, the local norm  $\|\cdot\|_{\psi}$  admits a closed-form characterization, as given in Proposition 3.2. This in turn gives a closed-form characterization of the space  $X_{\mathcal{F}}$ : it is just all the  $\text{BV}^2$  functions on  $[0, 1]$  that vanishes at the boundary. This also results in a closed-form characterization of  $\mathcal{M}$ . Furthermore, after a global transformation in (3.89), we can also characterize a geodesic connecting any two target functions in  $\mathcal{M}$ . With these characterizations, we can compute the distance  $d_{\mathcal{F}}$  exactly as Proposition 3.1 by the geodesic characterization. Finally, we have the explicit expression for  $d_{\mathcal{F}}$ :

$$(5.4) \quad d_{\mathcal{F}}(\psi_1, \psi_2) = \|\ln \psi'_1 - \ln \psi'_2\|_{\text{TV}([0,1])} \int_0^1 \left| \frac{\psi''_1(x)}{\psi'_1(x)} - \frac{\psi''_2(x)}{\psi'_2(x)} \right| dx.$$

5.1.2. *Discussions on the closed-form results for 1D ReLU.* Now, let us take a closer look at the closed-form representation of the complexity  $C_{\mathcal{F}}$ :

$$(5.5) \quad C_{\mathcal{F}}(\psi) = d_{\mathcal{F}}(\text{Id}, \psi) = \int_0^1 \left| \frac{\psi''(x)}{\psi'(x)} \right| dx.$$

We can see that the complexity depends on the ratio between the second derivative and the first derivative of the target function  $\psi$ . Therefore, if a map  $\psi \in \mathcal{M}$  has first order derivative bounded below by some  $c > 0$ , and second order derivative bounded above by some  $C > 0$ , then it has a complexity bounded by  $C/c$ . If  $C$  is small and  $c$  is relatively large, then the function is easy to approximate with ReLU flows.

On the other hand, if the first order derivative  $\psi'$  is close to zero at some point, or the second order derivative  $\psi''$  is large at some point, then the complexity becomes large. For example, consider  $\psi_{\varepsilon}(x) := \varepsilon x + x^2$  for small  $\varepsilon > 0$ . Then, we have

$$(5.6) \quad C_{\mathcal{F}}(\psi_{\varepsilon}) = \int_0^1 \left| \frac{2}{\varepsilon + 2x} \right| dx = 2 \ln \left( 1 + \frac{2}{\varepsilon} \right),$$

which goes to infinity as  $\varepsilon \rightarrow 0$ . This is consistent with the intuition that when  $\varepsilon$  is small, the function  $\psi_{\varepsilon}$  has a very small first order derivative near  $x = 0$ , which makes approximation by flow maps hard. Also, if we consider  $\xi_n := x + \frac{1}{2n\pi} \sin(n\pi x)$  for positive integer  $n$ , then we have

$$(5.7) \quad \xi'_n(x) = 1 + \frac{1}{2} \cos(n\pi x) \in \left[ \frac{1}{2}, \frac{3}{2} \right]$$

We have

$$(5.8) \quad C_{\mathcal{F}}(\xi_n) = \int_0^1 \left| \frac{-\frac{n\pi}{2} \sin(n\pi x)}{1 + \frac{1}{2} \cos(n\pi x)} \right| dx = \int_0^1 \left| \frac{n\pi \sin(n\pi x)}{2 + \cos(n\pi x)} \right| dx \geq \frac{1}{3} \int_0^1 n\pi |\sin(n\pi x)| dx = \frac{2}{3}n,$$

which goes to infinity as  $n \rightarrow \infty$ . This is also consistent with the intuition that when  $n$  is large, the derivative of  $\xi_n$  oscillates rapidly, making flow approximation hard.

We also notice that this complexity measure is very different from the classical function space norms, such as Sobolev norms or Besov norms, which mainly depend on the absolute values of the derivatives of different orders. Instead, our complexity measure depends on the first order derivative relative to the second order derivative, which is more related to the geometry of the function graph.

For a more intuitive understanding of this difference, we provide a visualization of the distance  $d_{\mathcal{F}}(\cdot, \cdot)$  compared to the classical  $L^2$  distance with respect to the Lebesgue measure on a set of functions in  $\mathcal{M}$ . Specifically, we consider three functions in  $\mathcal{M}$  defined as

$$(5.9) \quad \psi_1(x) = x + \sin(2\pi x)/7\pi, \quad \psi_2(x) = x + \sin(4\pi x)/7\pi, \quad \psi_3(x) = x - \sin(2\pi x)/7\pi - \sin(4\pi x)/7\pi.,$$

By the characterization of  $\mathcal{M}$ , their convex combinations  $a\psi_1 + b\psi_2 + c\psi_3$ , with  $a, b, c \geq 0$  and  $a + b + c = 1$ , also belong to  $\mathcal{M}$ . We then parametrize the function  $\psi = a\psi_1 + b\psi_2 + c\psi_3$  by the barycentric coordinates  $(a, b, c)$  in the triangle with vertices  $(1, 0, 0), (0, 1, 0), (0, 0, 1)$ . Notice that the point  $(\frac{1}{3}, \frac{1}{3}, \frac{1}{3})$  in the triangle corresponds to the identity map Id. We then visualize the contours of the distances  $d_{\mathcal{F}}(\psi_0, \psi)$  and  $\|\psi_0 - \psi\|_{L^2([0,1])}$  to the identity in the triangle. The results are shown in Figure 2. From the figure, the contours of  $L^2$  distance are elliptical, which is consistent with the fact

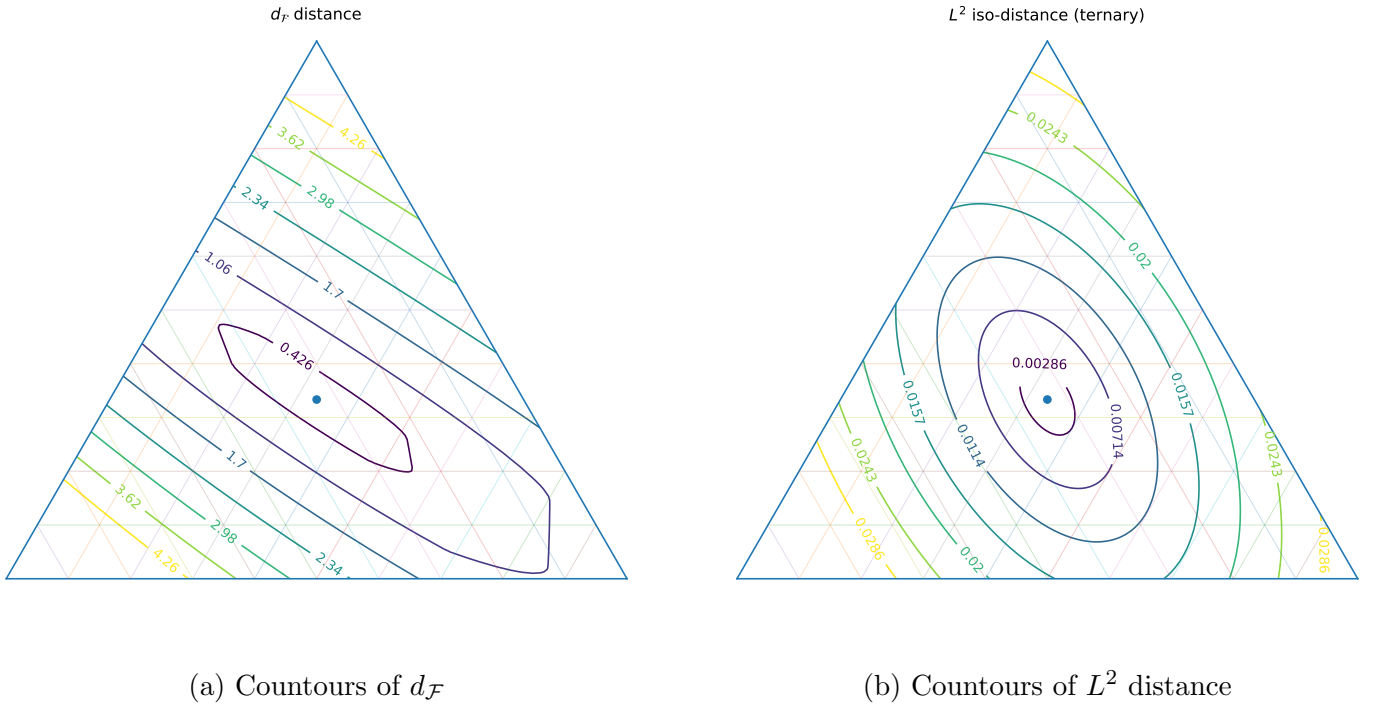


FIGURE 2. Comparison of distance contours between  $d_{\mathcal{F}}$  and  $L^2$  on the convex hull of three functions in  $\mathcal{M}$

that it is the affine transformation of the Euclidean distance in  $\mathbb{R}^3$ . However, the contours of  $d_{\mathcal{F}}$  are highly non-elliptical, which reflects the difference of the complexity measure from classical norms.

5.1.3. *Connections with flow-based generative models.* Another interesting observation is that the distance  $d_{\mathcal{F}}(\psi_1, \psi_2) = |\ln \psi'_1 - \ln \psi'_2|_{\text{TV}([0,1])}$  has a connection to the learning of distributions. Specifically, functions in  $\mathcal{M}$  can be naturally identified as the cumulative distribution functions (CDFs) of some probability distributions supported on  $[0, 1]$ . For a given  $\psi \in \mathcal{M}$ , we denote its corresponding probability distribution as  $\mu_{\psi}$ , which has the density function  $p_{\psi} = \psi'$ . Then, the metric  $d_{\mathcal{F}}(\cdot, \cdot)$  naturally induces a metric between probability distributions supported on  $[0, 1]$  as:

$$(5.10) \quad d_{\mathcal{F}}(\mu_{\psi_1}, \mu_{\psi_2}) := d_{\mathcal{F}}(\psi_1, \psi_2) = \int_{[0,1]} |(\ln p_{\psi_1})' - (\ln p_{\psi_2})'|_{\text{TV}([0,1])} dx,$$

where  $\mu_{\psi_1}, \mu_{\psi_2}$  are measures whose positive density functions that are bounded and bounded away from zero, and have bounded variance. Notice that the term  $(\ln p_\psi)'$  is known as the score function of the distribution  $\mu_\psi$  in statistics [24], which is widely used in modern generative models, such as score-based diffusion models [40, 21, 41]. The metric  $d_{\mathcal{F}}(\cdot, \cdot)$  actually measures  $L^1$  distance between the score functions of two distributions. Therefore, the results indicates that the complexity of transforming one distribution to another using flow maps of ReLU networks is closely related to the distance between their score functions. This provides a new perspective to understand the learning of distributions via flow-based models. Similar connections in higher dimensional distributions are worthy of further investigations in the future.

5.1.4. *New ways to build models: insights from connected components.* From the geometric perspective, the distance  $d_{\mathcal{F}}(\cdot, \cdot)$  offers a more general understanding of the approximation complexity  $C_{\mathcal{F}}$ : this distance can be defined between any two diffeomorphisms on  $M$ . Our discussion in Section 3 just focuses on the target set  $\mathcal{T}$ , which is the connected components of the identity map under the topology induced by  $d_{\mathcal{F}}$ .

More generally, for any  $\psi \in \text{Diff}([0, 1])$ , we can consider its connected component:

$$(5.11) \quad \mathcal{T}_\psi := \{\tilde{\psi} \in \text{Diff}([0, 1]) \mid d_{\mathcal{F}}(\psi, \tilde{\psi}) < \infty\}.$$

Then, according to our general results,  $\mathcal{T}_\psi$  is also a Finsler Banach manifold modeled on  $X_{\mathcal{F}}$ , with similar characterizations of the local norm and geodesic distance.

This generalization offers us new understandings on function approximation: it is not necessarily to approximate a target function starting from the identity map. A simple example is, if we choose  $\psi = -\text{Id}$  as the opposite of identity map, then  $\mathcal{T}_{-\text{Id}}$  contains orientation-reversing diffeomorphisms. Notice that it is well-known that it is impossible to uniformly approximate a orientation-reversing diffeomorphism by flow maps (i.e. from the identity map). However, if we start from the opposite map  $-\text{Id}$ , the problem becomes feasible.

In most of applications of deep learning, including ResNets [20], transformers [48], and flow-based generative models [31, 21, 43], the networks are usually initialized as the identity map. This is of course a natural choice, since the identity map is the simplest function that preserves all information of the input data. However, an insight from our geometric framework is that approximation may be easier if we start from a proper initial function that is closer to the target function, at least in a topological sense. With this perspective, our geometric framework provides a way of understanding the approximation complexity between any two functions, instead of only from the identity map to the target function. This and its algorithmic consequences will be explored in future work.

5.2. **Other applications.** We further consider some other examples of control families and investigate the corresponding target function spaces and complexity measures using the geometric framework.

5.2.1. *Transport time on  $\text{SO}(3)$ .* Although the goal of our framework is to study flows generated by neural networks for deep learning and artificial intelligence applications, it can be applied to general flows on manifolds. Here, we consider a case where such a flow gives very familiar objects in geometry, and discuss what our distance correspond to in these settings.

We consider a finite-dimensional example where the reachable diffeomorphisms form a Lie subgroup of  $\text{Diff}(M)$ . Let  $M = S^2$  (unit sphere) and consider the family of constant fields

$$(5.12) \quad x \mapsto Ax, \quad A \in \mathfrak{so}(3),$$

i.e.  $A$  is skew-symmetric. Writing the  $\hat{\cdot}$ -map

$$(5.13) \quad \widehat{(a_x, a_y, a_z)} := \begin{pmatrix} 0 & -a_z & a_y \\ a_z & 0 & -a_x \\ -a_y & a_x & 0 \end{pmatrix}, \quad \text{vee}(\hat{a}) = a,$$

the vector field is  $x \mapsto \hat{a}x$  with body angular velocity  $a \in \mathbb{R}^3$ . Flows are rotations  $x \mapsto Rx$  with  $R = \exp(t\hat{a}) \in \text{SO}(3)$ . Hence the reachable set of diffeomorphisms is the finite-dimensional submanifold

$$\mathcal{M} = \text{SO}(3) \subset \text{Diff}(S^2).$$

For  $\psi \in \text{SO}(3)$ , define the principal rotation angle and principal logarithm

$$(5.14) \quad \theta(\psi) := \arccos\left(\frac{\text{tr}(\psi) - 1}{2}\right) \in [0, \pi], \quad \text{Log}(\psi) := \frac{\theta(\psi)}{2 \sin \theta(\psi)} (\psi - \psi^\top) \in \mathfrak{so}(3),$$

so that  $\exp(\text{Log} \psi) = \psi$  and  $\text{Log}(\psi) = \hat{\omega}$  with  $\|\omega\|_2 = \theta(\psi)$ .

We may identify  $T_R \text{SO}(3) \equiv R \mathfrak{so}(3)$ , and define the anchored bundle  $(\mathcal{E}, \pi, \rho)$  by

$$(5.15) \quad \mathcal{E} := \text{SO}(3) \times \mathbb{R}^3, \quad \pi(R, a) = R, \quad \rho_R(a) = R\hat{a} \in T_R \text{SO}(3).$$

Thus  $\rho$  is onto at each  $R$  (full actuation), so  $\mathcal{D} = \rho(\mathcal{E}) = T \text{SO}(3)$  and the induced sub-Finsler structure is in fact a *Finsler* structure. Choosing a fiber norm on  $a \in \mathbb{R}^3$  yields a left-invariant metric with length

$$(5.16) \quad L(\gamma) = \int_0^1 \|a(t)\| dt, \quad \dot{R}(t) = R(t)\hat{a}(t).$$

We discuss two choices for the control family to realize rotations that will lead to different approximation rates.

**(A)  $\ell^2$ -fiber norm (Riemannian).** Let

$$(5.17) \quad \mathcal{F}_2 := \{x \mapsto \hat{a}x \mid \|a\|_2 \leq 1\}.$$

By convexity, the atomic norm coincides with  $\|a\|_2$ :

$$(5.18) \quad \|R\hat{a}\|_R = \|a\|_2.$$

This norm is induced by the inner product  $\langle \hat{a}, \hat{b} \rangle = a \cdot b$  on  $\mathfrak{so}(3)$ , hence we obtain the standard bi-invariant Riemannian metric on  $\text{SO}(3)$  [23]. Geodesics are one-parameter subgroups  $R(t) = R_0 \exp(t\hat{\omega})$  with constant  $\omega$ , and the geodesic (minimal-time) distance is

$$(5.19) \quad d_{\mathcal{F}_2}(\psi_1, \psi_2) = \|\text{vee}(\text{Log}(\psi_2\psi_1^\top))\|_2 = \theta(\psi_2\psi_1^\top),$$

in particular  $d_{\mathcal{F}_2}(I, \psi) = \theta(\psi)$ . This distance is also called the angle metric on  $\text{SO}(3)$  in the literature [19], since it measures the scale of the angle between two rotations.

**(B)  $\ell^1$ -fiber norm (Finsler).** Let the control family be the six axial generators

$$\mathcal{F}_1 := \{\pm \hat{e}_1x, \pm \hat{e}_2x, \pm \hat{e}_3x\},$$

so the atomic norm on  $a \in \mathbb{R}^3$  is  $\|a\|_1$ :

$$(5.20) \quad \|R\hat{a}\|_R = \|a\|_1.$$

The induced distance  $d_{\mathcal{F}_1}$  is the Finsler distance associated with  $\ell^1$  on the Lie algebra. Using the constant-velocity path  $R(t) = \exp(t \text{Log} \psi)$  gives the explicit *upper bound*

$$(5.21) \quad d_{\mathcal{F}_1}(I, \psi) \leq \|\text{vee}(\text{Log} \psi)\|_1, \quad d_{\mathcal{F}_1}(\psi_1, \psi_2) \leq \|\text{vee}(\text{Log}(\psi_2\psi_1^\top))\|_1.$$

Moreover, since  $\|a\|_1 \geq \|a\|_2$  for all  $a \in \mathbb{R}^3$ , the  $\ell^1$ -Finsler norm dominates the  $\ell^2$ -Riemannian norm pointwise; hence the *lower bound*

$$(5.22) \quad d_{\mathcal{F}_1}(\psi_1, \psi_2) \geq d_{\mathcal{F}_2}(\psi_1, \psi_2) = \theta(\psi_2\psi_1^\top).$$

Combining (5.21)-(5.22) and the norm equivalence  $\|v\|_1 \leq \sqrt{3}\|v\|_2$  yields the two-sided estimate

$$(5.23) \quad \theta(\psi_2\psi_1^\top) \leq d_{\mathcal{F}_1}(\psi_1, \psi_2) \leq \sqrt{3}\theta(\psi_2\psi_1^\top).$$

Thus the  $\ell^1$ -Finsler transport time is quantitatively comparable to the canonical geodesic distance, with anisotropy encoded by the polyhedral  $\ell^1$  unit ball on the Lie algebra.

5.2.2. *Finite time approximation of smooth functions using additional dimensions.* In this example, we will consider an application of our framework to the approximation of general smooth functions  $f : \mathbb{R}^d \rightarrow \mathbb{R}^d$  over compact sets, by using flows in higher dimensional spaces.

For  $R > 0$ , let  $B_R \subset \mathbb{R}^{2d}$  denote the open Euclidean ball of radius  $R$  centered at the origin. We will consider the following control family  $\mathcal{F}$  on  $\mathbb{R}^{2d}$ :

$$(5.24) \quad \mathcal{F} := \{x \rightarrow \rho(x)\sigma(Ax + b) \mid A \in \mathbb{R}^{2d \times 2d}, b \in \mathbb{R}^{2d}, \|A\|_2 \leq 1, \|b\|_2 \leq 1\}$$

where  $\sigma$  is the ReLU activation function which is applied elementwise, and  $\rho \in C_c^\infty(\mathbb{R}^{2d})$  is a smooth cutoff function such that  $\rho \equiv 1$  on  $B_1$  and  $\rho \equiv 0$  outside  $B_{7/4}$ , and is positive on  $B_{7/4} \setminus B_1$ .

Applying our results together with Theorem 2.1 in [52], we have the following result:

**Proposition 5.1.** *Let  $r \geq d + 2$  be a positive integer. For any given compact set  $K \subset \mathbb{R}^d$  and any  $C^r$  function  $f : \mathbb{R}^d \rightarrow \mathbb{R}^d$ , there exists  $T > 0$  and two linear maps  $\alpha : \mathbb{R}^d \rightarrow \mathbb{R}^{2d}$ ,  $\beta : \mathbb{R}^{2d} \rightarrow \mathbb{R}^d$  such that*

$$(5.25) \quad f \in \overline{\{\beta \circ \varphi \circ \alpha \mid \varphi \in \mathcal{A}_{\mathcal{F}}(T)\}}^{C^0}.$$

*That is, one can approximate a function with enough smoothness in  $d$ -dimension arbitrarily well using a continuous-time neural network with layer-wise architecture given by  $\mathcal{F}$  in  $2d$ -dimension in a uniform time  $T$ .*

The application of our framework uses the following proposition:

**Proposition 5.2.** *Given a compact set  $K \subset \mathbb{R}^d$ . For any  $C^r$  function  $f : \mathbb{R}^d \rightarrow \mathbb{R}^d$ , there exists linear maps  $\alpha : \mathbb{R}^d \rightarrow \mathbb{R}^{2d}$ ,  $\beta : \mathbb{R}^{2d} \rightarrow \mathbb{R}^d$  and a  $C^r$  diffeomorphism  $\Phi : \mathbb{R}^{2d} \rightarrow \mathbb{R}^{2d}$  such that*

$$(5.26) \quad \beta \circ \Phi \circ \alpha|_K = f|_K,$$

*$\alpha(K) \subset B_1$ ,  $\Phi$  is equal to the identity on  $B_2 \setminus B_{3/2}$ , and  $\Phi$  maps  $B_2$  onto itself, and maps  $\alpha(K)$  to  $B_1$ .*

*Proof.* First, let  $\alpha : \mathbb{R}^d \rightarrow \mathbb{R}^{2d}$  be the embedding  $\alpha_0(u) = (\lambda u, 0)$ , and  $\beta_0 : \mathbb{R}^{2d} \rightarrow \mathbb{R}^d$  be the projection  $\beta_0(u, v) = v/\kappa$ , where  $\lambda, \kappa > 0$ . Since  $K$  and  $f(K)$  are compact, there exists  $\lambda, \kappa > 0$  such that  $\alpha_0(K) \subset B_1 \subset B_2 \subset \mathbb{R}^{2d}$  and  $K \times f(K) \subset \mathbb{R}^{2d}$ . Choose such  $\lambda, \kappa > 0$ , and consider the map  $\Psi : \mathbb{R}^{2d} \rightarrow \mathbb{R}^{2d}$  by  $\Psi(u, v) = (u, v + \kappa f(1/\lambda u))$ . Then, we have  $\beta \circ \Psi \circ \alpha|_K = f|_K$ . Moreover,  $\Psi$  is a  $C^r$  diffeomorphism of  $\mathbb{R}^{2d}$ , with inverse  $\Psi^{-1}(u, v) = (u, v - \kappa f(1/\lambda u))$ . Also,  $\Psi$  maps  $\alpha(K) \subset B_1$  to  $B_1$ .

Next, we will modify  $\Psi$  to obtain a diffeomorphism  $\Phi$  that is equal to the identity on  $B_2 \setminus B_{3/2}$ , and is equal to  $\Psi$  on  $\alpha(K)$ . This is done by the following lemma:

**Lemma 5.1.** *There exists a family  $(\Phi_t)_{t \in [0,1]}$  such that, for every  $t \in [0, 1]$ ,*

$$(5.27) \quad \Phi_t : B_2 \rightarrow B_2$$

*is a  $C^r$  diffeomorphism, and the following properties hold:*

$$\begin{aligned} \Phi_0 &= \text{id}_{B_2}, \\ \Phi_1|_K &= \Psi|_K, \\ \Phi_t &= \text{id} \quad \text{on } B_2 \setminus B_{3/2}. \end{aligned}$$

*In particular,  $(\Phi_t)_{t \in [0,1]}$  is an isotopy of  $B_2$  from  $\text{id}_{B_2}$  to  $\Phi_1$ , and every  $\Phi_t$  is equal to the identity in a neighborhood of  $\partial B_2$ .*

*Proof of the lemma.* Denote  $\tilde{f}(x) := \kappa f(x/\lambda)$ . Choose  $\eta \in C_c^r(B_{3/2})$  such that

$$(5.28) \quad 0 \leq \eta \leq 1, \quad \eta \equiv 1 \quad \text{on } B_1.$$

Extend  $\eta$  by zero outside  $B_{3/2}$ , and define a  $C^r$  vector field on  $\mathbb{R}^{2d}$  by

$$(5.29) \quad X(u, v) := \eta(u, v) (0, \tilde{f}(u)).$$

Since  $X$  has compact support, its flow  $(\Phi_t)_{t \in \mathbb{R}}$  is globally defined, and each  $\Phi_t$  is a  $C^r$  diffeomorphism of  $\mathbb{R}^{2d}$ . Moreover,

$$(5.30) \quad X \equiv 0 \quad \text{on } \mathbb{R}^{2d} \setminus B_{3/2},$$

hence

$$(5.31) \quad \Phi_t = \text{id} \quad \text{on } \mathbb{R}^{2d} \setminus B_{3/2}$$

for every  $t \in \mathbb{R}$ . In particular,

$$(5.32) \quad \Phi_t = \text{id} \quad \text{on } B_2 \setminus B_{3/2}.$$

We next show that each  $\Phi_t$  maps  $B_2$  onto itself. Since  $\Phi_t$  fixes every point of  $\mathbb{R}^{2d} \setminus B_{3/2}$ , it fixes in particular every point of  $\mathbb{R}^{2d} \setminus B_2$ . If there were  $x \in B_2$  such that  $\Phi_t(x) \notin B_2$ , then  $\Phi_t(\Phi_t(x)) = \Phi_t(x)$  as well, contradicting injectivity of  $\Phi_t$ . Thus  $\Phi_t(B_2) \subset B_2$ . Applying the same argument to  $\Phi_t^{-1}$  gives  $\Phi_t(B_2) = B_2$ .

Finally, let  $x = (u, v) \in K$ , and define

$$(5.33) \quad \gamma_x(t) := (u, v + t\tilde{f}(u)) = (1-t)x + t\Psi(x), \quad t \in [0, 1].$$

Since  $x \in B_1$  and  $\Psi(x) \in B_1$ , and  $B_1$  is convex, we have  $\gamma_x(t) \in B_1$  for all  $t \in [0, 1]$ . Hence  $\eta(\gamma_x(t)) = 1$  for all  $t$ , and therefore

$$(5.34) \quad \dot{\gamma}_x(t) = (0, \tilde{f}(u)) = X(\gamma_x(t)).$$

Also  $\gamma_x(0) = x$ . By uniqueness of solutions to the ODE generated by  $X$ , it follows that

$$(5.35) \quad \Phi_t(x) = \gamma_x(t) \quad \text{for all } t \in [0, 1].$$

In particular,

$$(5.36) \quad \Phi_1(x) = \gamma_x(1) = \Psi(x).$$

Since  $x \in K$  was arbitrary, we conclude that

$$(5.37) \quad \Phi_1|_K = \Psi|_K.$$

This proves the result. □

The lemma implies that we can extend  $\psi|_{\alpha(K)}$  to a  $C^r$  diffeomorphism  $\Phi$  of  $\mathbb{R}^{2d}$  that is equal to the identity on  $B_2 \setminus B_{3/2}$ , and maps  $B_1, B_2$  onto themselves. Then, we have  $\beta \circ \Phi \circ \alpha|_K = f|_K$ , which completes the proof of the proposition. □

Now, we can provide the proof of Proposition 5.1.

*Proof of Proposition 5.1.* With Proposition 5.2, we can apply our framework on the diffeomorphism  $\Phi$  from  $B_2$  to itself in  $\mathbb{R}^{2d}$ . We choose  $\mathcal{M}$  as the set of  $W^{1,\infty}$  diffeomorphisms of  $B_2$  to itself that fixes the boundary.

For any map  $g : \mathbb{R}^{2d} \rightarrow \mathbb{R}^{2d}$  that is supported on  $B_{3/2}$  and of class  $C^r$ , there exists a  $C^r$  smooth function  $h$  supported on  $B_2 \subset \mathbb{R}^{2d}$  such that  $g(x) = h(x)\rho(x)$  for all  $x \in \mathbb{R}^d$ . According to the discussion in Example 4.3, the pair  $(\mathcal{M}, \mathcal{F})$  is a compatible pair. According to Theorem 2.1 in [52], the  $C^0$  closure of the convex hull of the following family

$$(5.38) \quad \tilde{\mathcal{F}} : \{x \rightarrow \sigma(Ax + b) \mid A \in \mathbb{R}^{2d \times 2d}, b \in \mathbb{R}^{2d}, \|A\|_2 \leq 1, \|b\|_2 \leq 1\}$$

contains a ball in the space  $C^r(B_2)$ . Therefore, the closure of the convex hull of  $\mathcal{F}$  contains a ball in  $C^r(B_2)$  intersected with the set of functions supported on  $B_{3/2}$ . Furthermore, by the proof of Lemma 5.1 above, the diffeomorphism  $\Phi$  can be connected to the identity map by a path of diffeomorphisms that keeps to be the identity map on  $B_2 \setminus B_{3/2}$ . This means that the path  $\gamma(t)$  from Id to  $\Phi$  can be generated

by a flow of  $C^r$  vector fields supported on  $B_{3/2}$ , and therefore  $\|\dot{\gamma}(t)\|_{\gamma(t)}$  is finite for all  $t$ . This implies that

$$(5.39) \quad d_{\mathcal{F}}(\text{Id}, \Phi) = \int_0^1 \|\dot{\gamma}(t)\|_{\gamma(t)} dt < \infty.$$

□

**5.2.3. Deep ResNet with layer normalisation.** We now return to learning problems, where we demonstrate how our framework can be used as a recipe to estimate approximation complexities even when exact computations are difficult.

Let us consider a two-dimensional control family with normalization, i.e., a projection onto the unit circle. Our base manifold is the unit circle  $M = S^1 \subset \mathbb{R}^2$ . Fix  $b \in [-1, 1]$  and introduce a control family  $\mathcal{G}_b \subset \text{Vec}(\mathbb{R}^2)$  by

$$(5.40) \quad \mathcal{G}_b := \{x \mapsto W \sigma(Ax + b\mathbf{1}) \mid W, A \in \mathbb{R}^{2 \times 2}, W \text{ diagonal}, \|W\|_F \leq 1, \|A_i\|_2 = 1, i = 1, 2\},$$

where  $\sigma$  is the ReLU activation and  $\mathbf{1} = (1, 1)^\top$ . Let  $\text{Proj} : \text{Vec}(\mathbb{R}^2) \rightarrow \text{Vec}(S^1)$  be the orthogonal projection onto the tangent bundle:

$$(5.41) \quad \text{Proj}(V)(x) := (I - xx^\top)V(x), \quad x \in S^1, V \in \text{Vec}(\mathbb{R}^2).$$

Define the projected control family on  $S^1$  by

$$(5.42) \quad \mathcal{F}_b := \{\text{Proj}(g) \mid g \in \mathcal{G}_b\} \subset \text{Vec}(S^1).$$

We introduce the manifold  $\mathcal{M} := \text{Diff}^{W^{1,\infty}}(S^1)$ , the set of diffeomorphisms of  $S^1$  that are bi-Lipschitz and have Lipschitz inverses, which is a Banach manifold modeled on  $W^{1,\infty}(S^1)$ .

This construction is motivated by layer normalization in deep learning [4]: in a continuous-time idealization, normalization corresponds to projecting the ambient vector field onto the tangent space of a sphere; here the projection  $\text{Proj}$  plays exactly that role. Layer-normalised networks are core building blocks for deep ResNets (of the transformer type) used in practical applications, especially in large language models [4, 48, 51].

Now, we check that  $(\mathcal{M}, \mathcal{F}_b)$  satisfies Definition 4.8.

(1) *Exponential charts /  $C^1$  Banach manifold structure.* Identify  $S^1$  with  $\mathbb{R}/2\pi\mathbb{Z}$  via the angle coordinate  $\theta$  and write diffeomorphisms as  $\psi(\theta) = \theta + h(\theta)$  with  $h \in W^{1,\infty}(S^1)$  and  $\|h'\|_{L^\infty}$  sufficiently small (so that  $\psi$  is bi-Lipschitz). In these coordinates, local charts are given by addition,

$$\beta_\psi(u) := \psi + u, \quad u \in W^{1,\infty}(S^1) \text{ small,}$$

which is the exponential chart on the circle (geodesics in  $\theta$  are affine). Hence  $\mathcal{M} = \text{Diff}^{W^{1,\infty}}(S^1)$  admits a  $C^1$  Banach manifold structure modeled on  $W^{1,\infty}(S^1)$ .

(2) *Right translation is  $C^1$ .* For fixed  $\varphi \in \mathcal{M}$ , right translation is  $R_\varphi(\eta) = \eta \circ \varphi$ . In the angle coordinate, composition by a fixed bi-Lipschitz map acts boundedly on  $W^{1,\infty}(S^1)$ , and the induced map on charts is  $u \mapsto u \circ \varphi$ , which is  $C^1$  (indeed affine in these coordinates).

(3) *Admissible velocities.* Each  $g \in \mathcal{G}_b$  is globally Lipschitz on  $\mathbb{R}^2$ , and  $\text{Proj}$  is smooth on  $S^1$  with uniformly bounded derivative. Thus every  $f \in \mathcal{F}_b$  belongs to  $W^{1,\infty} \text{Vec}(S^1)$  with a uniform  $W^{1,\infty}$  bound, and consequently  $X_{\mathcal{F}_b}$  embeds continuously into  $W^{1,\infty}(S^1)$ . Therefore, for any  $\psi \in \mathcal{M}$  and  $f \in X_{\mathcal{F}_b}$ , the composition  $f \circ \psi$  gives a tangent direction at  $\psi$  in the  $W^{1,\infty}$  manifold structure.

(4) *Invariance under Carathéodory controls.* Let  $u(\cdot) : [0, T] \rightarrow X_{\mathcal{F}_b}$  be measurable. Since  $X_{\mathcal{F}_b} \subset W^{1,\infty}(S^1)$  and the uniform  $W^{1,\infty}$  bound imply that  $u(t, \cdot)$  is Lipschitz in space with an integrable Lipschitz modulus. Hence the Carathéodory ODE  $\dot{\gamma}(t) = u(t) \circ \gamma(t)$  admits a unique absolutely continuous solution. Moreover, Grönwall's inequality yields a bi-Lipschitz bound on  $\gamma(t)$ , so  $\gamma(t) \in \mathcal{M}$  for all  $t \in [0, T]$ .

The family  $\mathcal{F}_b$  induces an anchored bundle  $(E, \pi, \rho)$  over  $\mathcal{M}$ , with horizontal distribution  $\mathcal{D} = \rho(\mathcal{E}) \subset T\mathcal{M}$  and fiberwise atomic norms yielding a sub-Finsler structure  $\|\cdot\|_{\mathcal{D},x}$ . Identifying the *full* norm

$\|\cdot\|_{\mathcal{D},x}$  on all of  $\mathcal{D}_x$  is difficult in this example. Instead, we estimate the norm on a fiberwise linear subspace  $\tilde{\mathcal{D}}_x \subset \mathcal{D}_x$  on which the explicit bound is easy to compute. This collection  $\{\tilde{\mathcal{D}}_x\}_{x \in \mathcal{M}}$  actually defines a subbundle of the anchored bundle  $(E, \pi, \rho)$ .

Specifically, we work on the subset

$$\bar{\mathcal{M}} := \{\psi \in \text{Diff}(S^1) \mid \psi, \psi^{-1} \in C^3, \psi \text{ orientation preserving}\},$$

composed of smooth orientation-preserving diffeomorphisms whose inverses are also smooth. We parametrize  $S^1$  by the angle  $\theta \in \mathbb{R}$  and identify  $\psi \in \bar{\mathcal{M}}$  with its  $2\pi$ -periodic lift  $\bar{\psi} : \mathbb{R} \rightarrow \mathbb{R}$  satisfying

$$(5.43) \quad \bar{\psi}(\theta + 2\pi) = \bar{\psi}(\theta) + 2\pi, \quad \bar{\psi}'(\theta) > 0, \quad \forall \theta \in \mathbb{R}, \quad \bar{\psi}(0) \in [0, 2\pi).$$

We use the identification

$$(5.44) \quad C_{\text{per}}^3([0, 2\pi]) = \{u \in C^3(\mathbb{R}) \mid u(\theta + 2\pi) = u(\theta) \text{ for all } \theta\}$$

to represent a *chosen* fiberwise subspace  $\tilde{\mathcal{D}}_\psi \subset \mathcal{D}_\psi$  on which we can compute explicit bounds; in what follows  $u \in C_{\text{per}}^3([0, 2\pi])$  should be read as  $u \in \tilde{\mathcal{D}}_\psi$ .

We then have the following estimate on the local norm over  $\tilde{\mathcal{D}}_\psi$  for each  $\psi \in \bar{\mathcal{M}}$ :

**Proposition 5.3.** *Suppose  $b = \cos \beta$  with  $\beta/\pi \notin \mathbb{Q}$ . There exist constants  $C_{b,1}, C_{b,2} > 0$  such that for any  $u \in C_{\text{per}}^3([0, 2\pi])$  and  $\psi \in \bar{\mathcal{M}}$ ,*

$$(5.45) \quad \|u\|_{\mathcal{D},\psi} \leq C_{b,1} \|(u \circ \psi^{-1})^{(3)}\|_{L^2([0, 2\pi])} + C_{b,2} \|u \circ \psi^{-1}\|_{C([0, 2\pi])}.$$

While a closed form of the geodesic distance on  $\bar{\mathcal{M}}$  is still unavailable, we can estimate  $d_{\mathcal{F}_b}$  by integrating the above bound along an explicit (not necessarily optimal) curve whose velocity always lies in the subbundle  $\tilde{\mathcal{D}}$ , consisting of  $C^3$  diffeomorphisms over  $[0, 2\pi]$ . Consider the linear interpolation of lifts

$$(5.46) \quad \bar{\psi}_t := (1-t)\bar{\psi}_1 + t\bar{\psi}_2, \quad t \in [0, 1],$$

which connects  $\psi_1, \psi_2 \in \bar{\mathcal{M}}$ . Since  $\dot{\bar{\psi}}_t \in C_{\text{per}}^3([0, 2\pi]) = \tilde{\mathcal{D}}_{\bar{\psi}_t}$ , integrating the estimate in Proposition 5.3 along  $\{\bar{\psi}_t\}$  yields:

**Proposition 5.4** (A global upper bound via curves tangent to the subbundle). *Suppose  $b = \cos \beta$  with  $\beta/\pi \notin \mathbb{Q}$ . Then there exist constants  $C_{b,3}, C_{b,4} > 0$  such that for all  $\psi_1, \psi_2 \in \bar{\mathcal{M}}$ ,*

$$(5.47) \quad d_{\mathcal{F}_b}(\psi_1, \psi_2) \leq C_{b,3} \int_0^{2\pi} \left[ A(\rho) (D^2 \rho)^2 + B(\rho) (D\rho)^2 (D^2 \rho) + C(\rho) (D\rho)^4 \right] dx + C_{b,4} \|\psi_1 - \psi_2\|_{C([0, 2\pi])},$$

where

$$(5.48) \quad \rho(x) := \frac{\psi_1'}{\psi_2'}(\psi_2^{-1}(x)) > 0, \quad D := \frac{d}{dz},$$

and

$$A(\rho) = \frac{67\rho^6 + 67\rho^5 + 67\rho^4 + 67\rho^3 + 172\rho^2 - 80\rho + 60}{420\rho^7},$$

$$B(\rho) = -\frac{17\rho^6 + 34\rho^5 + 51\rho^4 + 68\rho^3 + 295\rho^2 - 150\rho + 105}{140\rho^8},$$

$$C(\rho) = \frac{3(\rho^5 + 3\rho^4 + 6\rho^3 + 10\rho^2 + 15\rho + 21)}{56\rho^8}.$$

Although the bound appears complicated, it depends primarily on the geometric quantity  $\rho$ , i.e., the ratio between the first derivatives of  $\psi_1$  and  $\psi_2$ . When higher-order derivatives of  $\rho$  are small and  $\rho$  is bounded away from zero, the length of the above admissible curve (hence  $d_{\mathcal{F}_b}(\psi_1, \psi_2)$ ) is small, indicating that the approximation from  $\psi_1$  to  $\psi_2$  is easy.

By identifying  $\psi$  with an increasing function on  $[0, 2\pi]$ , this setting resembles the 1D ReLU case. As there, the local norm admits an upper bound in terms of Sobolev-type quantities; here, however, higher-order terms emerge due to composition on the circle. Consequently, unlike the 1D ReLU case, there is no global reparametrization (such as (3.89)) that flattens the local norm into a classical norm; the global complexity remains governed by  $\rho$  and its higher derivatives, as reflected in the estimate above. The qualitative message is similar: if  $\rho$  stays uniformly away from 0 and its derivatives up to order 4 are small, then the approximation (in the sub-Finsler, minimal-time sense) from  $\psi_1$  to  $\psi_2$  is easy.

**Computations for the layer-normalization example.** Recall the control family  $\mathcal{G}_b$  and its projected family  $\mathcal{F}_b$  introduced in the previous subsection. For completeness, we keep the explicit parametrizations needed for the estimates below.

For a given (scalar) bias parameter  $b \in \mathbb{R}$  (we write  $b$  for  $b\mathbf{1} \in \mathbb{R}^2$ ), we consider functions of the form

$$(5.49) \quad x \rightarrow W\sigma(Ax + b), \quad x \in \mathbb{R}^2, \quad W, A \in \mathbb{R}^{2 \times 2}, \quad W \text{ is diagonal}, \quad \|W\|_F \leq 1, \quad \|A_i\|_2 = 1, \quad i = 1, 2,$$

where  $A_i$  is the  $i$ -th row of  $A$ , and denote by  $\mathcal{G}_b$  the collection of all such vector fields.

We then introduce an associated control family on the circle  $S^1 \subset \mathbb{R}^2$  by projection:

$$(5.50) \quad \mathcal{F}_b := \{\text{Proj}(g) \mid g \in \mathcal{G}_b\} \subset \text{Vec}(S^1),$$

where the projection operator is defined as:

$$\text{Proj}(V)(x) := (I - xx^T)V(x), \quad \text{for all } x \in S^1.$$

Parameterizing the circle by  $\theta \in [0, 2\pi)$ , any tangent vector field  $V$  on  $S^1$  can be identified with a  $2\pi$ -periodic continuous function  $f(\theta) : \mathbb{R} \rightarrow \mathbb{R}$  by setting  $f(\theta) = V((\cos \theta, \sin \theta)) \cdot (-\sin \theta, \cos \theta)$ . Under this identification, the control family  $\mathcal{F}_b$  can be written as

$$(5.51) \quad \bar{\mathcal{F}}_b := \{\theta \rightarrow -w_1\sigma(a_1 \cdot (\sin \theta, \cos \theta) + b_1) \sin \theta + w_2\sigma(a_2 \cdot (\sin \theta, \cos \theta) + b_2) \cos \theta \mid |w_1|, |w_2|, |a_1|, |a_2| \leq 1\}.$$

In what follows we work with the induced local norm  $\|\cdot\|_{\text{Id}}$  (defined in the general theory) on the tangent space of the smooth submanifold  $\bar{\mathcal{M}}$  introduced earlier; the corresponding estimate at a general base point  $\varphi \in \bar{\mathcal{M}}$  is then obtained by right-translation (composition with  $\varphi^{-1}$ ), as summarized before.

For each  $\phi \in \bar{\mathcal{M}}$ , the tangent space  $T_\phi \bar{\mathcal{M}}$  can be identified as the set of all  $C^3$ -vector fields on  $S^1$ , which can be identified as

$$(5.52) \quad C_{\text{per}}^3([0, 2\pi]) := \{f \in C^3(\mathbb{R}) \mid f(\theta + 2\pi) = f(\theta), \forall \theta \in \mathbb{R}\}.$$

Now, we first give an estimate of the local norm  $\|\cdot\|_\phi$  at  $\phi \in \bar{\mathcal{M}}$  by estimating the local norm at the identity map  $\text{Id}$ .

First, we can decompose a given  $f \in C_{\text{per}}^3([0, 2\pi])$  in the tangent space as the following:

$$(5.53) \quad f(\theta) = (f(\theta) \cos \theta) \cos \theta + (f(\theta) \sin \theta) \sin \theta.$$

We notice that if  $|a| \leq 1$ , we can write  $a = (\cos \varphi, \sin \varphi)$  for some  $\varphi \in [0, 2\pi)$ . Then, we have

$$(5.54) \quad a \cdot x = \cos(\theta - \varphi),$$

which gives a reparameterization of the control family. We then approximate  $f(\theta) \cos \theta$  by  $\sum_{i=1}^N w_i \sigma(\cos(\theta - \varphi_i) + b_1)$  and  $f(\theta) \sin \theta$  by  $\sum_{i=1}^M w_i \sigma(\cos(\theta - \varphi_i) + b_2)$ ; our complexity measure is the sum of  $|w_i|$ .

For the subproblem, notice that any linear combination

$$(5.55) \quad \sum_{k=1}^m w_k \sigma(\cos(\theta - \varphi_i) + b)$$

can be identified as a convolution of  $g_b(\theta) := \sigma(\cos \theta - b)$  with a discrete measure  $\rho = \sum_{k=1}^m w_k \delta_{\varphi_k}$ , where  $\delta_{\varphi}$  is the Dirac measure at  $\varphi$ .

Based on this observation, we have the following proposition:

**Proposition 5.5.** *Suppose that there exists a function  $\rho \in L^1([0, 2\pi])$  such that*

$$(5.56) \quad \int_0^{2\pi} g_b(x+t)\rho(t)dt = u(x).$$

Then, we have that

$$(5.57) \quad \inf\{s \mid u \in \overline{\mathbf{CH}_s(\mathcal{F}_b)}\} \leq \int_{[0,2\pi]} |\rho(t)| dt.$$

*Proof.* Fix  $\varepsilon > 0$ . Choose a continuous  $\rho_\varepsilon$  with  $\|\rho - \rho_\varepsilon\|_{L^1([0,2\pi])} \leq \varepsilon$ . Then

$$(5.58) \quad \left\| \int_0^{2\pi} g_b(\cdot+t)\rho(t) dt - \int_0^{2\pi} g_b(\cdot+t)\rho_\varepsilon(t) dt \right\|_{C([0,2\pi])} \leq \|g_b\|_{C([0,2\pi])} \varepsilon.$$

Since  $g_b$  and  $\rho_\varepsilon$  are continuous on  $[0, 2\pi]$ , a Riemann-sum approximation gives points  $t_k$  and weights  $w_k := \rho_\varepsilon(t_k)\Delta t$  such that

$$(5.59) \quad \left\| \int_0^{2\pi} g_b(\cdot+t)\rho_\varepsilon(t) dt - \sum_{k=1}^m w_k g_b(\cdot+t_k) \right\|_{C([0,2\pi])} \leq \varepsilon, \quad \sum_{k=1}^m |w_k| \leq \int_0^{2\pi} |\rho_\varepsilon(t)| dt + \varepsilon.$$

By construction,  $\sum_{k=1}^m w_k g_b(\cdot+t_k) \in \mathbf{CH}_s(\mathcal{F}_b)$  with  $s := \sum_k |w_k|$ , hence  $u$  lies in the  $C([0, 2\pi])$ -closure of  $\mathbf{CH}_{\|\rho\|_{L^1} + C\varepsilon}(\mathcal{F}_b)$  for a constant  $C$  independent of  $\varepsilon$ . Letting  $\varepsilon \rightarrow 0$  yields the claim.  $\square$

Now, we will show that there exists some  $b$  such that such  $\rho$  exists for any  $u \in C_{\text{per}}^3([0, 2\pi])$ .

**Proposition 5.6.** *Let  $b = \cos \beta$ , where  $\beta$  is a quadratic irrational multiple of  $\pi$ , i.e.  $\beta = \pi\alpha$  where  $\alpha$  is a quadratic irrational number. Then, for any  $f \in C_{\text{per}}^3([0, 2\pi])$ , there exists  $\rho \in L^1([0, 2\pi])$  such that*

$$(5.60) \quad \int_0^{2\pi} g_b(x+t)\rho(t)dt = f(x).$$

Moreover, there exists a constant  $C_b$  depending only on  $b$  such that

$$(5.61) \quad \|\rho\|_{L^1([0,2\pi])} \leq C_b \|f\|_{W^{3,2}([0,2\pi])}.$$

*Proof.* Notice that  $g_b(x)$  is an even function, we have that its sine coefficients in the Fourier series are all zero. Its cosine coefficients can be calculated as:

$$\begin{aligned}
a_n &= \frac{1}{2\pi} \int_0^{2\pi} \sigma(\cos x - \cos \beta) \cos(nx) dx \\
&= \frac{1}{2\pi} \int_{-\beta}^{\beta} (\cos x - \cos \beta) \cos(nx) dx \\
&= \frac{1}{2\pi} \left( \int_{-\beta}^{\beta} \cos x \cos(nx) dx - \cos \beta \int_{-\beta}^{\beta} \cos(nx) dx \right) \\
&= \frac{1}{2\pi} \left( \frac{1}{2} \int_{-\beta}^{\beta} (\cos((n-1)x) + \cos((n+1)x)) dx - \cos \beta \int_{-\beta}^{\beta} \cos(nx) dx \right) \\
(5.62) \quad &= \frac{1}{2\pi} \left( \frac{1}{2} \left[ \frac{\sin((n-1)x)}{n-1} + \frac{\sin((n+1)x)}{n+1} \right]_{-\beta}^{\beta} - \cos \beta \left[ \frac{\sin(nx)}{n} \right]_{-\beta}^{\beta} \right) \\
&= \frac{1}{2\pi} \left( \frac{\sin((n-1)\beta)}{n-1} + \frac{\sin((n+1)\beta)}{n+1} - \frac{2 \cos \beta \sin(n\beta)}{n} \right) \\
&= \frac{1}{2\pi} \left( \frac{\sin((n-1)\beta)}{n-1} + \frac{\sin((n+1)\beta)}{n+1} - \frac{\sin((n+1)\beta) + \sin((n-1)\beta)}{n} \right) \\
&= \frac{1}{2\pi} \left( \sin((n-1)\beta) \left( \frac{1}{n-1} - \frac{1}{n} \right) + \sin((n+1)\beta) \left( \frac{1}{n+1} - \frac{1}{n} \right) \right) \\
&= \begin{cases} \frac{1}{2\pi} \left( \frac{\sin((n-1)\beta)}{n(n-1)} - \frac{\sin((n+1)\beta)}{n(n+1)} \right), & n \geq 2, \\ \frac{1}{2\pi} \left( \beta - \frac{\sin(2\beta)}{2} \right), & n = 1. \end{cases}
\end{aligned}$$

Notice that

$$(5.63) \quad \frac{1}{2\pi} \left( \frac{\sin((n-1)\beta)}{n(n-1)} - \frac{\sin((n+1)\beta)}{n(n+1)} \right) = -\frac{2}{n^2} \sin \beta \cos n\beta + \mathcal{O}\left(\frac{1}{n^3}\right).$$

By the continued fraction approximation of quadratic irrational numbers, we have that

$$(5.64) \quad \inf_n |n \cos n\beta| > 0.$$

This indicates that there exists some constant  $C_{1,b} > 0$ , only depending on  $b$ , such that

$$(5.65) \quad |\hat{g}_b(n)| \geq \frac{C_{1,b}}{n^3}, \text{ for all integer } n \neq 0.$$

If we assume  $f$  to be  $C^5$ -smooth (can be weaker, say  $f \in H^4([0, 2\pi])$ ), we have that

$$(5.66) \quad |\hat{f}(n)| \leq \frac{C}{n^5}, \text{ for some } C > 0, \text{ for all integer } n \neq 0.$$

Therefore, the Fourier coefficients of  $\rho$  satisfies

$$(5.67) \quad \frac{\hat{f}(n)}{\hat{g}_b(n)} \leq \frac{C}{C_{1,b}n^2}, \text{ for all integer } n.$$

This indicates that there exists a function  $\rho \in H^1([0, 2\pi])$  with Fourier coefficients  $\hat{\rho}(n) = \frac{\hat{f}(n)}{\hat{g}_b(n)}$  such that:

$$(5.68) \quad f(x) = \int_0^{2\pi} g_b(x+t)\rho(t)dt.$$

Moreover, we have that

$$(5.69) \quad \begin{aligned} \|\rho\|_{L^1([0,2\pi])} &\leq \sqrt{2\pi}\|\rho\|_{L^2([0,2\pi])} \leq \sqrt{2\pi} \left( \left(\frac{C}{C_{1,b}}\right)^2 \sum_{n \in \mathbb{Z} \setminus \{0\}} (n^3 |\hat{f}(n)|)^2 + \left(\frac{\hat{f}(0)}{\hat{g}(0)}\right)^2 \right)^{\frac{1}{2}} \\ &\leq C_{b,2} \|f^{(3)}\|_{L^2([0,2\pi])} + C_{b,3} \|f\|_{C([0,2\pi])} \end{aligned}$$

here  $C_{b,2}$  and  $C_{b,3}$  are two constants that only depend on  $b$ .  $\square$

Combining the above two propositions, we have an estimate of the local norm:

$$(5.70) \quad \|u\|_{\varphi} \leq C_{b,2} \|(u \circ \varphi^{-1})^{(3)}\|_{L^2[0,2\pi]} + C_{b,3} \|u \circ \varphi^{-1}\|_{C([0,2\pi])}.$$

Now, we provide a global distance estimation between two diffeomorphisms  $\phi_1, \phi_2 \in \mathcal{M}$ .

For any  $\psi \in \bar{\mathcal{M}}$ , there exists a natural path (homotopy) from Id to  $\psi$ . Specifically, consider the cover

$$(5.71) \quad p : \mathbb{R} \rightarrow S^1, \theta \rightarrow e^{i\theta}.$$

For any  $\varphi \in \bar{\mathcal{M}}$ , there exists a lift  $\tilde{\psi} \in \text{Diff}(\mathbb{R})$  which is orientation preserving such that  $\tilde{\psi}(x + 2\pi) = \tilde{\psi}(x) + 2\pi$  and  $p \circ \tilde{\psi} = \psi \circ p$ . Therefore, we identify the  $C^5$ -diffeomorphism  $\psi$  on  $S^1$  as the set of functions:

$$(5.72) \quad \begin{aligned} \mathcal{N} := \{ \psi \in C^5([0, 2\pi]) \mid \psi'(x) > 0 \text{ for all } x \in (0, 2\pi), \\ \psi(0) + 2\pi = \psi(2\pi), \psi^{(i)}(0) = \psi^{(i)}(2\pi) \text{ for } i = 1, 2, 3, 4, 5 \} \end{aligned}$$

For any  $\psi_1, \psi_2 \in \mathcal{N}$ ,

$$(5.73) \quad \psi_t := (1-t)\psi_1 + t\psi_2$$

gives a homotopy from  $\psi_1$  to  $\psi_2$  on  $\mathcal{N}$ . Therefore, we can estimate the global distance  $d_{\mathcal{F}}(\psi_1, \psi_2)$  by estimating the length of this path:

$$(5.74) \quad \begin{aligned} \int_0^1 \left\| \frac{\partial}{\partial t} \psi_t \right\|_{\psi_t} dt &= \int_0^1 \|(\psi_2 - \psi_1) \circ \psi_t^{-1}\|_{\text{Id}} dt \\ &\leq \left( \int_0^1 C_{b,2} \|((\psi_2 - \psi_1) \circ \psi_t^{-1})^{(3)}\|_{L^2[0,2\pi]} + C_{b,3} \|(\psi_2 - \psi_1) \circ \psi_t^{-1}\|_{C([0,2\pi])} dt \right) \end{aligned}$$

Denote  $u := \psi_2 - \psi_1$ . For the first term, we have

$$(5.75) \quad \int_0^1 C_{b,2} \|(u \circ \psi_t^{-1})^{(3)}\|_{L^2[0,2\pi]} dt \leq C_{b,2} \left( \int_0^1 \|(u \circ \psi_t^{-1})^{(3)}\|_{L^2[0,2\pi]}^2 dt \right)^{1/2}$$

Now, for given  $t \in [0, 1]$ , denote

$$(5.76) \quad y = \psi_t^{-1}(x), z := \psi_2(y).$$

Define

$$(5.77) \quad \rho(z) := \frac{\psi_1'}{\psi_2'}(\psi_2^{-1}(z)) > 0, \quad D := \frac{d}{dz}, \quad \rho_t = t + (1-t)\rho.$$

Then, we have

$$(5.78) \quad \frac{d}{dx} = \frac{1}{\psi_t'(y)} \frac{d}{dy} = \frac{\psi_2'}{\psi_t} \frac{d}{dz} = \frac{1}{h} D$$

We also have:

$$(5.79) \quad Du = 1 - \rho, \quad D^2u = -D\rho, \quad D^3u = -D^2\rho.$$

Then, we have

$$(5.80) \quad \frac{d}{dx}(u \circ \psi_t^{-1}) = \frac{1}{h} Du = \frac{1-\rho}{h}$$

$$(5.81) \quad \frac{d^2}{dx^2}(u \circ \psi_t^{-1})'' = \frac{1}{h} D \left( \frac{1-\rho}{h} \right) = \frac{1}{h} \left( \frac{-D\rho}{h} + \frac{-(1-\rho)Dh}{h^2} \right).$$

Notice that

$$(5.82) \quad h + (1-t)(1-\rho) = (t + (1-t)\rho) + (1-t)(1-\rho) = 1,$$

we have

$$(5.83) \quad \frac{d^2}{dx^2}(u \circ \psi_t^{-1}) = -\frac{D\rho}{h^3}$$

Finally, we have

$$(5.84) \quad \begin{aligned} \frac{d^3}{dx^3}(u \circ \psi_t^{-1}) &= \frac{1}{h} D \left( -\frac{D\rho}{h^3} \right) = -\frac{1}{h} \left( \frac{D^2\rho}{h^3} - \frac{3, Dh}{h^4} D\rho \right) \\ &= -\frac{D^2\rho}{h^4} + 3(1-t) \frac{(D\rho)^2}{h^5} \\ &= -\frac{D^2\rho}{(t + (1-t)\rho)^4} + 3(1-t) \frac{(D\rho)^2}{(t + (1-t)\rho)^5} \end{aligned}$$

Therefore, by switching the order of integration, we have

$$(5.85) \quad \int_0^1 \|(u \circ \psi_t^{-1})'''_x\|_{L^2}^2 dt = \int_0^{2\pi} \left[ A(\rho) (D^2\rho)^2 + B(\rho) (D\rho)^2 (D^2\rho) + C(\rho) (D\rho)^4 \right] dx,$$

where

$$\begin{aligned} A(\rho) &= \frac{67\rho^6 + 67\rho^5 + 67\rho^4 + 67\rho^3 + 172\rho^2 - 80\rho + 60}{420\rho^7}, \\ B(\rho) &= -\frac{17\rho^6 + 34\rho^5 + 51\rho^4 + 68\rho^3 + 295\rho^2 - 150\rho + 105}{140\rho^8}, \\ C(\rho) &= \frac{3(\rho^5 + 3\rho^4 + 6\rho^3 + 10\rho^2 + 15\rho + 21)}{56\rho^8}. \end{aligned}$$

For the second term, since  $\psi_t$  is a diffeomorphism, it directly follows that

$$(5.86) \quad \int_0^1 \|(\psi_2 - \psi_1) \circ \psi_t^{-1}\|_{C([0,2\pi])} dt = \int_0^1 \|(\psi_2 - \psi_1)\|_{C([0,2\pi])} dt = \|\psi_1 - \psi_2\|_{C([0,2\pi])}$$

Combine these, we have the estimation:

$$(5.87) \quad d_{\mathcal{F}}(\psi_1, \psi_2) \leq C_{b,2} \int_0^{2\pi} \left[ A(\rho) (D^2\rho)^2 + B(\rho) (D\rho)^2 (D^2\rho) + C(\rho) (D\rho)^4 \right] dx + C_{b,3} \|\psi_1 - \psi_2\|_{C([0,2\pi])}$$

That is, the complexity is mainly related to the regularity of  $\rho$ .

## REFERENCES

- [1] Andrei Agrachev, Davide Barilari, and Ugo Boscain. *A comprehensive introduction to sub-Riemannian geometry*, volume 181. Cambridge University Press, 2019.
- [2] Andrei Agrachev and Andrey Sarychev. Control on the manifolds of mappings with a view to the deep learning. *Journal of Dynamical and Control Systems*, 28(4):989–1008, 2022.
- [3] Sylvain Arguillere. Sub-riemannian geometry and geodesics in banach manifolds. *The Journal of Geometric Analysis*, 30(3):2897–2938, 2020.
- [4] Jimmy Lei Ba, Jamie Ryan Kiros, and Geoffrey E Hinton. Layer normalization. *arXiv preprint arXiv:1607.06450*, 2016.
- [5] John M Ball. A version of the fundamental theorem for young measures. In *PDEs and Continuum Models of Phase Transitions: Proceedings of an NSF-CNRS Joint Seminar Held in Nice, France, January 18–22, 1988*, pages 207–215. Springer, 2005.
- [6] Andrew R Barron. Universal approximation bounds for superpositions of a sigmoidal function. *IEEE Transactions on Information theory*, 39(3):930–945, 2002.
- [7] Venkat Chandrasekaran, Benjamin Recht, Pablo A. Parrilo, and Alan S. Willsky. The convex geometry of linear inverse problems. *Foundations of Computational Mathematics*, 12(6):805–849, 2012.
- [8] Jingpu Cheng, Qianxiao Li, Ting Lin, and Zuwei Shen. Interpolation, approximation, and controllability of deep neural networks. *SIAM Journal on Control and Optimization*, 63(1):625–649, 2025.
- [9] Jingpu Cheng, Ting Lin, Zuwei Shen, and Qianxiao Li. A unified framework for establishing the universal approximation of transformer-type architectures. In *The Thirty-ninth Annual Conference on Neural Information Processing Systems*, 2025.
- [10] Christa Cuchiero, Martin Larsson, and Josef Teichmann. Deep neural networks, generic universal interpolation, and controlled odes. *SIAM Journal on Mathematics of Data Science*, 2(3):901–919, 2020.
- [11] George Cybenko. Approximation by superpositions of a sigmoidal function. *Mathematics of control, signals and systems*, 2(4):303–314, 1989.
- [12] Klaus Deimling. *Nonlinear functional analysis*. Springer Science & Business Media, 2013.
- [13] Jacob Devlin, Ming-Wei Chang, Kenton Lee, and Kristina Toutanova. Bert: Pre-training of deep bidirectional transformers for language understanding. In *Proceedings of the 2019 conference of the North American chapter of the association for computational linguistics: human language technologies, volume 1 (long and short papers)*, pages 4171–4186, 2019.
- [14] Ronald A DeVore and George G Lorentz. *Constructive approximation*, volume 303. Springer Science & Business Media, 1993.
- [15] Alexey Dosovitskiy, Lucas Beyer, Alexander Kolesnikov, Dirk Weissenborn, Xiaohua Zhai, Thomas Unterthiner, Mostafa Dehghani, Matthias Minderer, Georg Heigold, Sylvain Gelly, et al. An image is worth 16x16 words: Transformers for image recognition at scale. *arXiv preprint arXiv:2010.11929*, 2020.
- [16] Yifei Duan and Yongqiang Cai. A minimal control family of dynamical systems for universal approximation. *IEEE Transactions on Automatic Control*, 2025.
- [17] Borjan Geshkovski, Philippe Rigollet, and Domènec Ruiz-Balet. Measure-to-measure interpolation using transformers. *arXiv preprint arXiv:2411.04551*, 2024.
- [18] Yury Gorishniy, Ivan Rubachev, Valentin Khrukov, and Artem Babenko. Revisiting deep learning models for tabular data. *Advances in neural information processing systems*, 34:18932–18943, 2021.
- [19] Richard Hartley, Jochen Trumpf, Yuchao Dai, and Hongdong Li. Rotation averaging. *International journal of computer vision*, 103(3):267–305, 2013.
- [20] Kaiming He, Xiangyu Zhang, Shaoqing Ren, and Jian Sun. Deep residual learning for image recognition. In *Proceedings of the IEEE Conference on Computer Vision and Pattern Recognition (CVPR)*, pages 770–778, 2016.
- [21] Jonathan Ho, Ajay Jain, and Pieter Abbeel. Denoising diffusion probabilistic models. In *Advances in Neural Information Processing Systems*, volume 33, pages 6840–6851, 2020.
- [22] Kurt Hornik. Approximation capabilities of multilayer feedforward networks. *Neural networks*, 4(2):251–257, 1991.
- [23] Du Q Huynh. Metrics for 3d rotations: Comparison and analysis. *Journal of Mathematical Imaging and Vision*, 35(2):155–164, 2009.
- [24] Erich L. Lehmann and George Casella. *Theory of Point Estimation*. Springer, New York, NY, 2nd edition, 1998.
- [25] Qianxiao Li, Long Chen, Cheng Tai, et al. Maximum principle based algorithms for deep learning. *Journal of Machine Learning Research*, 18(165):1–29, 2018.
- [26] Qianxiao Li, Ting Lin, and Zuwei Shen. Deep learning via dynamical systems: An approximation perspective. *Journal of the European Mathematical Society*, 25(5):1671–1709, 2023.
- [27] Yaron Lipman, Ricky T. Q. Chen, Heli Ben-Hamu, Maximilian Nickel, and Matt Le. Flow matching for generative modeling. *arXiv preprint arXiv:2210.02747*, 2022.

- [28] Jianfeng Lu, Zuowei Shen, Haizhao Yang, and Shijun Zhang. Deep network approximation for smooth functions. *SIAM Journal on Mathematical Analysis*, 53(5):5465–5506, 2021.
- [29] Chao Ma, Lei Wu, et al. The barron space and the flow-induced function spaces for neural network models. *Constructive Approximation*, 55(1):369–406, 2022.
- [30] Richard Montgomery. *A tour of subriemannian geometries, their geodesics and applications*. Number 91. American Mathematical Soc., 2002.
- [31] Danilo Rezende and Shakir Mohamed. Variational inference with normalizing flows. In *International conference on machine learning*, pages 1530–1538. PMLR, 2015.
- [32] R. Tyrrell Rockafellar. *Convex Analysis*, volume 28 of *Princeton Mathematical Series*. Princeton University Press, Princeton, NJ, 1970.
- [33] Domenc Ruiz-Balet and Enrique Zuazua. Neural ode control for classification, approximation, and transport. *SIAM Review*, 65(3):735–773, 2023.
- [34] Lars Ruthotto and Eldad Haber. Deep neural networks motivated by partial differential equations. *Journal of Mathematical Imaging and Vision*, 62(3):352–364, 2020.
- [35] Zuowei Shen, Haizhao Yang, and Shijun Zhang. Deep network approximation characterized by number of neurons. *arXiv preprint arXiv:1906.05497*, 2019.
- [36] Zuowei Shen, Haizhao Yang, and Shijun Zhang. Neural network approximation: Three hidden layers are enough. *Neural Networks*, 141:160–173, 2021.
- [37] Zuowei Shen, Haizhao Yang, and Shijun Zhang. Optimal approximation rate of relu networks in terms of width and depth. *Journal de Mathématiques Pures et Appliquées*, 157:101–135, 2022.
- [38] Jonathan W Siegel and Jinchao Xu. Approximation rates for neural networks with general activation functions. *Neural Networks*, 128:313–321, 2020.
- [39] Jonathan W Siegel and Jinchao Xu. Characterization of the variation spaces corresponding to shallow neural networks. *Constructive Approximation*, 57(3):1109–1132, 2023.
- [40] Yang Song and Stefano Ermon. Generative modeling by estimating gradients of the data distribution. In *Advances in Neural Information Processing Systems*, volume 32, pages 11895–11907, 2019. NeurIPS 2019.
- [41] Yang Song, Jascha Sohl-Dickstein, Diederik P. Kingma, Abhishek Kumar, Stefano Ermon, and Ben Poole. Improved techniques for training score-based generative models. *arXiv preprint*, 2020. See also subsequent journal/conference versions on score-based / SDE formulations (Song et al., 2021).
- [42] Yang Song, Jascha Sohl-Dickstein, Diederik P Kingma, Abhishek Kumar, Stefano Ermon, and Ben Poole. Score-based generative modeling through stochastic differential equations. *arXiv preprint arXiv:2011.13456*, 2020.
- [43] Yang Song, Jascha Sohl-Dickstein, Diederik P. Kingma, Abhishek Kumar, Stefano Ermon, and Ben Poole. Score-based generative modeling through stochastic differential equations. In *International Conference on Learning Representations*. OpenReview.net, 2021.
- [44] Eduardo D Sontag. *Mathematical control theory: deterministic finite dimensional systems*, volume 6. Springer Science & Business Media, 2013.
- [45] Paulo Tabuada and Bahman Ghahserifard. Universal approximation power of deep residual neural networks through the lens of control. *IEEE Transactions on Automatic Control*, 68(5):2715–2728, 2022.
- [46] Ilya O Tolstikhin, Neil Houlsby, Alexander Kolesnikov, Lucas Beyer, Xiaohua Zhai, Thomas Unterthiner, Jessica Yung, Andreas Steiner, Daniel Keysers, Jakob Uszkoreit, et al. Mlp-mixer: An all-mlp architecture for vision. *Advances in neural information processing systems*, 34:24261–24272, 2021.
- [47] Hugo Touvron, Piotr Bojanowski, Mathilde Caron, Matthieu Cord, Alaaeldin El-Nouby, Edouard Grave, Gautier Izacard, Armand Joulin, Gabriel Synnaeve, Jakob Verbeek, et al. Resmlp: Feedforward networks for image classification with data-efficient training. *IEEE transactions on pattern analysis and machine intelligence*, 45(4):5314–5321, 2022.
- [48] Ashish Vaswani, Noam Shazeer, Niki Parmar, Jakob Uszkoreit, Llion Jones, Aidan N. Gomez, Łukasz Kaiser, and Illia Polosukhin. Attention is all you need. *Advances in Neural Information Processing Systems (NeurIPS)*, 30, 2017.
- [49] Ee Weinan. A proposal on machine learning via dynamical systems. *Communications in Mathematics and Statistics*, 5(1):1–11, 2017.
- [50] Johannes Wittmann. The banach manifold  $ck(m, n)$ . *Differential Geometry and its Applications*, 63:166–185, 2019.
- [51] Ruibin Xiong, Yunchang Yang, Di He, Kai Zheng, Shuxin Zheng, Chen Xing, Huishuai Zhang, Yanyan Lan, Liwei Wang, and Tieyan Liu. On layer normalization in the transformer architecture. In *International conference on machine learning*, pages 10524–10533. PMLR, 2020.
- [52] Yunfei Yang and Ding-Xuan Zhou. Optimal rates of approximation by shallow relu k neural networks and applications to nonparametric regression. *Constructive Approximation*, 62(2):329–360, 2025.
- [53] Dmitry Yarotsky. Error bounds for approximations with deep relu networks. *Neural networks*, 94:103–114, 2017.
- [54] Dmitry Yarotsky. Optimal approximation of continuous functions by very deep relu networks. In *Conference on learning theory*, pages 639–649. PMLR, 2018.